Climate: Observations, projections and impacts: Indonesia

Met Office
Simon N. Gosling, University of Nottingham
Robert Dunn, Met Office
Fiona Carrol, Met Office
Nikos Christidis, Met Office
John Fullwood, Met Office
Diogo de Gusmao, Met Office
Nicola Golding, Met Office
Lizzie Good, Met Office
Trish Hall, Met Office
Lizzie Kendon, Met Office
John Kennedy, Met Office
Kirsty Lewis, Met Office
Rachel McCarthy, Met Office
Carol McSweeney, Met Office
Colin Morice, Met Office
David Parker, Met Office
Matthew Perry, Met Office
Peter Stott, Met Office
Kate Willett, Met Office
Myles Allen, University of Oxford
Nigel Arnell, Walker Institute, University of Reading
Dan Bernie, Met Office
Richard Betts, Met Office
Niel Bowerman, Centre for Ecology and Hydrology
Bastiaan Brak, University of Leeds
John Caesar, Met Office
Andy Challinor, University of Leeds
Rutger Dankers, Met Office
Fiona Hewer, Fiona's Red Kite
Chris Huntingford, Centre for Ecology and Hydrology
Alan Jenkins, Centre for Ecology and Hydrology
Nick Klingaman, Walker Institute, University of Reading
Kirsty Lewis, Met Office
Ben Lloyd-Hughes, Walker Institute, University of Reading
Jason Lowe, Met Office
Rachel McCarthy, Met Office
James Miller, Centre for Ecology and Hydrology
Robert Nicholls, University of Southampton
Maria Noguer, Walker Institute, University of Reading
Friedreike Otto, Centre for Ecology and Hydrology
Paul van der Linden, Met Office
Rachel Warren, University of East Anglia

The country reports were written by a range of climate researchers, chosen for their subject expertise, who were drawn from institutes across the UK. Authors from the Met Office and the University of Nottingham collated the contributions in to a coherent narrative which was then reviewed. The authors and contributors of the reports are as above.

Climate: Observations, projections and impacts

Indonesia

We have reached a critical year in our response to climate change. The decisions that we made in Cancún put the UNFCCC process back on track, saw us agree to limit temperature rise to 2 °C and set us in the right direction for reaching a climate change deal to achieve this. However, we still have considerable work to do and I believe that key economies and major emitters have a leadership role in ensuring a successful outcome in Durban and beyond.

To help us articulate a meaningful response to climate change, I believe that it is important to have a robust scientific assessment of the likely impacts on individual countries across the globe. This report demonstrates that the risks of a changing climate are wide-ranging and that no country will be left untouched by climate change.

I thank the UK's Met Office Hadley Centre for their hard work in putting together such a comprehensive piece of work. I also thank the scientists and officials from the countries included in this project for their interest and valuable advice in putting it together. I hope this report will inform this key debate on one of the greatest threats to humanity.

The Rt Hon. Chris Huhne MP, Secretary of State for Energy and Climate Change

There is already strong scientific evidence that the climate has changed and will continue to change in future in response to human activities. Across the world, this is already being felt as changes to the local weather that people experience every day.

Our ability to provide useful information to help everyone understand how their environment has changed, and plan for future, is improving all the time. But there is still a long way to go. These reports – led by the Met Office Hadley Centre in collaboration with many institutes and scientists around the world – aim to provide useful, up to date and impartial information, based on the best climate science now available. This new scientific material will also contribute to the next assessment from the Intergovernmental Panel on Climate Change.

However, we must also remember that while we can provide a lot of useful information, a great many uncertainties remain. That's why I have put in place a long-term strategy at the Met Office to work ever more closely with scientists across the world. Together, we'll look for ways to combine more and better observations of the real world with improved computer models of the weather and climate; which, over time, will lead to even more detailed and confident advice being issued.

Julia Slingo, Met Office Chief Scientist

Introduction

Understanding the potential impacts of climate change is essential for informing both adaptation strategies and actions to avoid dangerous levels of climate change. A range of valuable national studies have been carried out and published, and the Intergovernmental Panel on Climate Change (IPCC) has collated and reported impacts at the global and regional scales. But assessing the impacts is scientifically challenging and has, until now, been fragmented. To date, only a limited amount of information about past climate change and its future impacts has been available at national level, while approaches to the science itself have varied between countries.

In April 2011, the Met Office Hadley Centre was asked by the United Kingdom's Secretary of State for Energy and Climate Change to compile scientifically robust and impartial information on the physical impacts of climate change for more than 20 countries. This was done using a consistent set of scenarios and as a pilot to a more comprehensive study of climate impacts. A report on the observations, projections and impacts of climate change has been prepared for each country. These provide up to date science on how the climate has already changed and the potential consequences of future changes. These reports complement those published by the IPCC as well as the more detailed climate change and impact studies published nationally.

Each report contains:

• A description of key features of national weather and climate, including an analysis of new data on extreme events.

• An assessment of the extent to which increases in greenhouse gases and aerosols in the atmosphere have altered the probability of particular seasonal temperatures compared to pre-industrial times, using a technique called 'fraction of attributable risk.'

• A prediction of future climate conditions, based on the climate model projections used in the Fourth Assessment Report from the IPCC.

• The potential impacts of climate change, based on results from the UK's Avoiding Dangerous Climate Change programme (AVOID) and supporting literature.
  For details visit: http://www.avoid.uk.net

The assessment of impacts at the national level, both for the AVOID programme results and the cited supporting literature, were mostly based on global studies. This was to ensure consistency, whilst recognising that this might not always provide enough focus on impacts of most relevance to a particular country. Although time available for the project was short, generally all the material available to the researchers in the project was used, unless there were good scientific reasons for not doing so. For example, some impacts areas were omitted, such as many of those associated with human health. In this case, these impacts are strongly dependant on local factors and do not easily lend themselves to the globally consistent framework used. No attempt was made to include the effect of future adaptation actions in the assessment of potential impacts. Typically, some, but not all, of the impacts are avoided by limiting global average warming to no more than 2 °C.

The Met Office Hadley Centre gratefully acknowledges the input that organisations and individuals from these countries have contributed to this study. Many nations contributed references to the literature analysis component of the project and helped to review earlier versions of these reports.

We welcome feedback and expect these reports to evolve over time. For the latest version of this report, details of how to reference it, and to provide feedback to the project team, please see the website at www.metoffice.gov.uk/climate-change/policy-relevant/obs-projections-impacts

In the longer term, we would welcome the opportunity to explore with other countries and organisations options for taking forward assessments of national level climate change impacts through international cooperation.

Summary

Climate observations

- Limited observational data is available over the Indonesian archipelago but where data are present over the period 1960 to 2010, there has been a warming trend.

- Over Sumatra and Borneo, where daily temperature data are available, there has been a trend between the late 1960s and 2003 towards fewer cool nights and more warm nights and warm days.

Climate change projections

- For the A1B emissions scenario projected temperature increases over Indonesia are generally in the range of 2-2.5°C. There are a few areas of Borneo and Sumatra where temperatures of 2.5-3°C are projected. There is good agreement between the CMIP3 models over all of Indonesia.

- Precipitation changes show quite low agreement between CMIP3 models over Indonesia, though there are some regions of good agreement over New Guinea. Over New Guinea, rainfall is projected to increase in the region of 10-20%. Further west, over Borneo, increases of 5-10% are projected, with smaller increases of 0-5% projected over Sumatra.

Climate change impacts projections

Crop yields

- A number of, but not all, Global- and regional-scale studies show that climate change could be associated with declines in maize yields but increases in rice yields, two of Indonesia's major crops, from 2050 onwards.

- In all studies the balance between detrimental ozone effects and ameliorating CO_2 fertilisation may determine whether projected losses or gains are realised under climate change.

- National-scale studies show that uncertainty in future crop production is dependent on potential changes to ENSO, which are not yet fully understood.

Food security

- Indonesia is currently a country with moderately low levels of undernourishment. Global-scale studies included here project that Indonesia could remain food-secure over the next 40 years, where food production from the land is concerned.

- However, the security of supply from marine sources is of concern. One study projects that Indonesia could experience some of the largest decreases in marine fish stocks across the globe; for example, the 10-year averaged maximum catch potential from 2005 to 2055 could decline by 23% under SRES A1B.

Water stress and drought

- There are currently few studies on the impact of climate change on water stress and drought in Indonesia, especially at the national scale.

- Recent simulations by the AVOID programme show no appreciable increases or decreases in the population projected to be exposed to water stress with climate change in Indonesia.

Pluvial flooding and rainfall

- The IPCC AR4 reported potential increases in precipitation over Indonesia under global climate change scenarios however few studies relevant to Indonesia have been published since.

- Large uncertainties remain, particularly regarding the response of the El Nino Southern Oscillation (ENSO) to climate change.

Fluvial flooding

- Results from a recent global-scale study suggest that extreme flooding could increase in Indonesia with climate change.

- Simulations by the AVOID programme support these results. A majority of the models show a tendency for increasing flood risk, particularly later in the century and in the A1B scenario, and in some models this increase is very large.

Tropical cyclones

- There remains large uncertainty in the current understanding of how tropical cyclones might be affected by climate change. To this end, caution should be applied in interpreting model-based results, even where the models are in agreement.

- Most global- and regional-scale studies reviewed here suggest that the frequency of landfalling tropical cyclones in Indonesia could decrease with climate change, for both West Pacific cyclones, which affect the eastern part of the country, and South Indian Ocean cyclones, which affect the western and southern regions.

- However, most studies reviewed here suggest that the intensity of cyclones could increase with climate change, particularly for the most severe storms.

Coastal regions

- Sea level rise (SLR) could have major impacts on Indonesia's coastal regions.

- A 10% intensification of the current 1-in-100-year storm surge combined with a prescribed 1m SLR could affect 39% of Indonesia's coastal GDP and 14,400km^2 of coastal land.

- Another study showed that the country's population exposed to SLR could increase from 600,000 in present, to 2.7 million under un-mitigated A1B emissions in the 2070s - aggressive mitigation policy could avoid exposure of around 156,000 people.

Table of Contents

Chapter 1 – Climate Observations

Rationale

Present day weather and climate play a fundamental role in the day to day running of society. Seasonal phenomena may be advantageous and depended upon for sectors such as farming or tourism. Other events, especially extreme ones, can sometimes have serious negative impacts posing risks to life and infrastructure and significant cost to the economy. Understanding the frequency and magnitude of these phenomena, when they pose risks or when they can be advantageous and for which sectors of society, can

Figure 1. *Location of boxes for the regional average time series (red dashed box) in Figures 3 and 4.*

significantly improve societal resilience. In a changing climate it is highly valuable to understand possible future changes in both potentially hazardous events and those reoccurring seasonal events that are depended upon by sectors such as agriculture and tourism. However, in order to put potential future changes in context, the present day must first be well understood both in terms of common seasonal phenomena and extremes.

The purpose of this chapter is to summarise the weather and climate from 1960 to present day. This begins with a general climate overview including an up to date analysis of changes in surface mean temperature. These changes may be the result of a number of factors including climate change, natural variability and changes in land use. There is then a focus on extremes of temperature and precipitation selected from 1997 onwards, reported in the World Meteorological Organization (WMO) Annual Statement on the Status of the Global Climate and/or the Bulletin of the American Meteorological Society (BAMS) State of the Climate reports. This is followed by a discussion of changes in moderate extremes from 1960 onwards using the HadEX extremes database (Alexander et al., 2006) which categorises extremes of temperature and precipitation. These are core climate variables which have received significant effort from the climate research community in terms of data acquisition and processing and for which it is possible to produce long high quality records for monitoring. The work presented here is the foundation of future plans to systematically

address the region's present and projected future weather and climate, and the associated impacts.

The methodology section that follows provides details of the data shown here and of the scientific analyses underlying the discussions of changes in the mean temperature and in temperature and precipitation extremes.

Climate overview

Indonesia consists of a large number of islands spanning the equator from 5°N to 10°S. The equatorial situation means that temperatures remain high throughout the year with little variation from month to month. The annual mean temperature is between 26°C and 29°C in most places. The maritime influence means that diurnal variation in temperature is small on the coast. Average daily maxima are approximately 31°C, and daily minimum temperatures average 23°C. At Jakarta, night-time temperatures are particularly warm with an average of 25°C. Most of the islands are very mountainous with volcanic peaks and mountain ranges exceeding 3000 m, and temperatures decrease with increasing altitude. The day-time sea breezes and strong monsoon winds provide some relief from the heat and humidity on the coast, while inland the nights are cooler.

There are two main seasonal wind systems which affect Indonesia. Between November and March, the inter-tropical convergence zone (ITCZ) is located to the south so the northerly winds of the north monsoon dominate. Between May and September, the ITCZ is located to the north, so Indonesia is affected by the south monsoon blowing from the Indian Ocean and Australia. For a few weeks in April and October, winds are light as the ITCZ, or Doldrum belt, passes over. The amount and season of maximum rainfall vary with the different exposure of the islands to these monsoon systems. Jakarta, on the northern side of the island of Java, has average annual rainfall of 1650 mm, most of which comes from the north monsoon between November and March, although April is also a wet month as the ITCZ passes from south to north. Ambon, on the southern side of the Moluccas to the east, is much wetter with an annual average rainfall of 3640 mm, and is most affected by the south monsoon from May to September. Medan, in north Sumatra, has rain throughout the year totalling 2260 mm on average, with October the wettest month as the ITCZ passes from north to south. Similarly, Balikpapan on Borneo has little seasonal variation in rainfall with an average annual amount of 2230 mm. Orographic enhancement leads to increased rainfall in the mountains.

Much of the rainfall is heavy and accompanied by thunder, and during thunderstorms wind squalls may occur. There is still a good amount of sunshine however, as when it is not raining it is generally fine and sunny. Warm phases of the El Niño Southern Oscillation (ENSO) tend to bring reduced rainfall which can lead to drought, especially for areas which have a pronounced dry season. Only the extreme southern islands such as Timor are occasionally affected by strong winds associated with tropical cyclones.

Analysis of long-term features in the mean temperature

CRUTEM3 data (Brohan et al., 2006) have been used to provide an analysis of mean temperatures from 1960 to 2010 over Indonesia using the median of pairwise slopes method to fit the trend (Sen, 1968; Lanzante, 1996). The methods are fully described in the methodology section that follows. There are limited data available over the Indonesian archipelago and so spatial coverage is incomplete. In concert with increasing global average temperatures (Sánchez-Lugo et al., 2011), where data are present, there is a predominant warming signal for temperature. For the majority of grid boxes shown in Figure 2 there is higher confidence in the warming shown in that the 5th to 95th percentiles of the slopes are of the same sign. This is consistent with previous research (Christensen et al. 2007). The signal is similar for both the dry months (June to August) and wet months (December to January). Regionally averaged trends (over grid boxes included in the red dashed box in Figure 1) calculated by the median of pairwise slopes show warming with higher confidence. For the dry season (JJA) the trend is 0.20°C per decade (5th to 95th percentile of slopes: 0.16 to 0.24°C per decade) and for the wet season (DJF) the trend is 0.1 °C per decade (5th to 95th percentile of slopes: 0.12 to 0.22°C per decade).
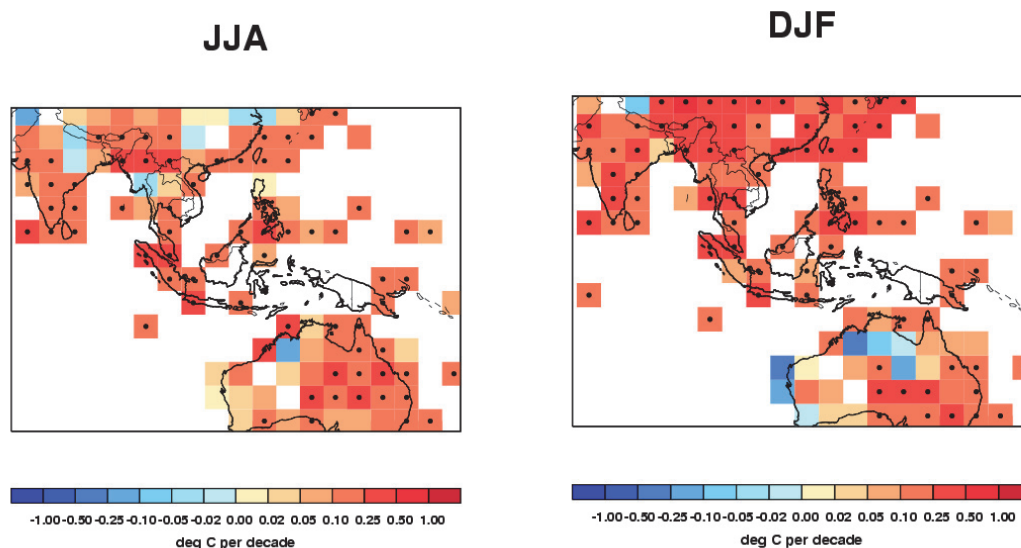
Figure 2. *Decadal trends in seasonally averaged temperatures for Indonesia and the surrounding area over the period 1960 to 2010. Monthly mean anomalies from CRUTEM3 (Brohan et al. 2006) are averaged over each 3 month season (June-July-August – JJA and December-January-February – DJF). Trends are fitted using the median of pairwise slopes method (Sen 1968, Lanzante 1996). There is higher confidence in the trends shown if the 5th to 95th percentiles of the pairwise slopes do not encompass zero because here the trend is considered to be significantly different from a zero trend (no change). This is shown by a black dot in the centre of the respective grid box.*

Temperature extremes

Both hot and cold temperature extremes can place many demands on society. While seasonal changes in temperature are normal and indeed important for a number of societal sectors (e.g. tourism, farming etc.), extreme heat or cold can have serious negative impacts. Importantly, what is 'normal' for one region may be extreme for another region that is less well adapted to such temperatures.

Indonesia experiences a narrow range of temperatures year round. There are few high impact extreme temperature events so none are included here. No significant extreme temperature event since 2000 was reported in WMO Statements on Status of the Global Climate and/or BAMS State of the Climate reports. The extremes that are experienced tend to be strongly associated with the wet and dry seasons, with excess cloud and rain leading to below-normal temperatures and vice versa.

Analysis of long-term features in moderate temperature extremes

HadEX extremes indices (Alexander et al. 2006) are used here for Indonesia from 1960 to 2003 using daily maximum and minimum temperatures. Here we discuss changes in the frequency of cool days and nights and warm days and nights which are moderate extremes. Cool days/nights are defined as being below the 10th percentile of daily maximum/minimum temperature and warm days/nights are defined as being above the 90th percentile of the daily maximum/minimum temperature. The methods are fully described in the methodology section.

There are few data available for the Indonesian archipelago and so spatial coverage is limited to Sumatra and Borneo. Between the late 1960s and 2003, the HadEX dataset (Alexander et al. 2006) shows a spatially consistent trend towards fewer cool nights and more warm nights and warm days (Figure 3). There is higher confidence in the majority of grid boxes and these signals are in concert with previous studies (Trenberth and Hoar, 1997; Aldhous, 2004) and the predominant pattern of increasing mean temperatures. However, there are spatially consistent increases in cool day frequency, also with higher confidence in the signal, over Borneo. The data presented here are annual totals, averaged across all

seasons, and so direct interpretation in terms of summertime heat waves and winter cold snaps is not possible. The small numbers of stations present in most grid boxes means that the grid box value will be biased towards the limited locations represented. Therefore, even if there is higher confidence in the signals shown, uncertainty in the signal representing the wider grid box is large.

Regional averages in the nighttime temperatures (daily minima) show high confidence in a signal of fewer cool nights and more warm nights. For daytime temperatures (daily maxima) confidence in the regional average trend of increasing warm days is high. There is no signal for cool days.

a) **cool nights (TN10p)**

-1.42 % per decade (-1.98 to -0.98)
-5.11 total change (%) (-7.12 to -3.52)

16

c) **warm nights (TN90p)**

<--cooler   % per decade   warmer-->

-5.00   -3.50   -2.00   -1.00   -0.50   -0.25   0.00   0.25   0.50   1.00   2.00   3.50   5.00

d)

4.98 % per decade (3.69 to 6.55)

17.93 total change (%) (13.27 to 23.59)

cool days (TX10p)

e)

<--warmer   % per decade   cooler-->

f)

0.08 % per decade (-0.04 to 0.16)

0.21 total change (%) (-0.11 to 0.43)

g) warm days (TX90p)

h)

4.27 % per decade (2.73 to 6.12)

15.38 total change (%) (9.84 to 22.02)
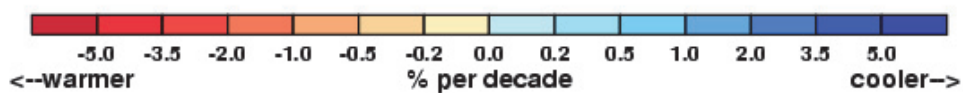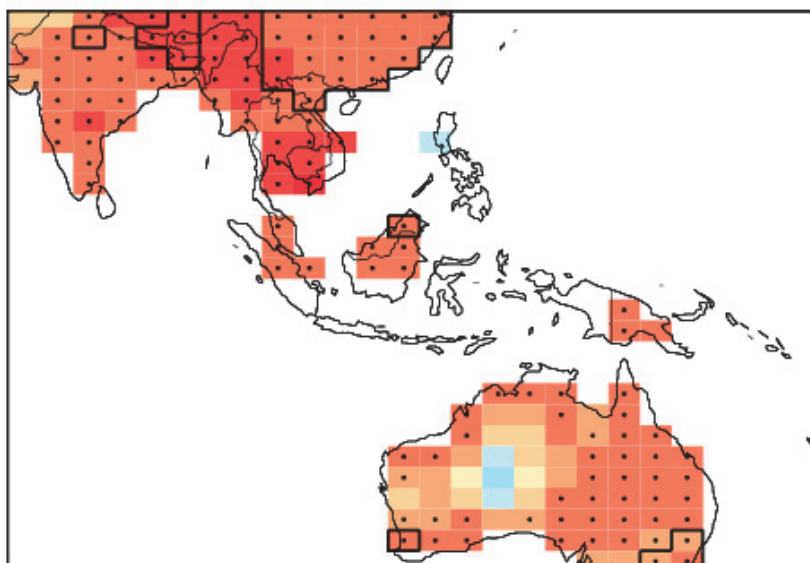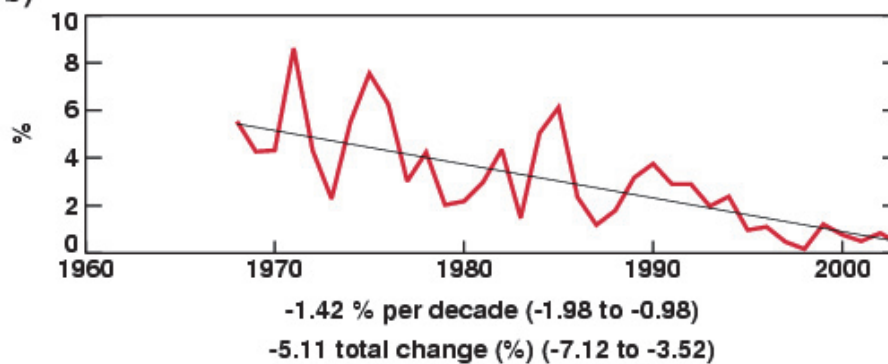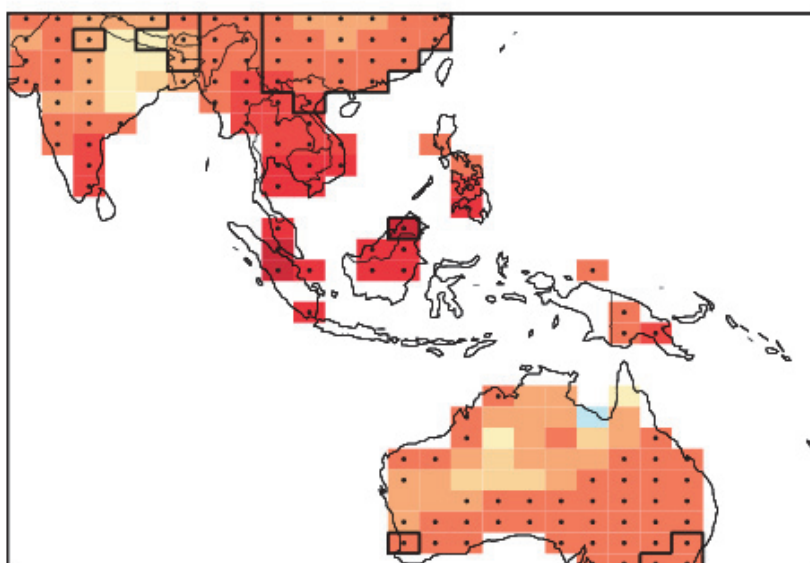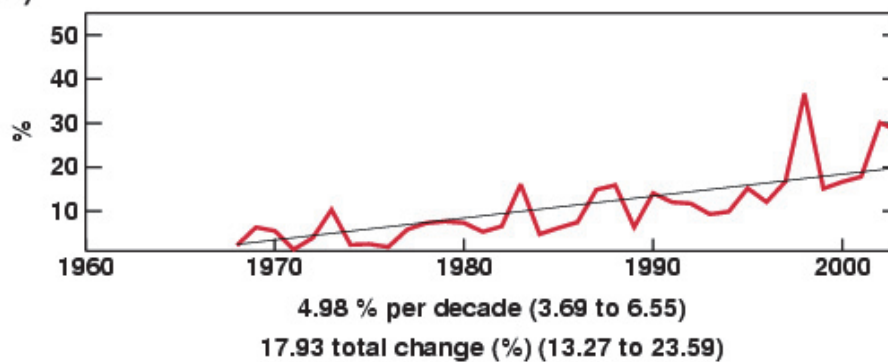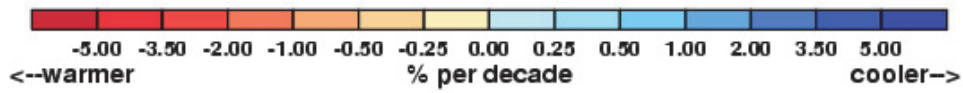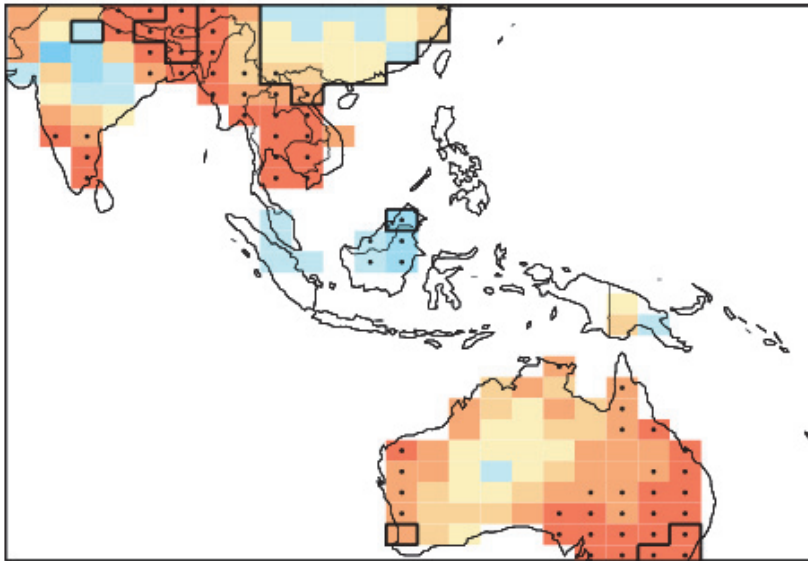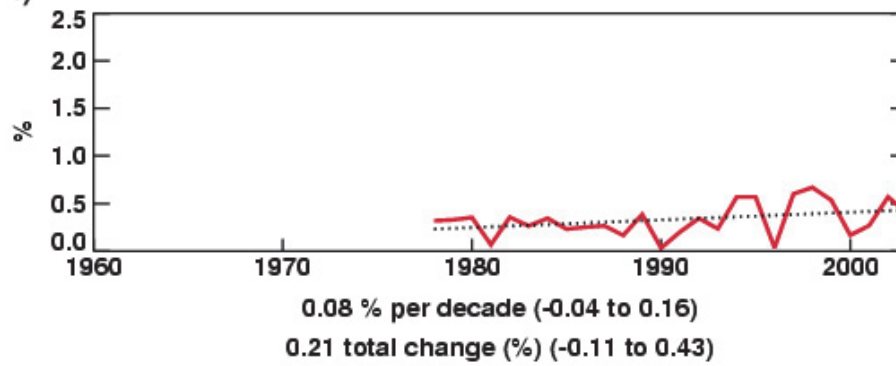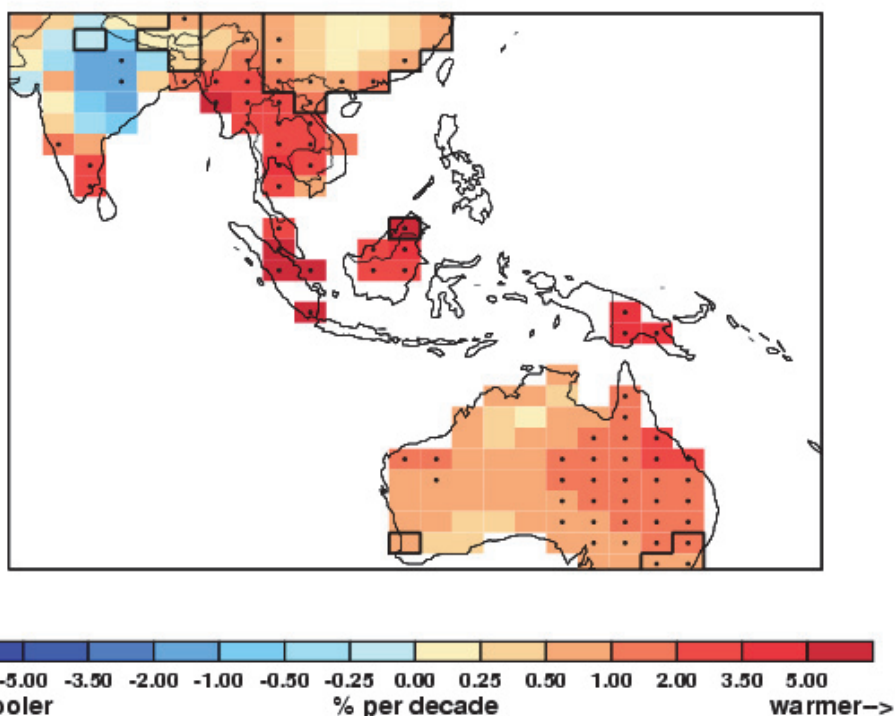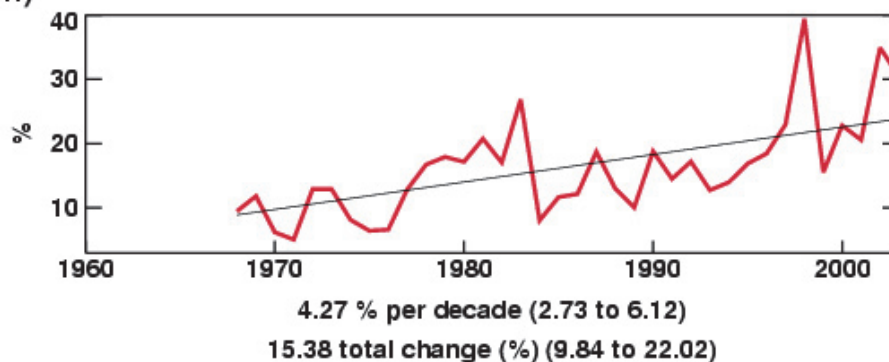
***Figure* 3.** *Percentage change in cool nights (a,b), warm nights (c,d), cool days (e,f) and warm days (g,h) for Indonesia over the period 1960 to 2003 relative to 1961-1990 from HadEX (Alexander et al. 2006). a,c,e,g) Grid box decadal trends. Grid boxes outlined in solid black contain at least 3 stations and so are likely to be more representative of the wider grid-box. Trends are fitted using the median of pairwise slopes method (Sen 1968, Lanzante 1996). Higher confidence in a long-term trend is shown by a black dot if the 5th to 95th percentile slopes are of the same sign. Differences in spatial coverage occur because each index has its own decorrelation length scale (see methodology section). b,d,f,h) Area averaged annual time series for 95.625 to 140.625° E, 6.25° N to 11.25° S as shown in the red box in Figure 1. Trends are fitted as described above. The decadal trend and its 5th to 95th percentile pairwise slopes are shown as well as the change over the period for which there are data. Higher confidence in the trends, as denoted above, is shown by a solid black line as opposed to a dotted one.*

19

Precipitation extremes

Precipitation extremes, either excess or deficit, can be hazardous to human health, societal infrastructure, and livestock and agriculture. While seasonal fluctuations in precipitation are normal and indeed important for a number of societal sectors (e.g. tourism, farming etc.), serious negative impacts can arise from flooding or drought. These are complex phenomena and often the result of accumulated excesses or deficits or other compounding factors such as high tides/storm surges or changes in land use. The analysis section below deals purely with precipitation amounts.

Table 1 shows selected extreme events since 1997 that are reported in WMO Statements on Status of the Global Climate and/or BAMS State of the Climate reports. The drought in association with the 1997-8 El Niño is highlighted below as an example of a recent extreme precipitation event that affected Indonesia. Floods in 2001 in association with La Niña are noted more briefly.

Year	Month	Event	Details	Source
1997	May-Oct	Drought	Severe drought. Regional deficits 400-1600mm	BAMS (Bell and Halpert, 1998)
1998-2000	Oct 1998-Dec 2000	Wet	Associated with La Niña.	WMO (2001)
2001	Feb	Flooding	Flooding (Java)	WMO (2002)
2003	Dec	Flooding	Heavy monsoon – flooding and landslides	WMO (2004)
2009	Mar	Flooding	Heavy rain	WMO (2010)

Table 1. Selected extreme precipitation events reported in WMO Statements on Status of the Global Climate and/or BAMS State of the Climate reports since 1997.

Recent extreme precipitation events

Drought, 1997 - 1998

Within the Indonesia area, a nearly complete lack of rainfall in parts of Sumatra and Borneo from mid-July 1997 through early September 1997, followed by substantially below-normal rainfall during the next three months, contributed to extensive wildfires and an ecological disaster (Bell et al., 1999). Although dry-season burning takes place each year to clear land for planting crops, these fires during 1997 quickly created an ecological disaster as they burned out of control due to large-scale drought. By mid-August large areas of tropical rain forest were completely engulfed. In the following three months, uncontrolled fires destroyed massive areas of tropical rain forest. Vast areas of smoke from the fires reduced visibility at times to less than 100 m, and caused serious respiratory problems hundreds of kilometres away from the smoke sources. The smoke also hindered, and sometimes completely stopped, traffic by land, sea, and air, and was a primary factor in several serious accidents. A large part of the country suffered from the severe drought, resulting in crop losses and malnutrition (Bell and Halpert, 1998).

Flooding event in 2001

Above-normal annual rainfall occurred in 2001 in association with La Niña (Waple et al.,2002). In February 2001, at least 100 people were killed in floods and landslips after several days of rain on the Indonesia island of Java. 20,000 homes and thousands of hectares of rice fields were destroyed (WMO, 2002).

Analysis of long-term features in precipitation

HadEX extremes indices (Alexander et al. 2006) are used here for Indonesia from 1960 to 2003 using daily precipitation totals. Here we discuss changes in the annual total precipitation. The methods are fully described in the methodology section.

There are few data available for the Indonesian archipelago and so spatial coverage is limited to Sumatra and Borneo. Also, the decorrelation length scales are short for precipitation and over this region in particular. Hence, there are very few grid-boxes with data and so very little can be said about precipitation between 1960 and 2003 (Figure 4) using the HadEX dataset. There is a mixed signal for total annual precipitation with sporadic

high confidence in decreasing precipitation totals for two grid-boxes. Regional averages are inconclusive. Other research suggests a slight decrease in precipitation over recent decades (Christensen et al. 2007).
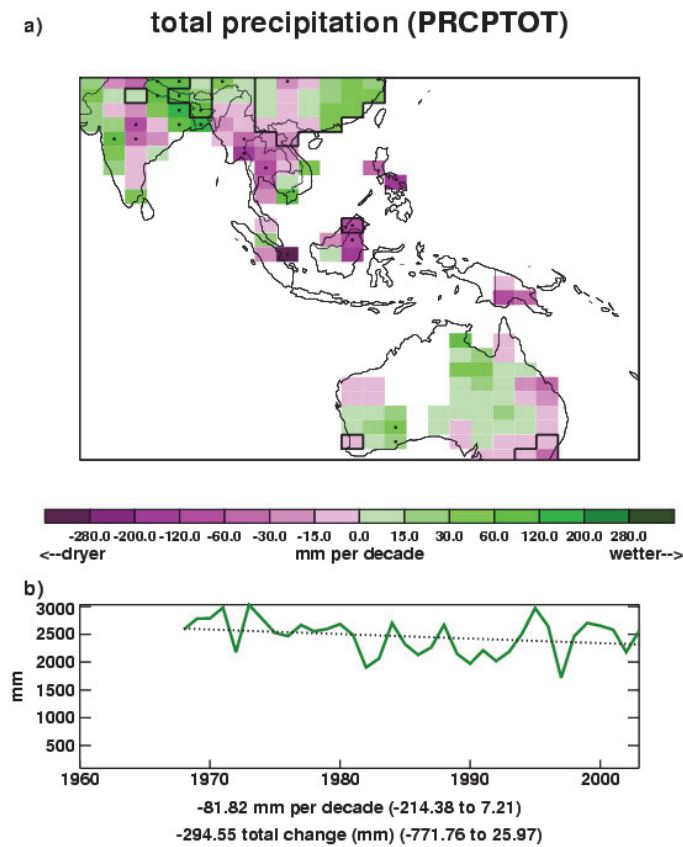
Figure 4. *Total annual precipitation for Indonesia over the period 1960 to 2003 relative to 1961-1990 from HadEX (Alexander et al. 2006). a) Decadal trends as described in Figure 3. b) Area average annual time series for 95.625 to 140.625 ° E, 6.25 ° N to 11.25 ° S as described in Figure 3.*

Summary

The main features seen in observed climate over Indonesia from this analysis are:

- Limited observational data is available over the Indonesian archipelago but where data are present over the period 1960 to 2010, there has been a warming trend.

- Over Sumatra and Borneo, where daily temperature data are available, there has been a trend between the late 1960s and 2003 towards fewer cool nights and more warm nights and warm days.

Methodology annex

Recent, notable extremes

In order to identify what is meant by 'recent' events the authors have used the period since 1994, when WMO Status of the Global Climate statements were available to the authors. However, where possible, the most notable events during the last 10 years have been chosen as these are most widely reported in the media, remain closest to the forefront of the memory of the country affected, and provide an example likely to be most relevant to today's society. By 'notable' the authors mean any event which has had significant impact either in terms of cost to the economy, loss of life, or displacement and long term impact on the population. In most cases the events of largest impact on the population have been chosen, however this is not always the case.

Tables of recent, notable extreme events have been provided for each country. These have been compiled using data from the World Meteorological Organisation (WMO) Annual Statements on the Status of the Global Climate. This is a yearly report which includes contributions from all the member countries, and therefore represents a global overview of events that have had importance on a national scale. The report does not claim to capture all events of significance, and consistency across the years of records available is variable. However, this database provides a concise yet broad account of extreme events per country. This data is then supplemented with accounts from the monthly National Oceanic and Atmospheric Administration (NOAA) State of the Climate reports which outline global extreme events of meteorological significance.

We give detailed examples of heat, precipitation and storm extremes for each country where these have had significant impact. Where a country is primarily affected by precipitation or heat extremes this is where our focus has remained. An account of the impact on human life, property and the economy has been given, based largely on media reporting of events, and official reports from aid agencies, governments and meteorological organisations. Some data has also been acquired from the Centre for Research on Epidemiological Disasters (CRED) database on global extreme events. Although media reports are unlikely to be completely accurate, they do give an indication as to the perceived impact of an extreme event, and so are useful in highlighting the events which remain in the national psyche.

Our search for data has not been exhaustive given the number of countries and events included. Although there are a wide variety of sources available, for many events, an official account is not available. Therefore figures given are illustrative of the magnitude of impact only (references are included for further information on sources). It is also apparent that the reporting of extreme events varies widely by region, and we have, where possible, engaged with local scientists to better understand the impact of such events.

The aim of the narrative for each country is to provide a picture of the social and economic vulnerability to the current climate. Examples given may illustrate the impact that any given extreme event may have and the recovery of a country from such an event. This will be important when considering the current trends in climate extremes, and also when examining projected trends in climate over the next century.

Observational record

In this section we outline the data sources which were incorporated into the analysis, the quality control procedure used, and the choices made in the data presentation. As this report is global in scope, including 23 countries, it is important to maintain consistency of methodological approach across the board. For this reason, although detailed datasets of extreme temperatures, precipitation and storm events exist for various countries, it was not possible to obtain and incorporate such a varied mix of data within the timeframe of this project. Attempts were made to obtain regional daily temperature and precipitation data from known contacts within various countries with which to update existing global extremes databases. No analysis of changes in storminess is included as there is no robust historical analysis of global land surface winds or storminess currently available.

Analysis of seasonal mean temperature

Mean temperatures analysed are obtained from the CRUTEM3 global land-based surface-temperature data-product (Brohan et al. 2006), jointly created by the Met Office Hadley Centre and Climatic Research Unit at the University of East Anglia. CRUTEM3 comprises of more than 4000 weather station records from around the world. These have been averaged together to create 5° by 5° gridded fields with no interpolation over grid boxes that do not contain stations. Seasonal averages were calculated for each grid box for the 1960 to 2010 period and linear trends fitted using the median of pairwise slopes (Sen 1968; Lanzante 1996). This method finds the slopes for all possible pairs of points in the data, and takes

their median. This is a robust estimator of the slope which is not sensitive to outlying points. High confidence is assigned to any trend value for which the 5th to 95th percentiles of the pairwise slopes are of the same sign as the trend value and thus inconsistent with a zero trend.

Analysis of temperature and precipitation extremes using indices

In order to study extremes of climate a number of indices have been created to highlight different aspects of severe weather. The set of indices used are those from the World Climate Research Programme (WCRP) Climate Variability and Predictability (CLIVAR) Expert Team on Climate Change Detection and Indices (ETCCDI). These 27 indices use daily rainfall and maximum and minimum temperature data to find the annual (and for a subset of the indices, monthly) values for, e.g., the 'warm' days where daily maximum temperature exceeds the 90th percentile maximum temperature as defined over a 1961 to 1990 base period. For a full list of the indices we refer to the website of the ETCCDI (http://cccma.seos.uvic.ca/ETCCDI/index.shtml).

Index	Description	Shortname	Notes
Cool night frequency	Daily minimum temperatures lower than the 10th percentile daily minimum temperature using the base reference period 1961-1990	TN10p	---
Warm night frequency	Daily minimum temperatures higher than the 90th percentile daily minimum temperature using the base reference period 1961-1990	TN90p	---
Cool day frequency	Daily maximum temperatures lower than the 10th percentile daily maximum temperature using the base reference period 1961-1990	TX10p	---
Warm day frequency	Daily maximum temperatures higher than the 90th percentile daily maximum temperature using the base reference period 1961-1990	TX90p	---
Dry spell duration	Maximum duration of continuous days within a year with rainfall <1mm	CDD	Lower data coverage due to the requirement for a 'dry spell' to be at least 6 days long resulting in intermittent temporal coverage
Wet spell duration	Maximum duration of continuous days with rainfall >1mm for a given year	CWD	Lower data coverage due to the requirement for a 'wet spell' to be at least 6 days long resulting in intermittent temporal coverage
Total annual precipitation	Total rainfall per year	PRCPTOT	---

Table 2. *Description of ETCCDI indices used in this document.*

A previous global study of the change in these indices, containing data from 1951-2003 can be found in Alexander et al. 2006, (HadEX; see http://www.metoffice.gov.uk/hadobs/hadex/). In this work we aimed to update this analysis to the present day where possible, using the most recently available data. A subset of the indices is used here because they are most easily related to extreme climate events (Table 2).

Use of HadEX for analysis of extremes

The HadEX dataset comprises all 27 ETCCDI indices calculated from station data and then smoothed and gridded onto a 2.5° x 3.75° grid, chosen to match the output from the Hadley Centre suite of climate models. To update the dataset to the present day, indices are calculated from the individual station data using the RClimDex/FClimDex software; developed and maintained on behalf of the ETCCDI by the Climate Research Branch of the

Meteorological Service of Canada. Given the timeframe of this project it was not possible to obtain sufficient station data to create updated HadEX indices to present day for a number of countries: Brazil; Egypt; Indonesia; Japan (precipitation only); South Africa; Saudi Arabia; Peru; Turkey; and Kenya. Indices from the original HadEX data-product are used here to show changes in extremes of temperature and precipitation from 1960 to 2003. In some cases the data end prior to 2003. Table 3 summarises the data used for each country. Below, we give a short summary of the methods used to create the HadEX dataset (for a full description see Alexander et al., 2006).

To account for the uneven spatial coverage when creating the HadEX dataset, the indices for each station were gridded, and a land-sea mask from the HadCM3 model applied. The interpolation method used in the gridding process uses a decorrelation length scale (DLS) to determine which stations can influence the value of a given grid box. This DLS is calculated from the e-folding distance of the individual station correlations. The DLS is calculated separately for five latitude bands, and then linearly interpolated between the bands. There is a noticeable difference in spatial coverage between the indices due to these differences in decorrelation length scales. This means that there will be some grid-box data where in fact there are no stations underlying it. Here we apply black borders to grid-boxes where at least 3 stations are present to denote greater confidence in representation of the wider grid-box area there. The land-sea mask enables the dataset to be used directly for model comparison with output from HadCM3. It does mean, however, that some coastal regions and islands over which one may expect to find a grid-box are in fact empty because they have been treated as sea.

Data sources used for updates to the HadEX analysis of extremes

We use a number of different data sources to provide sufficient coverage to update as many countries as possible to present day. These are summarised in Table 3. In building the new datasets we have tried to use exactly the same methodology as was used to create the original HadEX to retain consistency with a product that was created through substantial international effort and widely used, but there are some differences, which are described in the next section.

Wherever new data have been used, the geographical distributions of the trends were compared to those obtained from HadEX, using the same grid size, time span and fitting method. If the pattern of the trends in the temperature or precipitation indices did not match that from HadEX, we used the HadEX data despite its generally shorter time span. Differences in the patterns of the trends in the indices can arise because the individual

stations used to create the gridded results are different from those in HadEX, and the quality control procedures used are also very likely to be different. Countries where we decided to use HadEX data despite the existence of more recent data are Egypt and Turkey.

GHCND:

The Global Historical Climate Network Daily data has near-global coverage. However, to ensure consistency with the HadEX database, the GHCND stations were compared to those stations in HadEX. We selected those stations which are within 1500m of the stations used in the HadEX database and have a high correlation with the HadEX stations. We only took the precipitation data if its r>0.9 and the temperature data if one of its r-values >0.9. In addition, we required at least 5 years of data beyond 2000. These daily data were then converted to the indices using the *fclimdex* software.

ECA&D and SACA&D:

The European Climate Assessment and Dataset and the Southeast Asian Climate Assessment and Dataset data are pre-calculated indices comprising the core 27 indices from the ETCCDI as well as some extra ones. We kindly acknowledge the help of Albert Klein Tank, the KNMI[1] and the BMKG[2] for their assistance in obtaining these data.

Mexico:

The station data from Mexico has been kindly supplied by the SMN[3] and Jorge Vazquez. These daily data were then converted to the required indices using the *Fclimdex* software. There are a total of 5298 Mexican stations in the database. In order to select those which have sufficiently long data records and are likely to be the most reliable ones we performed a cross correlation between all stations. We selected those which had at least 20 years of data post 1960 and have a correlation with at least one other station with an *r*-value >0.95. This resulted in 237 stations being selected for further processing and analysis.

Indian Gridded:

The India Meteorological Department provided daily gridded data (precipitation 1951-2007, temperature 1969-2009) on a 1° x 1° grid. These are the only gridded daily data in our analysis. In order to process these in as similar a way as possible the values for each grid

---

[1] Koninklijk Nederlandsch Meteorologisch Instituut – The Royal Netherlands Meteorological Institute

[2] Badan Meteorologi, Klimatologi dan Geofisika – The Indonesian Meteorological, Climatological and Geophysical Agency

[3] Servicio Meteorológico Nacional de México – The Mexican National Meteorological Service

were assumed to be analogous to a station located at the centre of the grid. We keep these data separate from the rest of the study, which is particularly important when calculating the decorrelation length scale, which is on the whole larger for these gridded data.

Country	Region box (red dashed boxes in Fig. 1 and on each map at beginning of chapter)	Data source (T = temperature, P = precipitation)	Period of data coverage (T = temperature, P = precipitation)	Indices included (see Table 2 for details)	Temporal resolution available	Notes
Argentina	73.125 to 54.375 ° W, 21.25 to 56.25 ° S	Matilde Rusticucci (T,P)	1960-2010 (T,P)	TN10p, TN90p, TX10p, TX90p, PRCPTOT, CDD, CWD	annual	
Australia	114.375 to 155.625 ° E, 11.25 to 43.75 ° S	GHCND (T,P)	1960-2010 (T,P)	TN10p, TN90p, TX10p, TX90p, PRCPTOT, CDD, CWD	monthly, seasonal and annual	Land-sea mask has been been adapted to include Tasmania and the area around Brisbane
Bangladesh	88.125 to 91.875 ° E, 21.25 to 26.25 ° N	Indian Gridded data (T,P)	1960-2007 (P), 1970-2009 (T)	TN10p, TN90p, TX10p, TX90p, PRCPTOT, CDD, CWD	monthly, seasonal and annual	Interpolated from Indian Gridded data
Brazil	73.125 to 31.875 ° W, 6.25 ° N to 33.75 ° S	HadEX (T,P)	1960-2000 (P) 2002 (T)	TN10p, TN90p, TX10p, TX90p, PRCPTOT, CDD, CWD	annual	Spatial coverage is poor
China	73.125 to 133.125 ° E, 21.25 to 53.75 ° N	GHCND (T,P)	1960-1997 (P) 1960-2003 (T_{min}) 1960-2010 (T_{max})	TN10p, TN90p, TX10p, TX90p, PRCPTOT, CDD, CWD	monthly, seasonal and annual	Precipitation has very poor coverage beyond 1997 except in 2003-04, and no data at all in 2000-02, 2005-11
Egypt	24.375 to 35.625 ° E, 21.25 to 31.25 ° N	HadEX (T,P)	No data	TN10p, TN90p, TX10p, TX90p, PRCPTOT,	annual	There are no data for Egypt so all grid-box values have been interpolated from stations in Jordan, Israel, Libya and Sudan
France	5.625 ° W to 9.375 ° E, 41.25 to 51.25 ° N	ECA&D (T,P)	1960-2010 (T,P)	TN10p, TN90p, TX10p, TX90p, PRCPTOT, CDD, CWD	monthly, seasonal and annual	

Country	Coordinates	Source	Time period	Indices	Temporal resolution	Notes
Germany	5.625 to 16.875 °E, 46.25 to 56.25 °N	ECA&D (T,P)	1960-2010 (T,P)	TN10p, TN90p, TX10p, TX90p, PRCPTOT, CDD, CWD	monthly, seasonal and annual	
India	69.375 to 99.375 °E, 6.25 to 36.25 °N	Indian Gridded data (T,P)	1960-2003 (P), 1970-2009 (T)	TN10p, TN90p, TX10p, TX90p, PRCPTOT, CDD, CWD	monthly, seasonal and annual	
Indonesia	95.625 to 140.625 °E, 6.25 °N to 11.25 °S	HadEX (T,P)	1968-2003 (T,P)	TN10p, TN90p, TX10p, TX90p, PRCPTOT,	annual	Spatial coverage is poor
Italy	5.625 to 16.875 °E, 36.25 to 46.25 °N	ECA&D (T,P)	1960-2010 (T,P)	TN10p, TN90p, TX10p, TX90p, PRCPTOT, CDD, CWD	monthly, seasonal and annual	Land-sea mask has been adapted to improve coverage of Italy
Japan	129.375 to 144.375 °E, 31.25 to 46.25 °N	HadEX (P) GHCND (T)	1960-2003 (P) 1960-2000 (T_{min}) 1960-2010 (T_{max})	TN10p, TN90p, TX10p, TX90p, PRCPTOT,	monthly, seasonal and annual (T), annual (P)	
Kenya	31.875 to 43.125 °E, 6.25 °N to 6.25 °S	HadEX (T,P)	1960-1999 (P)	TN10p, TN90p, TX10p, TX90p, PRCPTOT	annual	There are no temperature data for Kenya and so grid-box values have been interpolated from neighbouring Uganda and the United Republic of Tanzania. Regional averages include grid-boxes from outside Kenya that enable continuation to 2003
Mexico	118.125 to 88.125 °W, 13.75 to 33.75 °N	Raw station data from the Servicio Meteorológico Nacional (SMN) (T,P)	1960-2009 (T,P)	TN10p, TN90p, TX10p, TX90p, PRCPTOT, CDD, CWD	monthly, seasonal and annual	237/5298 stations selected. Non uniform spatial coverage. Drop in T and P coverage in 2009.
Peru	84.735 to 65.625 °W, 1.25 °N to 18.75 °S	HadEX (T,P)	1960-2002 (T,P)	TN10p, TN90p, TX10p, TX90p, PRCPTOT, CDD, CWD	annual	Intermittent coverage in TX90p, CDD and CWD

Country					
Russia	ECA&D (T,P)	West Russia 28.125 to 106.875 °E, 43.75 to 78.75 °N, East Russia 103.125 to 189.375 °E, 43.75 to 78.75 °N	1960-2010 (T,P)	TN10p, TN90p, TX10p, TX90p, PRCPTOT, CDD, CWD	monthly, seasonal and annual	Country split for presentation purposes only.
Saudi Arabia	HadEX (T,P)	31.875 to 54.375 °E, 16.25 to 33.75 °N	1960-2000 (T,P)	TN10p, TN90p, TX10p, TX90p, PRCPTOT	annual	Spatial coverage is poor
South Africa	HadEX (T,P)	13.125 to 35.625 °E, 21.25 to 36.25 °S	1960-2000 (T,P)	TN10p, TN90p, TX10p, TX90p, PRCPTOT, CDD, CWD	annual	---
Republic of Korea	HadEX (T,P)	125.625 to 129.375 °E, 33.75 to 38.75 °N	1960-2003 (T,P)	TN10p, TN90p, TX10p, TX90p, PRCPTOT, CDD	annual	There are too few data points for CWD to calculate trends or regional timeseries
Spain	ECA&D (T,P)	9.375 °W to 1.875 °E, 36.25 to 43.75 °N	1960-2010 (T,P)	TN10p, TN90p, TX10p, TX90p, PRCPTOT, CDD, CWD	monthly, seasonal and annual	
Turkey	HadEX (T,P)	24.375 to 46.875 °E, 36.25 to 43.75 °N	1960-2003 (T,P)	TN10p, TN90p, TX10p, TX90p, PRCPTOT, CDD, CWD	annual	Intermittent coverage in CWD and CDD with no regional average beyond 2000
United Kingdom	ECA&D (T,P)	9.375 °W to 1.875 °E, 51.25 to 58.75 °N	1960-2010 (T,P)	TN10p, TN90p, TX10p, TX90p, PRCPTOT, CDD, CWD	monthly, seasonal and annual	
United States of America	GHCND (T,P)	125.625 to 65.625 °W, 23.75 to 48.75 °N	1960-2010 (T,P)	TN10p, TN90p, TX10p, TX90p, PRCPTOT, CDD, CWD	monthly, seasonal and annual	

Table 3. Summary of data used for each country

Quality control and gridding procedure used for updates to the HadEX analysis of extremes

In order to perform some basic quality control checks on the index data, we used a two-step process on the indices. Firstly, internal checks were carried out, to remove cases where the 5 day rainfall value is less than the 1 day rainfall value, the minimum T_min is greater than the minimum T_max and the maximum T_min is greater than the maximum T_max. Although these are physically impossible, they could arise from transcription errors when creating the daily dataset, for example, a misplaced minus sign, an extra digit appearing in the record or a column transposition during digitisation. During these tests we also require that there are at least 20 years of data in the period of record for the index for that station, and that some data is found in each decade between 1961 and 1990, to allow a reasonable estimation of the climatology over that period.

Weather conditions are often similar over many tens of kilometres and the indices calculated in this work are even more coherent. The correlation coefficient between each station-pair combination in all the data obtained is calculated for each index (and month where appropriate), and plotted as a function of the separation. An exponential decay curve is fitted to the data, and the distance at which this curve has fallen by a factor 1/e is taken as the decorrelation length scale (DLS). A DLS is calculated for each dataset separately. For the GHCND, a separate DLS is calculated for each hemisphere. We do not force the fitted decay curve to show perfect correlation at zero distance, which is different to the method employed when creating HadEX. For some of the indices in some countries, no clear decay pattern was observed in some data sets or the decay was so slow that no value for the DLS could be determined. In these cases a default value of 200km was used.

We then perform external checks on the index data by comparing the value for each station with that of its neighbours. As the station values are correlated, it is therefore likely that if one station measures a high value for an index for a given month, its neighbours will also be measuring high. We exploit this coherence to find further bad values or stations as follows. Although raw precipitation data shows a high degree of localisation, using indices which have monthly or annual resolution improves the coherence across wider areas and so this neighbour checking technique is a valid method of finding anomalous stations.

We calculate a climatology for each station (and month if appropriate) using the mean value for each index over the period 1961-1990. The values for each station are then anomalised using this climatology by subtracting this mean value from the true values, so that it is clear if the station values are higher or lower than normal. This means that we do not need to take

differences in elevation or topography into account when comparing neighbours, as we are not comparing actual values, but rather deviations from the mean value.

All stations which are within the DLS distance are investigated and their anomalised values noted. We then calculate the weighted median value from these stations to take into account the decay in the correlation with increasing distance. We use the median to reduce the sensitivity to outliers.

If the station value is greater than 7.5 median-absolute-deviations away from the weighted median value (this corresponds to about 5 standard deviations if the distribution is Gaussian, but is a robust measure of the spread of the distribution), then there is low confidence in the veracity of this value and so it is removed from the data.

To present the data, the individual stations are gridded on a 3.75^o x 2.5^o grid, matching the output from HadCM3. To determine the value of each grid box, the DLS is used to calculate which stations can reasonably contribute to the value. The value of each station is then weighted using the DLS to obtain a final grid box value. At least three stations need to have valid data and be near enough (within 1 DLS of the gridbox centre) to contribute in order for a value to be calculated for the grid point. As for the original HadEX, the HadCM3 land-sea mask is used. However, in three cases the mask has been adjusted as there are data over Tasmania, eastern Australia and Italy that would not be included otherwise (Figure 5).
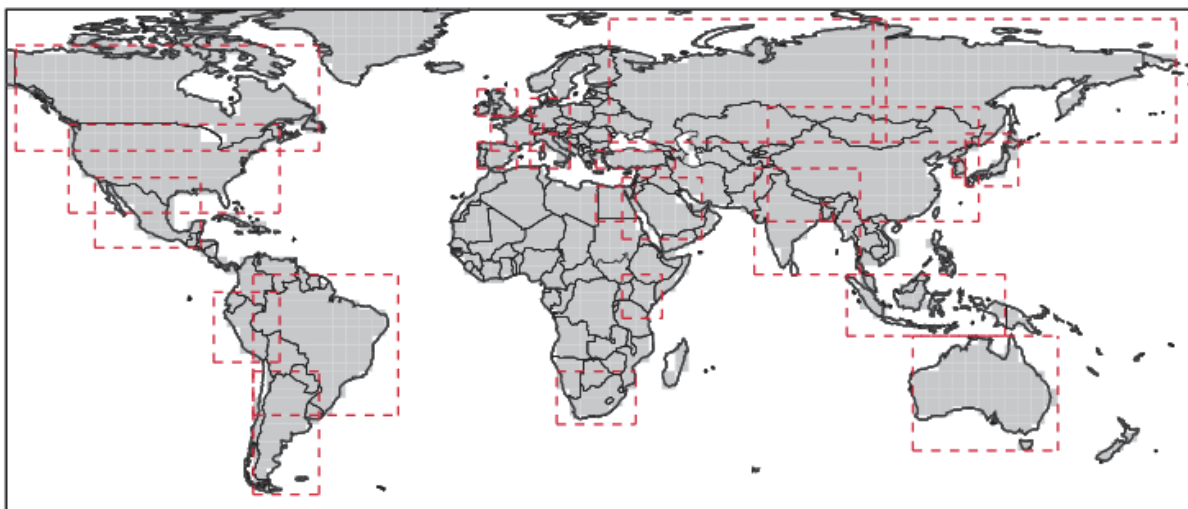
Figure 5. Land-sea mask used for gridding the station data and regional areas allocated to each country as described in Table 3.

Presentation of extremes of temperature and precipitation

Indices are displayed as regional gridded maps of decadal trends and regional average time-series with decadal trends where appropriate. Trends are fitted using the median of pairwise slopes method (Sen 1968, Lanzante 1996). Trends are considered to be significantly different from a zero trend if the 5th to 95th percentiles of the pairwise slopes do not encompass zero. This is shown by a black dot in the centre of the grid-box or by a solid line on time-series plots. This infers that there is high confidence in the sign (positive or negative) of the sign. Confidence in the trend magnitude can be inferred by the spread of the 5th to 95th percentiles of the pairwise slopes which is given for the regional average decadal trends. Trends are only calculated when there are data present for at least 50% of years in the period of record and for the updated data (not HadEX) there must be at least one year in each decade.

Due to the practice of data-interpolation during the gridding stage (using the DLS) there are values for some grid boxes when no actually station lies within the grid box. There is more confidence in grid boxes for which there are underlying data. For this reason, we identify those grid boxes which contain at least 3 stations by a black contour line on the maps. The DLS differs with region, season and index which leads to large differences in the spatial coverage. The indices, by their nature of being largely threshold driven, can be intermittent over time which also effects spatial and temporal coverage (see Table 2).

Each index (and each month for the indices for which there is monthly data) has a different DLS, and so the coverage between different indices and datasets can be different. The restrictions on having at least 20 years of data present for each input station, at least 50% of years in the period of record and at least one year in each decade for the trending calculation, combined with the DLS, can restrict the coverage to only those regions with a dense station network reporting reliably.

Each country has a rectangular region assigned as shown by the red dashed box on the map in Figure 1 and listed in Table 2, which is used for the creation of the regional average. This is sometimes identical to the attribution region shown in grey on the map in Figure 1. This region is again shown on the maps accompanying the time series of the regional averages as a reminder of the region and grid boxes used in the calculation. Regional averages are created by weighting grid box values by the cosine of their grid box centre latitude. To ensure consistency over time a regional average is only calculated when there are a sufficient number of grid boxes present. The full-period median number of grid-boxes present is calculated. For regions with a median of more than six grid-boxes there must be at

least 80% of the median number of grid boxes present for any one year to calculate a regional average. For regions with six or fewer median grid boxes this is relaxed to 50%. These limitations ensure that a single station or grid box which has a longer period of record than its neighbours cannot skew the timeseries trend. So sometimes there may be grid-boxes present but no regional average time series. The trends for the regional averages are calculated in the same way as for the individual grid boxes, using the median of pairwise slopes method (Sen 1968, Lanzante 1996). Confidence in the trend is also determined if the 5th to 95th percentiles of the pairwise slopes are of the same sign and thus inconsistent with a zero trend. As well as the trend in quantity per decade, we also show the full change in the quantity from 1960 to 2010 that this fitted linear trend implies.

Warm Nights (TN90p)

days/10yr
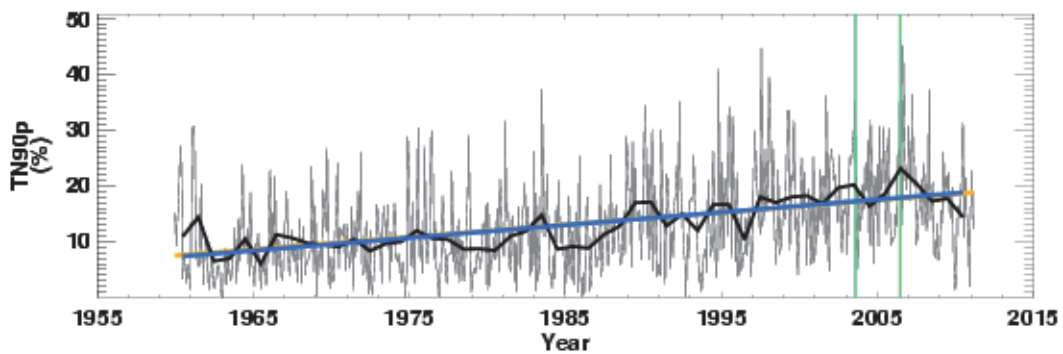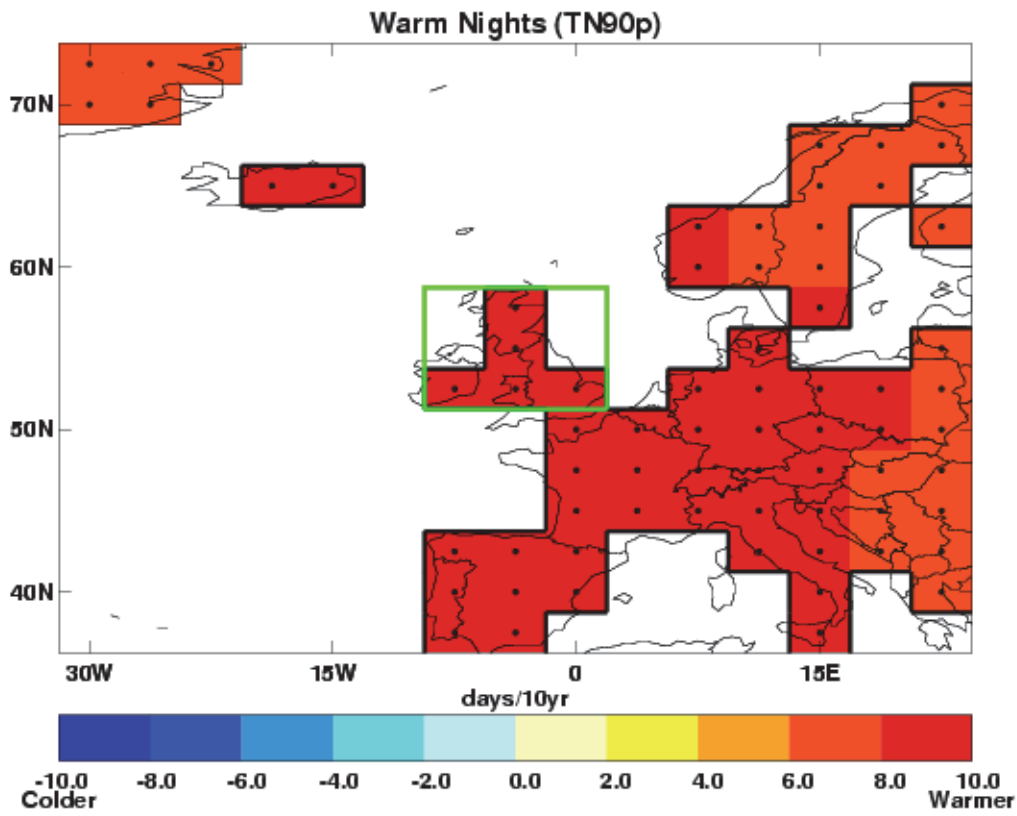
Monthly: 2.20% per decade (1.80 to 2.61)
Total change of 11.02% from 1960 to 2011 (9.00% to 13.06%)

Annual: 2.28% per decade (1.69 to 2.86)
Total change of 11.41% from 1960 to 2010 (8.43% to 14.28%)
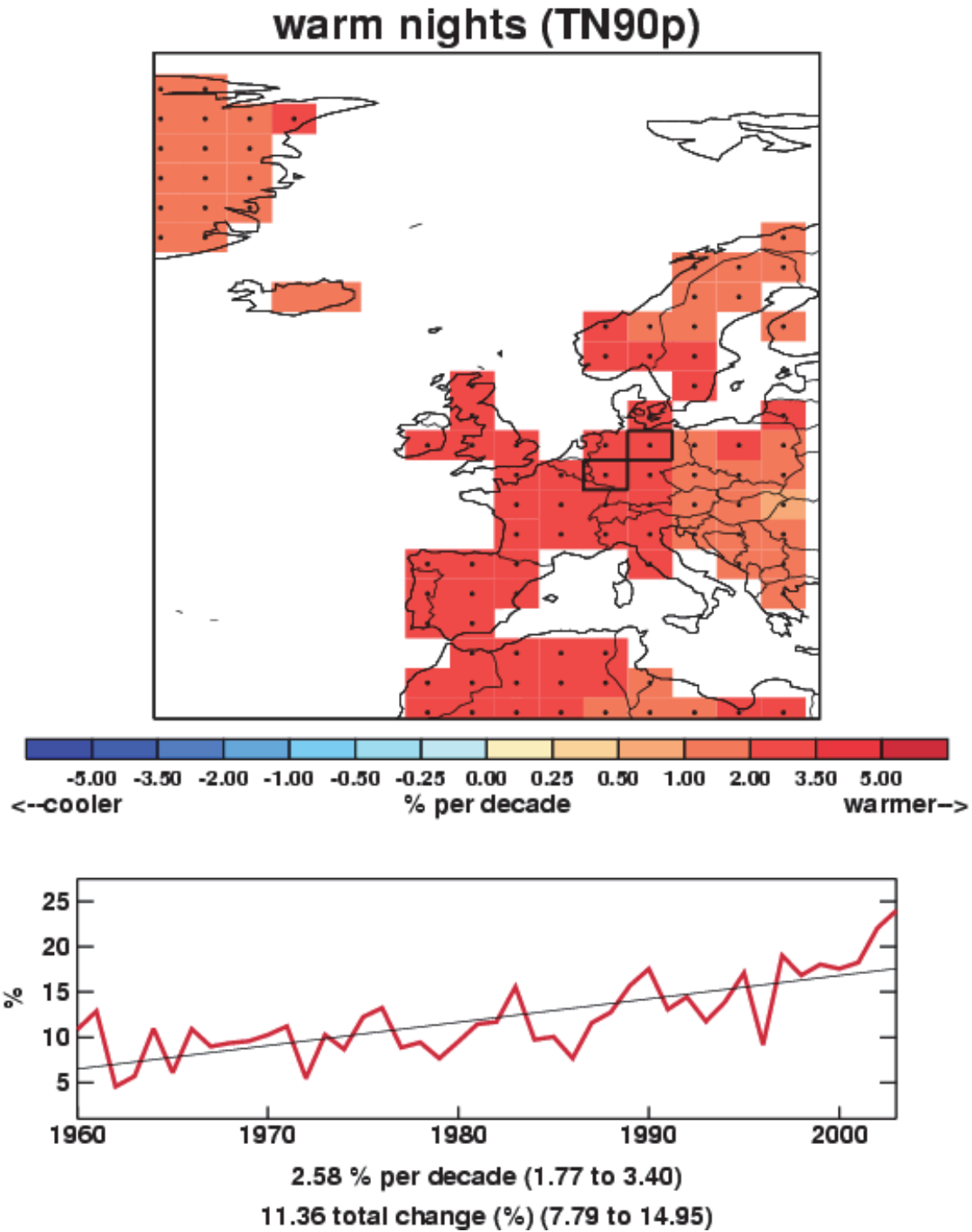
Figure 6. *Examples of the plots shown in the data section. Left: From ECA&D data between 1960-2010 for the number of warm nights, and Right: from HadEX data (1960-2003) for the total precipitation. A full explanation of the plots is given in the text below.*

The results are presented in the form of a map and a time series for each country and index.

The map shows the grid box decadal trend in the index over the period for which there are

data. High confidence, as determined above, is shown by a black dot in the grid box centre.

To show the variation over time, the values for each year (and month if available) are shown

in a time series for a regional average. The values of the indices have been normalised to a

39

base period of 1961-1990 (except the Indian gridded data which use a 1971 to 1990 period), both in HadEX and in the new data acquired for this project. Therefore, for example, the percentage of nights exceeding the 90th percentile for a temperature is 10% for that period.

There are two influences on whether a grid box contains a value or not – the land-sea mask, and the decorrelation length scale. The land-sea mask is shown in Figure 5. There are grid boxes which contain some land but are mostly sea and so are not considered. The decorrelation length scale sets the maximum distance a grid box can be from stations before no value is assigned to it. Grid boxes containing three or more stations are highlighted by a thick border. This indicates regions where the value shown is likely to be more representative of the grid box area mean as opposed to a single station location.

On the maps for the new data there is a box indicating which grid boxes have been extracted to calculate the area average for the time series. This box is the same as shown in Figure 1 at the beginning of each country's document. These selected grid boxes are combined using area (cosine) weighting to calculate the regional average (both annual [thick lines] and monthly [thin lines] where available). Monthly (orange) and annual (blue) trends are fitted to these time series using the method described above. The decadal trend and total change over the period where there are data are shown with 5th to 95th percentile confidence intervals in parentheses. High confidence, as determined above, is shown by a solid line as opposed to a dotted one. The green vertical lines on the time series show the dates of some of the notable events outlined in each section.

Attribution

Regional distributions of seasonal mean temperatures in the 2000s are computed with and without the effect of anthropogenic influences on the climate. The analysis considers temperatures averaged over the regions shown in Figure 7. These are also identified as grey boxes on the maps in Figure 1. The coordinates of the regions are given in Table 4. The methodology combines information from observations and model simulations using the approach originally introduced in Christidis et al., 2010 and later extended in Christidis et al., 2011, where more details can be found. The analysis requires spatial scales greater than about 2,500 km and for that reason the selected regions (Fig.7 and Table 4) are often larger than individual countries, or include several smaller countries in a single region (for example UK, Germany and France are grouped in one region).

Observations of land temperature come from the CRUTEM3 gridded dataset (Brohan et al., 2006) and model simulations from two coupled GCMs, namely the Hadley Centre HadGEM1 model (Martin et al., 2006) and version 3.2 of the MIROC model (K-1 Developers, 2004). The use of two GCMs helps investigate the sensitivity of the results to the model used in the analysis. Ensembles of model simulations from two types of experiments are used to partition the temperature response to external forcings between its anthropogenic and natural components. The first experiment (ALL) simulates the combined effect of natural and anthropogenic forcings on the climate system and the second (ANTHRO) includes anthropogenic forcings only. The difference of the two gives an estimate of the effect of the natural forcings (NAT). Estimates of the effect of internal climate variability are derived from long control simulations of the unforced climate. Distributions of the regional summer mean temperature are computed as follows:

a) A global optimal fingerprinting analysis (Allen and Tett, 1999; Allen and Stott, 2003) is first carried out that scales the global simulated patterns (fingerprints) of climate change attributed to different combinations of external forcings to best match them to the observations. The uncertainty in the scaling that originates from internal variability leads to samples of the scaled fingerprints, i.e. several realisations that are plausibly consistent with the observations. The 2000-2009 decade is then extracted from the scaled patterns and two samples of the decadal mean temperature averaged over the reference region are then computed with and without human influences, which provide the Probability Density Functions (PDFs) of the decadal mean temperature attributable to ALL and NAT forcings.

b) Model-derived estimates of noise are added to the distributions to take into account the uncertainty in the simulated fingerprints.

c) In the same way, additional noise from control model simulations is introduced to the distributions to represent the effect of internal variability in the annual values of the seasonal mean temperatures. The result is a pair of estimated distributions of the annual values of the seasonal mean temperature in the region with and without the effect of human activity on the climate. The temperatures throughout the analysis are expressed as anomalies relative to period 1961-1990.
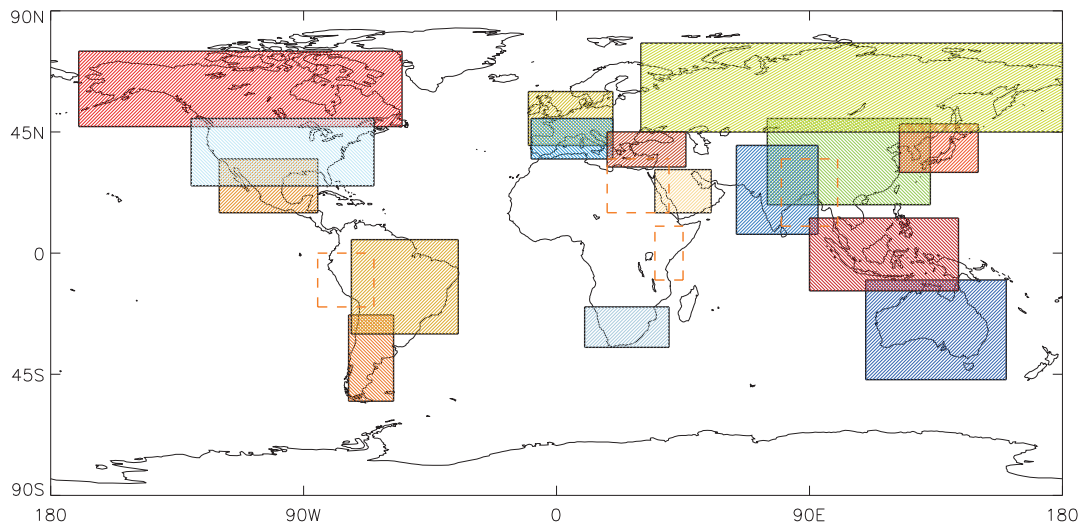
Figure 7. The regions used in the attribution analysis. Regions marked with dashed orange boundaries correspond to non-G20 countries that were also included in the analysis.

Region	Region Coordinates
Argentina	74-58W, 55-23S
Australia	110-160E, 47-10S
Bangladesh	80-100E, 10-35N
Brazil	73-35W, 30S-5N
Canada-Alaska	170-55W, 47-75N
China	75-133E, 18-50N
Egypt	18-40E, 15-35N
France-Germany-UK	10W-20E, 40-60N
India	64-93E, 7-40N
Indonesia	90-143E, 14S-13N
Italy-Spain	9W-20E, 35-50N
Japan-Republic of Korea	122-150E, 30-48N
Kenya	35-45E, 10S-10N
Mexico	120-85W, 15-35N
Peru	85-65W, 20-0S
Russia	30-185E, 45-78N
Saudi Arabia	35-55E, 15-31N
South Africa	10-40E, 35-20S
Turkey	18-46E, 32-45N

Table 4. The coordinates of the regions used in the attribution analysis.

References

ALDHOUS, P. 2004. Borneo is burning. *Nature* 432, 144-146.

ALEXANDER, L. V., ZHANG. X., PETERSON, T. C., CAESAR, J., GLEASON, B., KLEIN TANK, A. M. G., HAYLOCK, M., COLLINS, D., TREWIN, B., RAHIMZADEH, F., TAGIPOUR, A., RUPA KUMAR, K., REVADEKAR, J., GRIFFITHS, G., VINCENT, L., STEPHENSON, D. B., BURN, J., AGUILAR, E., BRUNET, M., TAYLOR, M., NEW, M., ZHAI, P., RUSTICUCCI, M. AND VAZQUEZ-AGUIRRE, J. L. 2006. Global observed changes in daily climate extremes of temperature and precipitation. *J. Geophys. Res*. 111, D05109. doi:10.1029/2005JD006290.

ALLEN, M. R., TETT S. F. B. 1999. Checking for model consistency in optimal fingerprinting. Clim Dyn 15: 419-434.

ALLEN M. R., STOTT P. A. 2003. Estimating signal amplitudes in optimal fingerprinting, part I: theory. Clim Dyn 21: 477-491.

BELL, G.D., AND HALPERT, M.S. 1998. Climate Assessment for 1997. *Bulletin of the American Meteorological Society* **79**, 5, S1-S50.

BELL, G.D., HALPERT, M.S., ROPELEWSKI, C.F., KOUSKY, V.E., DOUGLAS, A.V., SCHNELL, R.C., GELMAN, M.E. 1999. Climate Assessment for 1998. *Bulletin of the American Meteorological Society* **80**, 5, S1-S48.

BROHAN, P., KENNEDY, J.J., HARRIS, I., TETT, S.F.B. AND JONES, P.D. 2006. Uncertainty estimates in regional and global observed temperature changes: a new dataset from 1850. *J. Geophys. Res*. 111, D12106. doi:10.1029/2005JD006548.

CHRISTENSEN, J.H., HEWITSON, B., BUSUIOC, A., CHEN, A., GAO, X., HELD, I., JONES, R., KOLLI, R.K., KWON, W.-T., LAPRISE, R., MAGANA RUEDA, V., MEARNS, L., MENENDEZ, C.G., RÄISÄNEN, J., RINKE, A., SARR, A. AND WHETTON, P. 2007. Regional Climate Projections in *Climate Change 2007: The Physical Science Basis. Contribution of Working Group I to the Fourth Assessment Report of the Intergovernmental Panel on Climate Change* Solomon, S., D. Qin, M. Manning, Z. Chen, M. Marquis, K.B. Averyt, M. Tignor and H.L. Miller (eds.). Cambridge University Press, Cambridge, United Kingdom and New York, NY, USA.

CHRISTIDIS N., STOTT. P A., ZWIERS, F. W., SHIOGAMA, H., NOZAWA, T. 2010. Probabilistic estimates of recent changes in temperature: a multi-scale attribution analysis. Clim Dyn 34: 1139-1156.

CHRISTIDIS, N., PA STOTT, FW ZWIERS, H SHIOGAMA, T NOZAWA 2011. The contribution of anthropogenic forcings to regional changes in temperature during the last decade. Clim Dyn (submitted).

K-1 MODEL DEVELOPERS (2004) K-1 coupled GCM (MIROC) description, K-1 Tech Rep, H Hasumi and S Emori (eds), Centre for Clim Sys Res, Univ of Tokyo.

LANZANTE, J. R. 1996. Resistant, robust and non-parametric techniques for the analysis of climate data: theory and examples, including applications to historical radiosonde station data. *Int. J. Clim*. 16, 1197–226.

MARTIN G.M., RINGER. M. A., POPE V. D., JONES, A., DEARDEN, C., HINTON, T. 2006. The physical properties of the atmosphere in the new Hadley Centre Global Environmental Model (HadGEM1). Part I: Model description and global climatology. J Clim 19: 1274-1301.

SANCHEZ-LUGO, A., KENNEDY, J.J. AND BERRISFORD, P. 2011. [Global Climate] Surface Temperatures in State of the Climate 2010. *Bulletin of the American Meteorological Society* 92 (6), S36-S37.

SEN, P. K. 1968. Estimates of the regression coefficient based on Kendall's tau. *J. Am. Stat. Assoc*. 63, 1379–89.

TRENBERTH, K.E., AND HOAR, T.J. 1997. El Niño and climate change. *Geophys. Res. Lett*. 24, 3057-3060.

WAPLE, A. M., LAWRIMORE, J.H., HALPERT, M.S., BELL, G.D., HIGGINS, W., LYON, B., MENNE, M.J., GLEASON, K.L., SCHNELL, R.C., CHRISTY, J.R., THIAW, W., WRIGHT, W.J., SALINGER, M.J., ALEXANDER, L., STONE, R.S., AND CAMARGO, S.J. 2002. Climate Assessment for 2001. *Bulletin of the American Meteorological Society* 83 (6), S1-S62.

WMO WORLD METEOROLOGICAL ORGANIZATION. 2001. Statement on Status of the Global Climate in 2000, WMO-No. 920.
http://www.wmo.int/pages/prog/wcp/wcdmp/statement/wmostatement_en.html

WMO WORLD METEOROLOGICAL ORGANIZATION. 2002. Statement on Status of the Global Climate in 2001, WMO-No. 940.
http://www.wmo.int/pages/prog/wcp/wcdmp/statement/wmostatement_en.html

WMO WORLD METEOROLOGICAL ORGANIZATION. 2004. Statement on Status of the Global Climate in 2003, WMO-No. 966.
http://www.wmo.int/pages/prog/wcp/wcdmp/statement/wmostatement_en.html

WMO WORLD METEOROLOGICAL ORGANIZATION. 2010. Statement on Status of the Global Climate in 2009, WMO-NO. 1055.
http://www.wmo.int/pages/prog/wcp/wcdmp/statement/wmostatement_en.html

Acknowledgements

Chapter 2 – Climate Change Projections

Introduction

Climate models are used to understand how the climate will evolve over time and typically represent the atmosphere, ocean, land surface, cryosphere, and biogeochemical processes, and solve the equations governing their evolution on a geographical grid covering the globe. Some processes are represented explicitly within climate models, large-scale circulations for instance, while others are represented by simplified parameterisations. The use of these parameterisations is sometimes due to processes taking place on scales smaller than the typical grid size of a climate model (a Global Climate Model (GCM) has a typical horizontal resolution of between 250 and 600km) or sometimes to the current limited understanding of these processes. Different climate modelling institutions use different plausible representations of the climate system, which is why climate projections for a single greenhouse gas emissions scenario differ between modelling institutes. This gives rise to "climate model structural uncertainty".

In response to a proposed activity of the World Climate Research Programme's (WCRP's; http://www.wcrp-climate.org/) Working Group on Coupled Modelling (WGCM), the Program for Climate Model Diagnosis and Intercomparison (PCMDI; http://www-pcmdi.llnl.gov/) volunteered to collect model output contributed by leading climate modelling centres around the world. Climate model output from simulations of the past, present and future climate was collected by PCMDI mostly during the years 2005 and 2006, and this archived data constitutes phase 3 of the Coupled Model Intercomparison Project (CMIP3). In part, the WGCM organised this activity to enable those outside the major modelling centres to perform research of relevance to climate scientists preparing the IPCC Fourth Assessment Report (AR4). This unprecedented collection of recent model output is commonly known as the "CMIP3 multi-model dataset". The GCMs included in this dataset are referred to regularly throughout this review, although not exclusively.

The CMIP3 multi-model ensemble has been widely used in studies of regional climate change and associated impacts. Each of the constituent models was subject to extensive testing by the contributing institute, and the ensemble has the advantage of having been constructed from a large pool of alternative model components, therefore sampling alternative structural assumptions in how best to represent the physical climate system. Being assembled on an opportunity basis, however, the CMIP3 ensemble was not designed to represent model uncertainties in a systematic manner, so it does not, in isolation, support robust estimates of the risk of different levels of future climate change, especially at a regional level.

Since CMIP3, a new (CMIP5) generation of coupled ocean-atmosphere models has been developed, which is only just beginning to be available and is being used for new projections for the IPCC Fifth Assessment Report (AR5).

These newer models typically feature higher spatial resolution than their CMIP3 counterparts, including in some models a more realistic representation of stratosphere-troposphere interactions. The CMIP5 models also benefit from several years of development in their parameterisations of small scale processes, which, together with resolution increases, are expected to result in a general improvement in the accuracy of their simulations of historical climate, and in the credibility of their projections of future changes. The CMIP5 programme also includes a number of comprehensive Earth System Models (ESMs) which explicitly simulate the earth's carbon cycle and key aspects of atmospheric chemistry, and also contain more sophisticated representations of aerosols compared to CMIP3 models.

The CMIP3 results should be interpreted as a useful interim set of plausible outcomes. However, their neglect of uncertainties, for instance in carbon cycle feedbacks, implies that higher levels of warming outside the CMIP3 envelope cannot be ruled out. In future, CMIP5 coupled model and ESM projections can be expected to produce improved advice on future regional changes. In particular, ensembles of ESM projections will be needed to provide a more comprehensive survey of possible future changes and their relative likelihoods of occurrence. This is likely to require analysis of the CMIP5 multi-model ESM projections, augmented by larger ensembles of ESM simulations in which uncertainties in physical and biogeochemical feedback processes can be explored more systematically, for example via ensembles of model runs in which key aspects of the climate model are slightly adjusted. Note that such an exercise might lead to the specification of wider rather than narrower uncertainties compared to CMIP3 results, if the effects of representing a wider range of earth system processes outweigh the effects of refinements in the simulation of physical atmosphere-ocean processes already included in the CMIP3 models.

Climate projections

The Met Office Hadley Centre is currently producing perturbed parameter ensembles of a single model configuration known as HadCM3C, to explore uncertainties in physical and biogeochemical feedback processes. The results of this analysis will become available in the next year and will supplement the CMIP5 multi-model ESM projections, providing a more comprehensive set of data to help progress understanding of future climate change. However, many of the studies covered in the chapter on climate impacts have used CMIP3 model output. For this reason, and because it is still the most widely used set of projections available, the CMIP3 ensemble output for temperature and precipitation, for the A1B emission scenario, for Indonesia and the surrounding region is shown below.
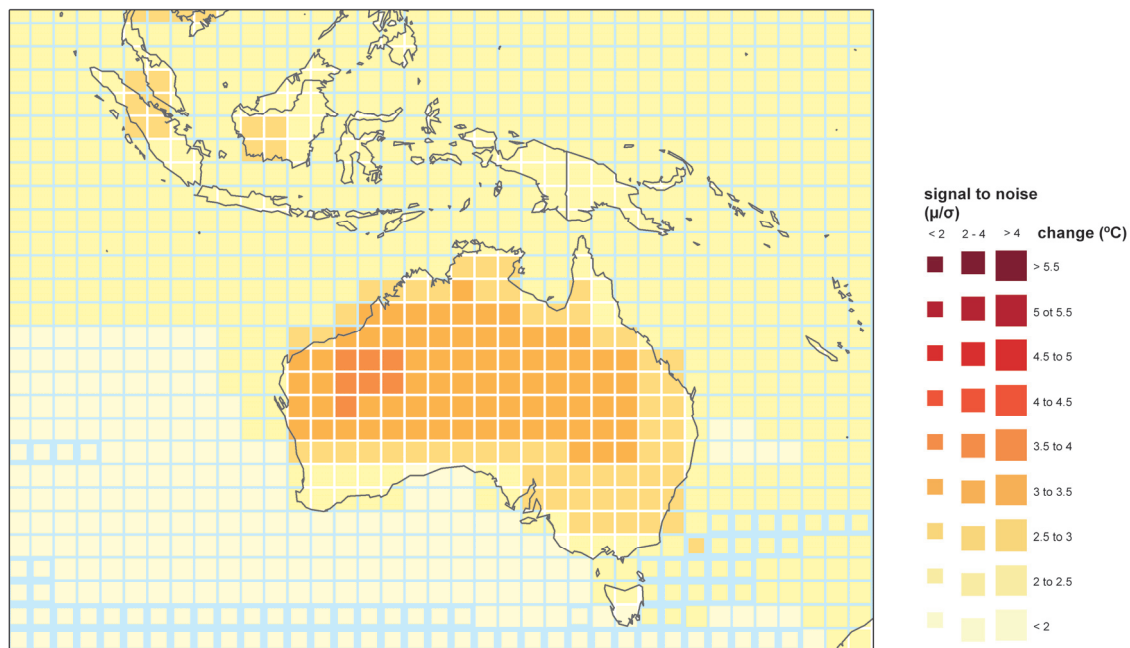
Figure 1. *Percentage change in average annual temperature by 2100 from 1960-1990 baseline climate, averaged over 21 CMIP3 models. The size of each pixel represents the level of agreement between models on the magnitude of the change.*
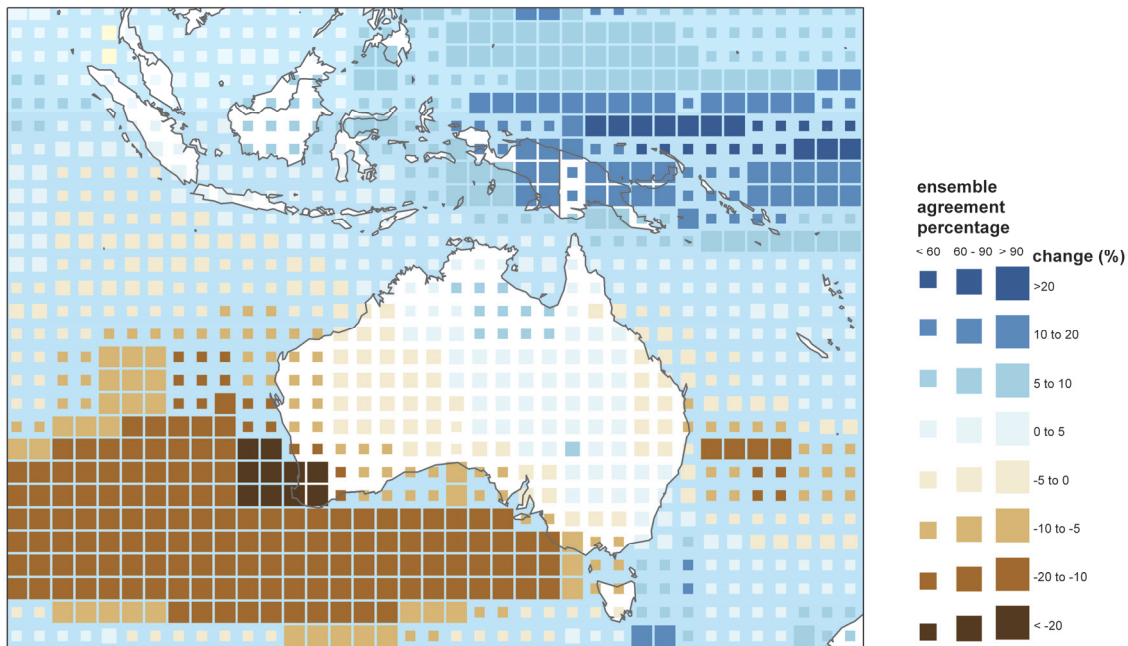
Figure 2. *Percentage change in average annual precipitation by 2100 from 1960-1990 baseline climate, averaged over 21 CMIP3 models. The size of each pixel represents the level of agreement between models on the sign of the change.*

Summary of temperature change in Indonesia

Figure 1 shows the percentage change in average annual temperature by 2100 from 1960-1990 baseline climate, averaged over 21 CMIP3 models. All of the models in the CMIP3 ensemble project increased temperatures in the future, but the size of each pixel indicates how well the models agree over the magnitude of the increase.

Projected temperature increases over Indonesia are generally consistent in the range of 2-2.5°C. There are a few grid boxes over Borneo and Sumatra where temperatures of 2.5-3°C are projected. There is good agreement between the models over all of Indonesia.

Summary of precipitation change in Indonesia

Figure 2 shows the percentage change in average annual precipitation by 2100 from 1960-1990 baseline climate, averaged over 21 CMIP3 models. Unlike for temperature, the models sometimes disagree over whether precipitation is increasing or decreasing over a region, so in this case the size of each pixel indicates the percentage of the models in the ensemble that agree on the sign of the change in precipitation.

For precipitation changes, there is quite low agreement between the models over Indonesia, though there are some regions of good agreement over New Guinea. Over New Guinea, rainfall is projected to increase in the region of 10-20%. Further west, over Borneo, increases of 5-10% are projected, with smaller increases of 0-5% projected over Sumatra.

Chapter 3 – Climate Change Impact Projections

Introduction

Aims and approach

This chapter looks at research on a range of projected climate change impacts, with focus on results for Indonesia. It includes projections taken from the AVOID programme, for some of the impact sectors.

The aim of this work is to take a 'top down' approach to assessing global impacts studies, both from the literature and from new research undertaken by the AVOID programme. This project covers 23 countries, with summaries from global studies provided for each of these. This global approach allows some level of comparison between countries, whilst presenting information on a scale most meaningful to inform international policy.

The literature covered in this chapter focuses on research published since the Fourth Assessment Report (AR4) of the Intergovernmental Panel on Climate Change (IPCC) and should be read in conjunction with IPCC AR4 WG1 and WG2 reports. For some sectors considered, an absence of research developments since the IPCC AR4, means earlier work is cited as this helps describe the current level of scientific understanding. This report focuses on assessing scientific research about climate change impacts within sectors; it does not present an integrated analysis of climate change adaptation policies.

Some national and sub-national scale literature is reported to a limited extent to provide some regional context.

Impact sectors considered and methods

This report reviews the evidence for the impact of climate change on a number of sectors, for Indonesia. The following sectors are considered in turn in this report:
- Crop yields
- Food security
- Water stress and drought
- Pluvial flooding and rainfall
- Fluvial flooding

- Tropical cyclones (where applicable)
- Coastal regions

Supporting literature

Literature searches were conducted for each sector with the Thomson Reuters Web of Science (WoS., 2011) and Google Scholar academic search engines respectively. Furthermore, climate change impact experts from each of the 23 countries reviewed were contacted. These experts were selected through a combination of government nomination and from experts known to the Met Office. They were asked to provide literature that they felt would be of relevance to this review. Where appropriate, such evidence has been included. A wide range of evidence was considered, including; research from international peer-reviewed journal papers; reports from governments, non-governmental organisations, and private businesses (e.g. reinsurance companies), and research papers published in national journals.

For each impact sector, results from assessments that include a global- or regional-scale perspective are considered separately from research that has been conducted at the national- or sub-national-scale. The consideration of global- and regional-scale studies facilitates a comparison of impacts across different countries, because such studies apply a consistent methodology for each country. While results from national- and sub-national-scale studies are not easily comparable between countries, they can provide a level of detail that is not always possible with larger-scale studies. However, the national- and sub-national scale literature included in this project does not represent a comprehensive coverage of regional-based research and cannot, and should not, replace individual, detailed impacts studies in countries. The review aims to present an up-to-date assessment of the impact of climate change on each of the sectors considered.

AVOID programme results

Much of the work in this report is drawn from modelling results and analyses coming out of the AVOID programme. The AVOID programme is a research consortium funded by DECC and Defra and led by the UK Met Office and also comprises the Walker Institute at the University of Reading, the Tyndall Centre represented through the University of East Anglia,

and the Grantham Institute for Climate Change at Imperial College. The expertise in the AVOID programme includes climate change research and modelling, climate change impacts in natural and human systems, socio-economic sciences, mitigation and technology. The unique expertise of the programme is in bringing these research areas together to produce integrated and policy-relevant results. The experts who work within the programme were also well suited to review the literature assessment part of this report. In this report the modelling of sea level rise impacts was carried out for the AVOID programme by the University of Southampton.

The AVOID programme uses the same emissions scenarios across the different impact sectors studied. These are a business as usual (IPCC SRES A1B) and an aggressive mitigation (the AVOID A1B-2016-5-L) scenario. Model output for both scenarios was taken from more than 20 GCMs and averaged for use in the impact models. The impact models are sector specific, and frequently employ further analytical techniques such as pattern scaling and downscaling in the crop yield models.

Data and analysis from AVOID programme research is provided for the following impact sectors:

- Crop yields
- Water stress and drought
- Fluvial flooding
- Coastal regions

Uncertainty in climate change impact assessment

There are many uncertainties in future projections of climate change and its impacts. Several of these are well-recognised, but some are not. One category of uncertainty arises because we don't yet know how mankind will alter the climate in the future. For instance, uncertainties in future greenhouse gas emissions depends on the future socio-economic pathway, which, in turn, depends on factors such as population, economic growth, technology development, energy demand and methods of supply, and land use. The usual approach to dealing with this is to consider a range of possible future scenarios.

Another category of uncertainties relate to our incomplete understanding of the climate system, or an inability to adequately model some aspects of the system. This includes:

- Uncertainties in translating emissions of greenhouse gases into atmospheric concentrations and radiative forcing. Atmospheric CO_2 concentrations are currently rising at approximately 50% of the rate of anthropogenic emissions, with the remaining 50% being offset by a net uptake of CO_2 into the oceans and land biosphere. However, this rate of uptake itself probably depends on climate, and evidence suggests it may weaken under a warming climate, causing more CO_2 to remain in the atmosphere, warming climate further. The extent of this feedback is highly uncertain, but it not considered in most studies. The phase 3 of the Coupled Model Intercomparison Project (CMIP3), which provided the future climate projections for the IPCC Fourth Assessment Report (AR4), used a single estimate of CO_2 concentration rise for each emissions scenario, so the CMIP3 projections (which were used in most studies presented here, including AVOID) do not account for this uncertainty.

- Uncertainty in climate response to the forcing by greenhouse gases and aerosols. One aspect of this is the response of global mean temperature ("climate sensitivity"), but a more relevant aspect for impacts studies is the response of regional climates, including temperature, precipitation and other meteorological variables. Different climate models can give very different results in some regions, while giving similar results in other regions. Confidence in regional projections requires more than just agreement between models: physical understanding of the relevant atmospheric, ocean and land surface processes is also important, to establish whether the models are likely to be realistic.

- Additional forcings of regional climate. Greenhouse gas changes are not the only anthropogenic driver of climate change; atmospheric aerosols and land cover change are also important, and unlike greenhouse gases, the strength of their influence varies significantly from place to place. The CMIP3 models used in most impacts studies generally account for aerosols but not land cover change.

- Uncertainty in impacts processes. The consequences of a given changes in weather or climatic conditions for biophysical impacts such as river flows, drought, flooding, crop yield or ecosystem distribution and functioning depend on many other processes which are often poorly-understood, especially at large scales. In particular, the extent to which different biophysical impacts interact with each other has been hardly studied, but may be crucial; for example, impacts of climate change on crop yield may depend not only on local climate changes affecting rain-fed crops, but also remote climate changes affecting river flows providing water for irrigation.

57

- Uncertainties in non-climate effects of some greenhouse gases. As well as being a greenhouse gas, CO_2 exerts physiological influences on plants, affecting photosynthesis and transpiration. Under higher CO_2 concentrations, and with no other limiting factors, photosynthesis can increase, while the requirements of water for transpiration can decrease. However, while this has been extensively studied under experimental conditions, including in some cases in the free atmosphere, the extent to which the ongoing rise in ambient CO_2 affects crop yields and natural vegetation functioning remains uncertain and controversial. Many impacts projections assume CO_2 physiological effects to be significant, while others assume it to be non-existent. Studies of climate change impacts on crops and ecosystems should therefore be examined with care to establish which assumptions have been made.

In addition to these uncertainties, the climate varies significantly through natural processes from year-to-year and also decade-to-decade, and this variability can be significant in comparison to anthropogenic forcings on shorter timescales (the next few decades) particularly at regional scales. Whilst we can characterise the natural variability it will not be possible to give a precise forecast for a particular year decades into the future.

A further category of uncertainty in projections arises as a result of using different methods to correct for uncertainties and limitations in climate models. Despite being painstakingly developed in order to represent current climate as closely as possible, current climate models are nevertheless subject to systematic errors such as simulating too little or too much rainfall in some regions. In order to reduce the impact of these, '*bias correction*' techniques are often employed, in which the climate model is a source of information on the *change* in climate which is then applied to the observed present-day climate state (rather than using the model's own simulation of the present-day state). However, these bias-corrections typically introduce their own uncertainties and errors, and can lead to inconsistencies between the projected impacts and the driving climate change (such as river flows changing by an amount which is not matched by the original change in precipitation). Currently, this source of uncertainty is rarely considered

When climate change projections from climate models are applied to climate change impact models (e.g. a global hydrological model), the climate model structural uncertainty carries through to the impact estimates. Additional uncertainties include changes in future emissions and population, as well as parameterisations within the impact models (this is rarely considered). Figure 1 highlights the importance of considering climate model structural uncertainty in climate change impacts assessment. Figure 1 shows that for 2°C prescribed

global-mean warming, the magnitude of, and sign of change in average annual runoff from present, simulated by an impacts model, can differ depending upon the GCM that provides the climate change projections that drive the impact model. This example also shows that the choice of impact model, in this case a global hydrological model (GHM) or catchment-scale hydrological model (CHM), can affect the magnitude of impact and sign of change from present (e.g. see IPSL CM4 and MPI ECHAM5 simulations for the Xiangxi). To this end, throughout this review, the number of climate models applied in each study reviewed, and the other sources of uncertainty (e.g. emissions scenarios) are noted. Very few studies consider the application of multiple impacts models and it is recommended that future studies address this.
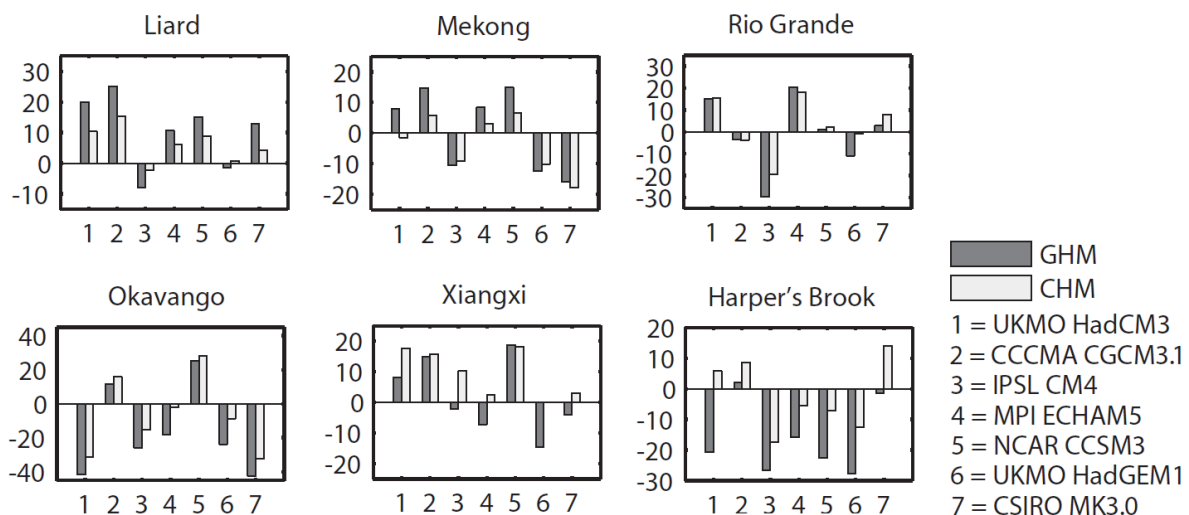
Figure 1. *Change in average annual runoff relative to present (vertical axis; %), when a global hydrological model (GHM) and a catchment-scale hydrological model (CHM) are driven with climate change projections from 7 GCMs (horizontal axis), under a 2°C prescribed global-mean warming scenario, for six river catchments. The figure is from Gosling et al. (2011).*

Uncertainties in the large scale climate relevant to Indonesia include changes in the El Niño-Southern Oscillation (ENSO) which could undergo rapid change with climate change. This could have a serious impact on large-scale atmospheric circulation, rainfall and seasonality in many parts of the world. Latif and Keenlyside (2009) concluded that, at this stage of understanding, it is not known how climate change might affect the tropical Pacific climate system. None of the global climate models (GCMs) they analysed showed rapid changes in behaviour. However, a threshold of abrupt change cannot be ruled out because whilst the GCMs that Latif and Keenlyside (2009) analysed (the CMIP3 multi-model dataset) are better than the previous generation of models (Reichler and Kim, 2008), these same models all show large biases in simulating the contemporary tropical Pacific, with no consensus on the sign of change in ENSO-like response.

Summary of findings for each sector

Crop yields

- Quantitative crop yield projections under climate change scenarios for Indonesia vary across studies due to the application of different models, assumptions and emissions scenarios.

- A number of, but not all, Global- and regional-scale studies included here indicate that climate change could be associated with declines in maize yields but increases in rice yields, two of Indonesia's major crops, from 2050 onwards.

- In all studies the balance between detrimental ozone effects and ameliorating CO_2 fertilisation may determine whether projected losses or gains are realised under climate change.

- National-scale studies show that uncertainty in future crop production is dependent on potential changes to ENSO, which are not yet fully understood.

- Other important knowledge gaps and key uncertainties include the quantification of yield increases due to CO_2 fertilisation, quantification of yield reductions due to ozone damage and the extent crop to which crop diseases could affect crop yields with climate change.

Food security

- Indonesia is currently a country with moderately low levels of undernourishment. Global-scale studies included here project that Indonesia could remain food-secure over the next 40 years, where food production from the land is concerned.

- However, the security of supply from marine sources is of concern. One study projects that Indonesia could experience some of the largest decreases in marine fish stocks across the globe; for example, the 10-year averaged maximum catch potential from 2005 to 2055 could decline by 23% under SRES A1B.

Water stress and drought

- There are currently few studies on the impact of climate change on water stress and drought in Indonesia, especially at the national scale. Important uncertainties concern the role of the Asian monsoon affecting drought occurrences in Indonesia under climate change scenarios, so additional research efforts should be focussed here.

- Recent simulations by the AVOID programme show no appreciable increases or decreases in the population projected to be exposed to water stress with climate change in Indonesia.

Pluvial flooding and rainfall

- The IPCC AR4 reported potential increases in precipitation over Indonesia under global climate change scenarios.

- However, few studies relevant to Indonesia have been published since.

- Large uncertainties remain, particularly regarding the response of the El Niño Southern Oscillation (ENSO) to climate change.

Fluvial flooding

- Results from a recent global-scale study suggest that extreme flooding could increase in Indonesia with climate change.

- Simulations by the AVOID programme support these results. A majority of the models show a tendency for increasing flood risk, particularly later in the century and in the A1B scenario, and in some models this increase is very large.

- Few studies have made projections of changes in flood hazard under climate change in Indonesia at national or local scale. Given that severe floods have affected Indonesia several times in recent history, a recommended avenue for further research is to better quantify the risk of flooding in Indonesia under climate change scenarios.

Tropical cyclones

- There remains large uncertainty in the current understanding of how tropical cyclones might be affected by climate change, including in theWest Pacific and South Indian Ocean, as conclusions are based upon a limited number of studies whose projections are from either coarse-resolution global models or from statistical or dynamical downscaling techniques. To this end, caution should be applied in interpreting model-based results, even where the models are in agreement.

- However, most global- and regional-scale studies reviewed here suggest that the frequency of landfalling tropical cyclones in Indonesia could decrease with climate change, for both West Pacific cyclones, which affect the eastern part of the country, and South Indian Ocean cyclones, which affect the western and southern regions.

- However, most studies reviewed here suggest that the intensity of cyclones could increase with climate change, particularly for the most severe storms.

- Future cyclone damages in Indonesia under climate change are uncertain, due to the uncertainties in the magnitude of projected changes in cyclone intensity and frequency.

Coastal regions

- Sea level rise (SLR) could have major impacts on Indonesia's coastal regions.

- A 10% intensification of the current 1-in-100-year storm surge combined with a prescribed 1m SLR could affect 39% of Indonesia's coastal GDP and 14,400km^2 of coastal land.

- Another study showed that the country's population exposed to SLR could increase from 600,000 in present, to 2.7 million under un-mitigated A1B emissions in the 2070s. An aggressive mitigation scenario could avoid around 156,000 people out of this total being exposed to SLR.

Crop yields

Headline

Crop yield projections under climate change scenarios for Indonesia vary greatly across studies due to the application of different models, assumptions and emissions scenarios. Nevertheless there is a general consensus that climate change could be associated with declines in maize yields but increases in rice yields, from 2050 onwards.

Studies imply that additional crop yield losses from ozone damage are low. However, there is high uncertainty associated with the intensity and frequency of ENSO events with climate change, which means crop yields associated with such events are also uncertain.

Other important knowledge gaps and key uncertainties, which are applicable to Indonesia as well as at the global-scale, include; the quantification of yield increases due to CO_2 fertilisation, and the extent crop diseases could affect crop yields with climate change (Luck et al., 2011).

Supporting literature

Introduction

The impacts of climate change on crop productivity are highly uncertain due to the complexity of the processes involved. Most current studies are limited in their ability to capture the uncertainty in regional climate projections, and often omit potentially important aspects such as extreme events and changes in pests and diseases. Importantly, there is a lack of clarity on how climate change impacts on drought are best quantified from an agricultural perspective, with different metrics giving very different impressions of future risk. The dependence of some regional agriculture on remote rainfall, snowmelt and glaciers adds to the complexity - these factors are rarely taken into account, and most studies focus solely on the impacts of local climate change on rain-fed agriculture. However, irrigated agricultural land produces approximately 40-45 % of the world's food (Doll and Siebert 2002), and the water for irrigation is often extracted from rivers which can depend on climatic conditions far from the point of extraction. Hence, impacts of climate change on crop productivity often

need to take account of remote as well as local climate changes. Indirect impacts via sea-level rise, storms and diseases have also not been quantified. Perhaps most seriously, there is high uncertainty in the extent to which the direct effects of CO_2 rise on plant physiology will interact with climate change in affecting productivity. Therefore, at present, the aggregate impacts of climate change on large-scale agricultural productivity cannot be reliably quantified (Gornall et al, 2010). This section summarises findings from a range of post IPCC AR4 assessments to inform and contextualise the analysis performed by AVOID programme for this project. The results from the AVOID work are discussed in the next section.

Rice is the most important food crop in Indonesia followed by maize and cassava. Other important crops include coconuts and oil palms. (see Table 1) (FAO, 2008).

Harvested area (ha)		Quantity (Metric ton)		Value ($1000)	
Rice, paddy	12300000	Rice, paddy	60200000	Rice, paddy	12400000
Oil palm fruit	5000000	Sugar cane	26000000	Palm oil	5110000
Maize	4000000	Cassava	21500000	Coconuts	1770000
Coconuts	2950000	Coconuts	19500000	Natural rubber	1560000
Natural rubber	2890000	Palm oil	18900000	Cassava	1520000
Cassava	1190000	Maize	16300000	Maize	1280000
Cocoa beans	990000	Bananas	5740000	Bananas	818000

Table 1. *The top 7 crops by harvested area, quantity and value according to the FAO (2008) in Indonesia. Crops that feature in all lists are shaded green; crops that feature in two top 7 lists are shaded amber. Data is from FAO (2008) and has been rounded down to three significant figures*.

A number of global, regional, national and sub-national impact model studies, which include results for some of the main crops in Indonesia, have been conducted. They applied a variety of methodological approaches, including using different climate model inputs and treatment of other factors that might affect yield, such as impact of increased CO_2 in the atmosphere on plant growth and adaption of agricultural practises to changing climate conditions. These different models, assumptions and emissions scenarios mean that there are a range of crop yield projections for Indonesia. However, the majority of studies explored in this report show that could be associated with declines in maize yields but increases in rice yields, from 2050 onwards.

Important knowledge gaps, which are applicable to Indonesia as well as at the global-scale, include; the quantification of yield reductions due to ozone damage (Ainsworth and McGrath, 2010, Iglesias et al., 2009), and the extent crop diseases could affect crop yields with climate change (Luck et al., 2011). Most crop simulation models do not include the direct effect of

extreme temperatures on crop development and growth, thus only changes in mean climate conditions are considered to affect crop yields for the studies included here.

Assessments that include a global or regional perspective

Recent past

Climate impacts on crop production in Indonesia, in particular rice, are manifested predominantly through the impacts of the El Niño-Southern Oscillation (ENSO) on the climate (Irawan, 2003, Naylor et al., 2007). Therefore numerous studies have investigated the sensitivity of crop yields in Indonesia to recent climate change.

Long-term records from 1830 to 1953 show that droughts occurred more frequently during El Niño years by more than ten-fold (Quinn et al., 1978). A recent analysis by the KNMI (2009) confirms the association of low rainfall and El Niño years. El Niño associated droughts can result in serious crop production losses: the 1997/98 El Niño event resulted in a huge shortfall in rice production that necessitated the import of over five million metric tons of rice to ensure food availability (Kishore et al., 2000). The potential impact of El Niño events on rice production relates mainly to the delayed onset of the monsoon rains that arrive between late October and December. Farmers switch to crops that are less water-demanding during early growth stages and may not (or be able to) compensate by increased planting at the second rice planting between April and May (Naylor and Mastrandrea, 2010). Conversely, La Niña tends to result in increased rainfall (NASA, 1999) and increases in crop production at the national level (Irawan, 2003), though in some cases it also results in crop losses due to flooding (e.g. IRIN, 2010, Agrimoney, 2010, Honorine, 2010).

Lobell et al. (2011) assessed the impacts of recent climate change (1980-2008) on maize, rice, wheat and soybean yields at the global-scale and national estimates for Indonesia were calculated (see Table 2).

Crop yield changes could be due to a variety of factors, which might include, but not be confined to, a changing climate. In order to assess the impact of recent climate change (1980-2008) on wheat, maize, rice and soybean, Lobell et al. (2011) looked at how the overall yield trend in these crops changed in response to changes in climate over the period studied. The study was conducted at the global-scale but national estimates for Indonesia were also calculated. Lobell et al. (2011) divided the climate-induced yield trend by the overall yield trend for 1980–2008, to produce a simple metric of the importance of climate relative to all other factors. The ratio produced indicates the influence of climate on the productivity trend overall. So for example a value of –0.1 represents a 10% reduction in

66

yield gain due to climate change, compared to the increase that could have been achieved without climate change, but with technology and other gains. This can also be expressed as 10 years of climate trend being equivalent to the loss of roughly 1 year of technology gains. For Indonesia, a negative effect on rice yield was estimated relative to what could have been achieved without the climate trends (see Table 2).

Crop	Trend
Maize	-0.1 to 0.0
Rice	-0.2 to -0.1
Wheat	n/a
Soybean	-0.1 to 0.0

Table 2. The estimated net impact of climate trends for 1980-2008 on crop yields. Climate-induced yield trend divided by overall yield trend. 'n/a' infers zero or insignificant crop production or unavailability of data. Data is from Lobell et al. (2011).

Welch et al. (2010) showed that irrigated rice yield at Sukamandi (Java) and other main rice producing locations in South Asia was negatively affected by higher minimum temperatures during the vegetative and ripening phases of growth. Higher maximum temperatures on the other hand, though still below the optimum, during these phases increased yield. Effects of solar radiation were negative during vegetative growth but positive during ripening. Combined, these effects of radiation and temperature suggested that if observed weather trends at the end of the 20th century had not occurred, annual rice growth rate could have been 12.3 kg ha^{-1} yr^{-1} higher during the main cropping season and 7.1 kg ha^{-1} yr^{-1} higher during the shorter, lower yielding cropping season.

Climate change studies

Included in this section are results from recent studies that have applied climate projections from Global Climate Models (GCMs) to crop yield models to assess the global-scale impact of climate change on crop yields, and which include impact estimates at the national-scale for Indonesia (Avnery et al., 2011, Masutomi et al., 2009, Iglesias and Rosenzweig, 2009).

The process of CO_2 fertilisation of some crops is usually included in climate impact studies of yields. However, other gases can influence crop growth, and are not always included in impact model projections. An example of this is ozone, (O_3) and so a study which attempts to quantify the potential impact of changes in the atmospheric concentration of this gas is also included Avnery et al., (2011).

In addition to these studies, the AVOID programme analysed the patterns of climate change for 21 GCMs to establish an index of 'climate suitability' of agricultural land. Climate suitability is not directly equivalent to crop yields, but is a means of looking at a standard metric across all countries included in this project, and of assessing the level of agreement on variables that affect crop production between all 21 GCMs.

Iglesias and Rosenzweig (2009) repeated an earlier study presented by Parry et al. (2004) by applying climate projections from the HadCM3 GCM (instead of HadCM2, which was applied by Parry et al. (2004)), under seven SRES emissions scenarios and for three future time periods. This study used consistent crop simulation methodology and climate change scenarios globally, and weighted the model site results by their contribution to regional and national, rain-fed and irrigated production. The study also applied a quantitative estimation of physiological CO_2 effects on crop yields and considered the affect of adaptation by assessing the potential of the country or region to reach optimal crop yield.

The results from the study are presented in Table 3 and Table 4. The simulations showed a rice yield deficit by 2020 turning, in the majority of scenarios, into a yield gain by 2050 and 2080, but a steadily increasing yield deficit with climate change for maize.

Scenario	Year	Rice	Maize
A1FI	2020	-1.02	-3.83
	2050	1.53	-7.52
	2080	-0.50	-10.60
A2a	2020	-0.32	-3.13
	2050	1.79	-6.29
	2080	4.78	-7.34
A2b	2020	-0.48	-3.13
	2050	1.62	-6.24
	2080	3.02	-9.44
A2c	2020	-1.50	-4.33
	2050	1.32	-6.78
	2080	2.76	-9.54
B1a	2020	-1.41	-3.86
	2050	0.00	-6.73
	2080	-2.29	-8.09
B2a	2020	-1.47	-4.44
	2050	0.23	-6.48
	2080	2.00	-6.94
B2b	2020	-1.59	-4.33
	2050	-0.54	-7.29
	2080	1.51	-7.42

Table 3. *Rice and maize yield changes (%) relative to baseline scenario (1970-2000) for different emission scenarios and future time periods. Some emissions scenarios were run in an ensemble simulation (e.g. A2a, A2b, A2c). Data is from Iglesias and Rosenzweig (2009).*

	Rice		Maize	
	Up	**Down**	**Up**	**Down**
Baseline to 2020	0	7	0	7
Baseline to 2050	5	1	0	7
Baseline to 2080	5	2	0	7
2020 to 2050	7	0	0	7
2050 to 2080	5	2	0	7

Table 4. *The number of emission scenarios that predict yield gains ("Up") or yield losses ("Down") for rice and maize between two points in time. Data is from Iglesias and Rosenzweig (2009).*

Masutomi et al. (2009) assessed the impact of climate change on rice production in Asia considering the process/parameter uncertainty in GCMs. The authors created climate scenarios based on the projections of GCMs for three emissions scenarios (18 GCMs for A1B, 14 GCMs for A2, and 17 GCMs for B1). The climate scenarios were then used as input to the M-GAEZ crop model to calculate the average change in production (ACP) and other parameters taking into account the effect of CO_2 fertilisation. Since land-use change was not

considered in the study, changes in crop production actually equate to changes in crop yield and the country-level results for Indonesia are presented in Table 5.

1990s - 2020s			1990s - 2050s			1990s - 2080s		
A2	**A1B**	**B1**	**A2**	**A1B**	**B1**	**A2**	**A1B**	**B1**
-2.9	-0.3	-1.5	3.7	5.5	1.9	-3.7	4.2	3.7

Table 5. Average change in rice production (%) taking CO_2 effect into consideration, for Indonesia. The values represent the average across all GCMs considered in the analysis (individual GCM results are not presented in the study). Data is from Masutomi et al. (2009).

Elsewhere, several recent studies have assessed the impact of climate change on a global-scale and include impact estimates for South Asia or Southeast Asia as a whole (Arnell et al., 2010, Nelson et al., 2009, Tatsumi et al., 2011, Lobell et al., 2008, Welch et al., 2010). Whilst these studies provide a useful indicator of crop yields under climate change for the *region*, it should be noted that the crop yields presented in such cases are not definitive *national* estimates. This is because the yields are averaged over the entire region, which includes other countries as well as Indonesia.

Nelson et al. (2009) applied two GCMs in combination with the DSSAT crop model under the SRES A2 emissions scenario to project future yields of rice, maize, soybean, wheat and groundnut with and without CO_2 enrichment, and for rain-fed and irrigated lands, for several regions across the globe. Table 6 represents the results for East Asia and the Pacific, the World Bank regional grouping in which Indonesia is included. It can be seen that increased CO_2 levels were of benefit to all crops simulated, whether rain-fed or irrigated. However the effects of CO_2 fertilisation in the case of irrigated maize and rain-fed wheat in particular are not projected to be large enough to fully compensate for factors which could lead to yield reductions, such as increasing temperatures, out to 2050.

GCM and CO_2 fertilisation	Rice		Maize		Soybean		Wheat		Groundnut	
	Rf.	Irr.	Rf.	Irr.	Rf.	Irr.	Rf.	Irr.	Rf.	Irr.
CSIRO NoCF	-4.5	-13.0	1.5	-1.3	-3.6	-8.2	-14.8	-2.7	-5.1	-11.1
NCAR NoCF	-5.8	-19.8	-3.9	-2.6	-8.6	-13.4	-16.1	-7.1	-6.5	-13.7
CSIRO CF	2.5	4.4	3.7	-0.8	17.0	9.1	-5.4	3.7	11.3	3.6
NCAR CF	1.8	-1.1	-2.0	-1.9	11.5	3.6	-9.2	-0.6	9.7	1.2

Table 6. Projected yield changes (%) by 2050 compared to baseline (yields with 2000 climate) using two GCMs with (CF) and without CO_2 fertilisation effect (NoCF). Rain-fed (Rf.) and Irrigated (Irr.) crop lands were assessed separately. Data is from Nelson et al. (2009).

Tatsumi et al. (2011) applied an improved version of the GAEZ crop model (iGAEZ) to simulate crop yields on a global scale for wheat, potato, cassava, soybean, rice, sweet potato, maize, green beans. The impact of global warming on crop yields from the 1990s to 2090s was assessed by projecting five GCM outputs under the SRES A1B scenario and comparing the results for crop yields as calculated using the iGAEZ model for the period of 1990-1999. The results for Southeast Asia, which includes Indonesia, are displayed in Table 7.

Wheat	Potato	Cassava	Soybean	Rice	Sweet	Maize	Green
-8.95	-1.87	17.48	3.09	3.66	1.29	6.87	-5.17

Table 7. Average change in yield (%), during 1990s-2090s in Southeast Asia. Data is from Tatsumi et al. (2011).

Arnell et al. (2010) used 5 GCMs to assess the effects of climate scenarios on crop productivity. Specifically, the crop simulation model GLAM-maize was used to simulate the effect of climate change on maize productivity. For Southeast Asia a loss of between approximately 33% and 40% of yield was projected, relative to the baseline (1961-1990) by 2050 in the absence of adaptation and mitigation strategies, under A1B emissions. Implementing the mitigation strategy A1B-2016-5-L (a 5%/year reduction in emissions from 2016 onwards to a low emissions floor) reduced the negative impact by approximately 20% and 30% in 2050 and 2100 respectively.

To identify appropriate adaptation priorities Lobell et al. (2008) conducted an analysis of climate risks for the major crops in 12 food-insecure regions. Statistical crop models were used in combination with climate projections for 2030 from 20 GCMs that have contributed to the World Climate Research Programme's Coupled Model Intercomparison Project phase 3. The results from the study for Southeast Asia, are presented in Figure 2. Lobell et al. (2008) found that in Southeast Asia, climate change had an adverse impact in 2030 on crop yield for soybean, maize, rice and wheat (at least 75% of projections were associated with yield losses) and a positive impact was projected for sugar cane (at least 95% of projections were associated with yield increases).
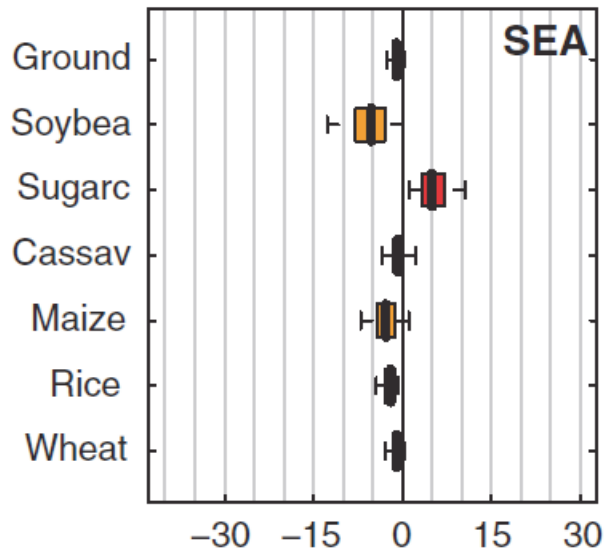
Figure 2. Probabilistic projections of production impacts in 2030 from climate change (expressed as a percentage of 1998 to 2002 average yields) for Southeast Asia. Red, orange, and yellow indicate a Hunger Importance Ranking of 1 to 30 (more important), 31 to 60 (important), and 61 to 94 (less important), respectively. Dashed lines extend from 5th to 95th percentile of projections, boxes extend from 25th to 75th percentile, and the middle vertical line within each box indicates the median projection. Figure is from Lobell et al. (2008).

In addition to the studies looking at the effect of changes in climate and CO_2 concentrations on crop yield Avnery et al. (2011) investigated the effects of ozone surface exposure on crop yield losses for soybeans, maize and wheat under the SRES A2 and B1 scenarios respectively. Two metrics of ozone exposure were investigated; seasonal daytime (08:00-19:59) mean O_3 ("M12") and accumulated O_3 above a threshold of 40 ppbv ("AOT40"). The results for Indonesia are presented in Table 8.

	A2		B1	
	M12	AOT40	M12	AOT40
Soybeans	-	-	-	-
Maize	2-4	0-2	0-2	0-2
Wheat	-	-	-	-

Table 8. National relative crop yield losses (%) for 2030 under A2 and B1 emission scenarios according to the M12 (seasonal daytime (08:00–19:59) mean) and AOT40 (accumulated O_3 above a threshold of 40 ppbv) metrics of O_3 exposure. Data is from Avnery et al. (2011).

National-scale or sub-national scale assessments

Climate change studies

Included in this section are results from recent studies that have conducted literature assessments and used empirical data and information from global climate model projections to investigate the impact of climate change on ENSO to further inform crop projections on a national and/or sub-national scale.

For Indonesia, much of future crop production depends on whether the frequency and intensity of El Niño-Southern Oscillation (ENSO) events and characteristics will change. After reviewing the literature, Philip (2009) concluded that GCMs do not agree on the impact of climate change on ENSO and that sometimes the sign of a change is even not consistent between GCMs. This conclusion is confirmed by Vecchi and Wittenberg (2010). Nevertheless, Naylor et al. (2007), using the CMIP3 multi-model dataset under SRES A2 and B1 emissions, found that the probability of exceeding a 30 day delay in the onset of monsoon rains could rise significantly by 2050, in particular for East Java / Bali. Empirical data collected over the period 1983-2004 showed that a 30-day delay of monsoon onset was associated with rice production declines around 6.5% and 11% in West / Central Java and East Java / Bali respectively. The authors concluded that regardless of the uncertainty in the response of large-scale circulation models to increased concentrations of greenhouse gases, a 30-day delay in monsoon onset is "*very likely* to occur more frequently in 2050 than it does today". It is important to emphasize that even if the 30-day monsoon onset delays may indeed become more frequent in the future, this may not necessarily lead to the scale of the production losses observed historically. Future crop production is also affected by the degree to which future ENSO events can be forecast allowing farmers to mitigate crop production / yield losses. Improvements in model skill such as demonstrated by D'Arrigo and Wilson (2008) may aid in reducing crop production losses with climate change.

AVOID Programme results

To further quantify the impact of climate change on crops, the AVOID programme simulated the effect of climate change on the suitability of land for crop cultivation for all countries reviewed in this literature assessment based upon the patterns of climate change from 21

GCMs (Warren et al., 2010). This ensures a consistent methodological approach across all countries and takes consideration of climate modelling uncertainties.

Methodology

The effect of climate change on the suitability of land for crop cultivation is characterised here by an index which defines the percentage of cropland in a region with 1) a decrease in suitability or 2) an increase in suitability. A threshold change of 5% is applied here to characterise decrease or increase in suitability. The crop suitability index is calculated at a spatial resolution of 0.5°x0.5°, and is based on climate and soil properties (Ramankutty et al., 2002). The baseline crop suitability index, against which the future changes are measured, is representative of conditions circa 2000. The key features of the climate for the crop suitability index are temperature and the availability of water for plants. Changes in these were derived from climate model projections of future changes in temperature and precipitation, with some further calculations then being used to estimate actual and potential evapotranspiration as an indicator of water availability. It should be noted that changes in atmospheric CO_2 concentrations can decrease evapotranspiration by increasing the efficiency of water use by plants (Ramankutty et al., 2002), but that aspect of the index was not included in the analysis here. Increased CO_2 can also increase photosynthesis and improve yield to a small extent, but again these effects are not included. Exclusion of these effects may lead to an overestimate of decreases in suitability.

The index here is calculated only for grid cells which contain cropland circa 2000, as defined in the global crop extent data set described by Ramankutty et al. (2008) which was derived from satellite measurements. It is assumed that crop extent does not change over time. The crop suitability index varies significantly for current croplands across the world (Ramankutty et al., 2002), with the suitability being low in some current cropland areas according to this index. Therefore, while climate change clearly has the potential to decrease suitability for cultivation if temperature and precipitation regimes become less favourable, there is also scope for climate change to increase suitability in some existing cropland areas if conditions become more favourable in areas where the suitability index is not at its maximum value of 1. It should be noted that some areas which are not currently croplands may already be suitable for cultivation or may become suitable as a result of future climate change, and may become used a croplands in the future either as part of climate change adaptation or changes in land use arising for other reasons. Such areas are not included in this analysis.

Results

Crop suitability was estimated under the pattern of climate change from 21 GCMs with two emissions scenarios; 1) SRES A1B and 2) an aggressive mitigation scenario where emissions follow A1B up to 2016 but then decline at a rate of 5% per year thereafter to a low emissions floor (denoted A1B-2016-5-L). The application of 21 GCMs is an attempt to quantify the uncertainty due to climate modelling, although it is acknowledged that only one crop suitability impacts model is applied. Simulations were performed for the years 2030, 2050, 2080 and 2100. The results for Indonesia are presented in Figure 3.

Under all the climate projections, no existing Indonesian cropland areas are projected to become more suitable under any model. Up to 2% of current croplands are projected to undergo declining suitability by 2030 in both scenarios.   By 2100, between 0 and 12% of current Indonesian cropland is projected to experience declining suitability under A1B, and 0 – 7% under the mitigation scenario.
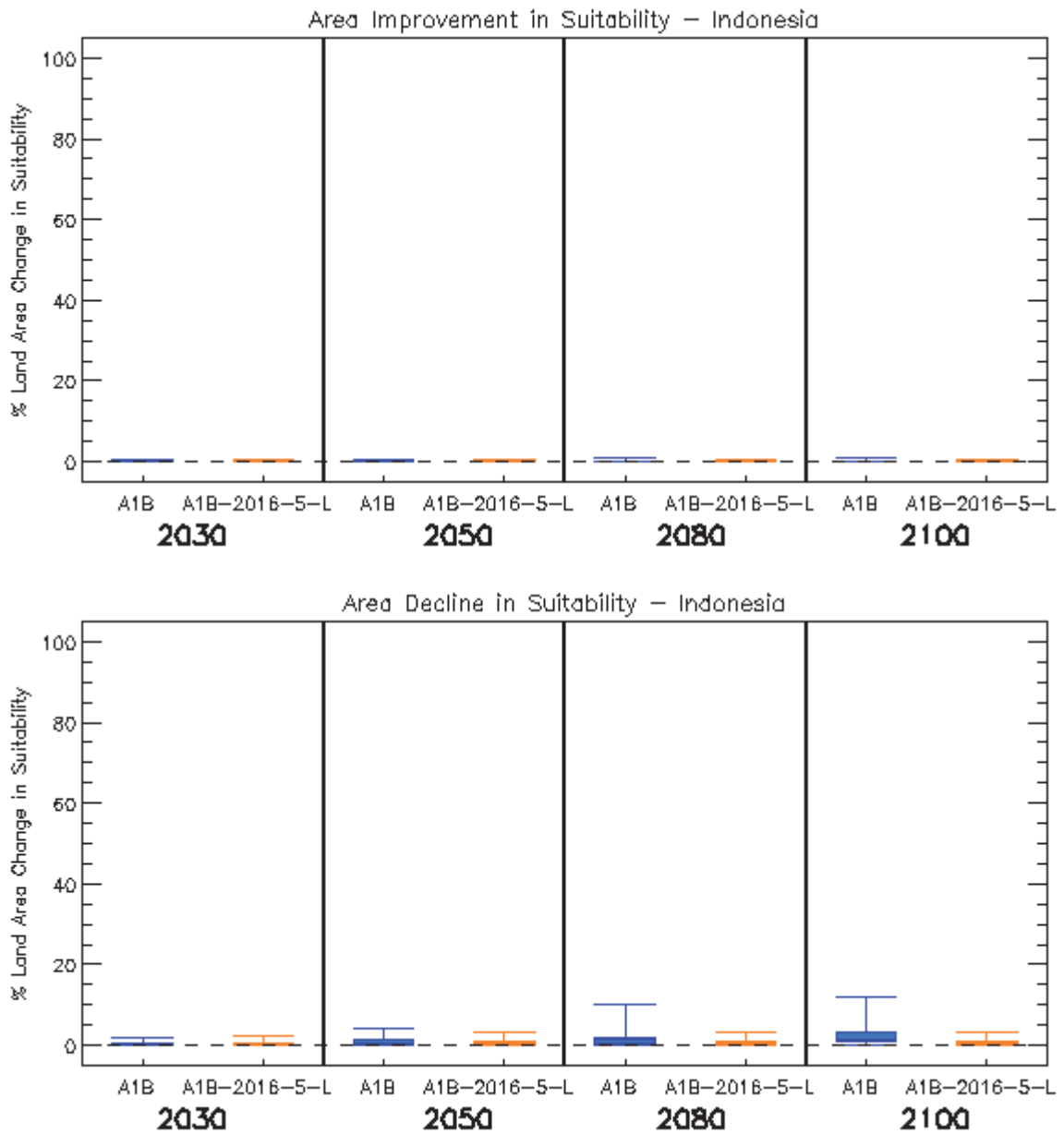
Figure 3. *Box and whisker plots for the impact of climate change on increased crop suitability (top panel) and decreased crop suitability (bottom panel) for Indonesia, from 21 GCMs under two emissions scenarios (A1B and A1B-2016-5-L), for four time horizons. The plots show the 25th, 50th, and 75th percentiles (represented by the boxes), and the maximum and minimum values (shown by the extent of the whiskers).*

Food security

Headline

Recent studies suggest that Indonesia could remain food-secure, when food production from the land is concerned. However, recent studies that explore the impacts of climate change on marine fisheries, suggests that Indonesia could experience some of the largest decreases in marine fish stocks across the globe, e.g. the 10-year averaged maximum catch potential from 2005 to 2055 could decline by 23% under SRES A1B. This represents new knowledge since the publication of the IPCC AR4 but further work should seek to address how the relative contributions from land-based and marine-based foods could affect food security under climate change scenarios for Indonesia.

Supporting literature

Introduction

Food security is a concept that encompasses more than just crop production, but is a complex interaction between food availability and socio-economic, policy and health factors that influence access to food, utilisation and stability of food supplies. In 1996 the World Food Summit defined food security as existing 'when all people, at all times, have physical and economic access to sufficient, safe and nutritious food to meet their dietary needs, and their food preferences are met for an active and healthy life'.

As such this section cannot be a comprehensive analysis of all the factors that are important in determining food security, but does attempt to assess a selection of the available literature on how climate change, combined with projections of global and regional population and policy responses, may influence food security.'

Assessments that include a global or regional perspective

According to the FAO's Food Security Country profiles (FAO, 2010) a moderately low proportion (10-19%) of Indonesia's population are currently undernourished.

With respect to food production from the land, under climate change scenarios, recent studies suggest that food security is not likely to become an issue. Indonesia is not likely to face severe food security over the next 40 years (Falkenmark et al., 2009, Wu et al., 2011). However, recent studies that explore the impacts of climate change on marine fisheries, suggests that Indonesia could experience some of the largest decreases in marine fish stocks across the globe (Allison et al., 2009, Cheung et al., 2010).

Wu et al. (2011) simulated crop yields with the GIS-based Environmental Policy Integrated Climate (EPIC) model. This was combined with crop areas simulated by a crop choice decision model to calculate total food production and per capita food availability across the globe, which was used to represent the status of food availability and stability. The study focussed on the SRES A1 scenario and applied climate change simulations for the 2000s (1991–2000) and 2020s (2011–2020). The climate simulations were performed by MIROC (Model for Interdisciplinary Research on Climate) version 3.2., which means the effects of climate model uncertainty were not considered. Downscaled population and GDP data from the International Institute for Applied Systems Analysis (IIASA) were applied in the simulations. Wu et al. (2011) conclude that Indonesia is not likely to face severe food insecurity in the next 20 years. Moreover, Indonesia might be able to improve their food security situation due to either an increase in per capita food availability or an increase in the capacity to import food between 2000 and 2020.

A global analysis of food security under climate change scenarios for the 2050s by Falkenmark et al. (2009) considered the importance of water availability for ensuring global food security. The study presents an analysis of water constraints and opportunities for global food production on current croplands and assesses five main factors:

1) how far improved land and water management might go towards achieving global food security,

2) the water deficits that would remain in regions currently experiencing water scarcity and which are aiming at food self-sufficiency,

3) how the water deficits above may be met by importing food,

4) the cropland expansion required in low income countries without the needed purchasing power for such imports, and

5) the proportion of that expansion pressure which will remain unresolved due to potential lack of accessible land.

78

Similar to the study presented by Wu et al. (2011), there is no major treatment of modelling uncertainty; simulations were generated by only the LPJml dynamic global vegetation and water balance model (Gerten et al. 2004) with population growth and climate change under the SRES A2 emission scenario. Falkenmark et al. (2009) summarise the impacts of future improvements (or lack thereof) in water productivity for each country across the globe and show that this generates either a deficit or a surplus of water in relation to food water requirements in each country. These can be met either by trade or by horizontal expansion (by converting other terrestrial ecosystems to crop land). The study estimated that in 2050 around one third of the world's population will live in each of three regions: those that export food, those that import food, and those that have to expand their croplands at the expense of other ecosystems because they do not have enough purchasing power to import their food. The simulations demonstrated that Indonesia was a food exporting country in 2050.

The International Food Policy Research Institute (IFPRI) have produced a report and online tool that describes the possible impact of climate change on two major indicators of food security; 1) the number of children aged 0-5 malnourished, and 2) the average daily kilocalorie availability (Nelson et al., 2010, IFPRI, 2010). The study considered three broad socio-economic scenarios; 1) a 'pessimistic' scenario, which is representative of the lowest of the four GDP growth rate scenarios from the Millennium Ecosystem Assessment GDP scenarios and equivalent to the UN high variant of future population change, 2) a 'baseline' scenario, which is based on future GDP rates estimated by the World Bank and a population change scenario equivalent to the UN medium variant, and 3) an 'optimistic' scenario that is representative of the highest of the four GDP growth rate scenarios from the Millennium Ecosystem Assessment GDP scenarios and equivalent to the UN low variant of future population change. Nelson et al. (2010) also considered climate modelling and emission uncertainty and included a factor to account for CO_2 fertilisation in their work. The study applied two GCMs, the CSIRO GCM and the MIROC GCM, and forced each GCM with two SRES emissions scenarios (A1B and B1). They also considered a no climate change emissions scenario, which they called 'perfect mitigation' (note that in most other climate change impact studies that this is referred to as the baseline). The perfect mitigation scenario is useful to compare the effect of climate change against what might have happened without, but is not a realistic scenario itself. Estimates for both indicators of food security from 2010 to 2050, for Indonesia, are presented in Table 9 and Table 10. Figure 4 displays the effect of climate change, calculated by comparing the 'perfect mitigation' scenario with each baseline, optimistic and pessimistic scenario. The results show that average kilocalorie availability increases from 2010 to 2050 under the optimistic and baseline scenarios. However, climate change has the effect of mitigating availability by

around 300 calories in 2050, relative to the situation in the absence of climate change. Moreover, up to an 11% decline in kilocalorie availability is attributable to climate change in 2050. Similarly, the number of malnourished children declines from 2010 to 2050 but the effect of climate change contributes around 300,000 of the number of malnourished children in 2050, relative to the no climate change scenario. The increase in malnourishment attributable to climate change is appreciable, at up to around 19% by 2050. Figure 5 and Figure 6 show how the changes projected for Indonesia compare with the projections for the rest of the globe (IFPRI, 2010). This highlights that whilst malnourishment declines during 2010-2050, it remains high within the global context.

Scenario	2010	2050
Baseline CSI A1B	2714	2701
Baseline CSI B1	2719	2735
Baseline MIR A1B	2697	2635
Baseline MIR B1	2706	2679
Baseline Perfect Mitigation	2765	2958
Pessimistic CSI A1B	2753	2389
Pessimistic CSI B1	2758	2420
Pessimistic MIR A1B	2736	2330
Pessimistic MIR B1	2744	2368
Pessimistic Perfect Mitigation	2806	2618
Optimistic CSI A1B	2810	3221
Optimistic CSI B1	2813	3241
Optimistic MIR A1B	2790	3114
Optimistic MIR B1	2798	3160
Optimistic Perfect Mitigation	2861	3504

Table 9*. Average daily kilocalorie availability simulated under different climate and socioeconomic scenarios, for Indonesia (IFPRI, 2010).*

Scenario	2010	2050
Baseline CSI A1B	5.57	3.74
Baseline CSI B1	5.56	3.68
Baseline MIR A1B	5.6	3.84
Baseline MIR B1	5.58	3.77
Baseline Perfect Mitigation	5.46	3.35
Pessimistic CSI A1B	5.49	4.91
Pessimistic CSI B1	5.48	4.84
Pessimistic MIR A1B	5.52	5.03
Pessimistic MIR B1	5.51	4.95
Pessimistic Perfect Mitigation	5.39	4.46
Optimistic CSI A1B	5.38	2.58
Optimistic CSI B1	5.37	2.56
Optimistic MIR A1B	5.42	2.7
Optimistic MIR B1	5.4	2.65
Optimistic Perfect Mitigation	5.28	2.27

Table 10. Number of malnourished children (aged 0-5; millions) simulated under different climate and socioeconomic scenarios, for Indonesia (IFPRI, 2010).
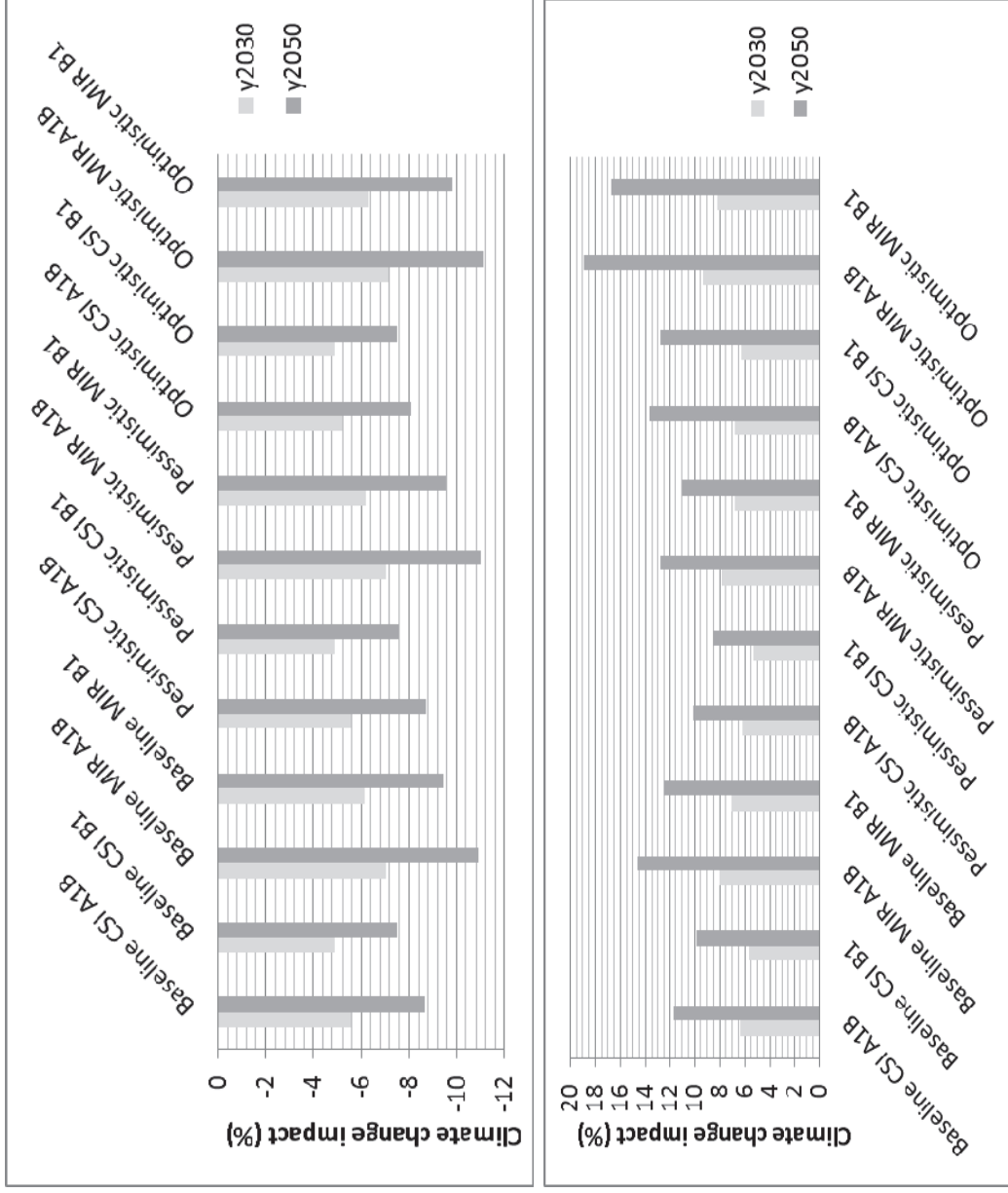
Figure 4. *The impact of climate change on average daily kilocalorie availability (top panel) and number of malnourished children (bottom) (IFPRI, 2010).*
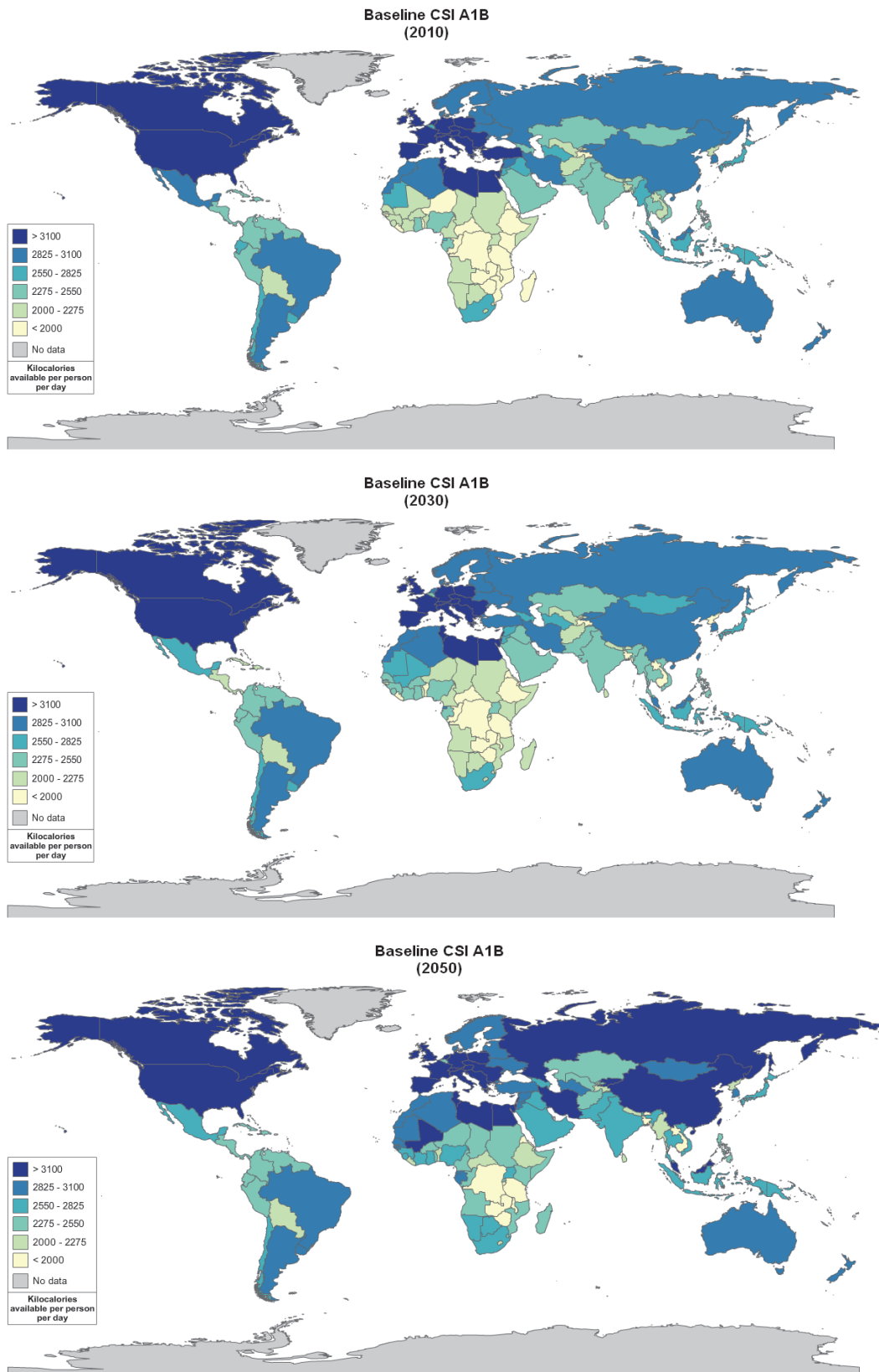
Figure 5. *Average daily kilocalorie availability simulated by the CSIRO GCM (CSI) under an A1B emissions scenario and the baseline socioeconomic scenario (IFPRI, 2010), for 2010 (top panel), 2030 (middle panel) and 2050 (bottom panel). The changes show the combination of both climate change and socio-economic changes.*

84
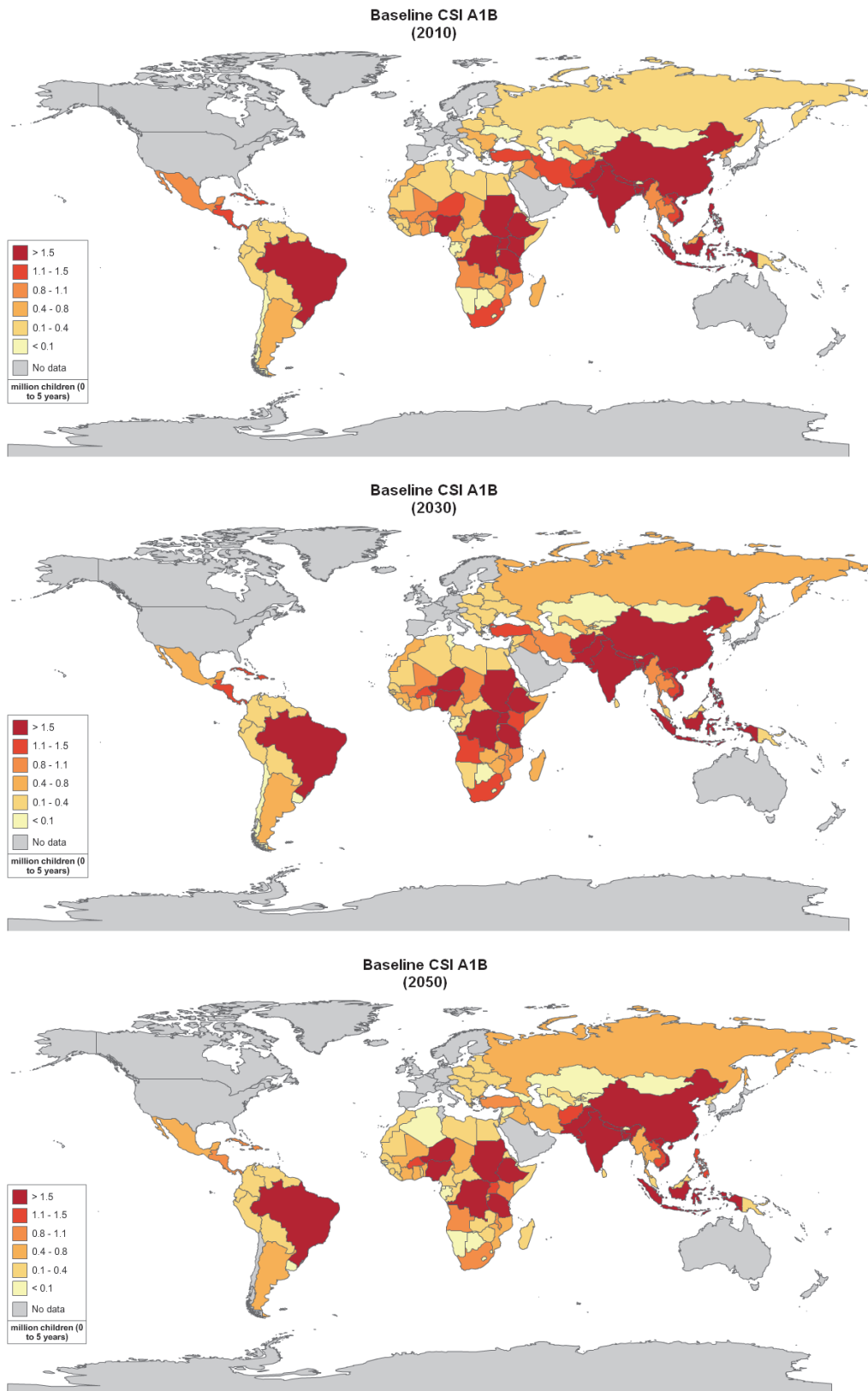
Figure 6. *Number of malnourished children (aged 0-5; millions) simulated by the CSIRO GCM (CSI) under an A1B emissions scenario and the baseline socioeconomic scenario (IFPRI, 2010), for 2010 (top panel), 2030 (middle panel) and 2050 (bottom panel). The changes show the combination of both climate change and socio-economic changes.*

It is important to note that up until recently, projections of climate change impacts on global food supply have tended to focus solely on production from terrestrial biomes, with the large contribution of animal protein from marine capture fisheries often ignored. However, recent studies have addressed this knowledge gap (Allison et al., 2009, Cheung et al., 2010). In addition to the direct affects of climate change, changes in the acidity of the oceans, due to increases in CO_2 levels, could also have an impact of marine ecosystems, which could also affect fish stocks. However, this relationship is complex and not well understood, and studies today have not been able to begin to quantify the impact of ocean acidification on fish stocks.

Allison et al. (2009) present a global analysis that compares the vulnerability of 132 national economies to potential climate change impacts on their capture fisheries. The study considered a country's vulnerability to be a function of the combined effect of projected climate change, the relative importance of fisheries to national economies and diets, and the national societal capacity to adapt to potential impacts and opportunities. Climate change projections from a single GCM under two emissions scenarios (SRES A1FI and B2) were used in the analysis. It should be noted, however, that results from studies that have applied only a single climate model or climate change scenario should be interpreted with caution. This is because they do not consider other possible climate change scenarios which could result in a different impact outcome, in terms of magnitude and in some cases sign of change. Allison et al. (2009) concluded that the national economy of Indonesia presented a moderate vulnerability to climate change impacts on fisheries. In contrast, countries in Central and Western Africa (e.g. Malawi, Guinea, Senegal, and Uganda), Peru and Colombia in north-western South America, and four tropical Asian countries (Bangladesh, Cambodia, Pakistan, and Yemen) were identified as most vulnerable (see Figure 7).
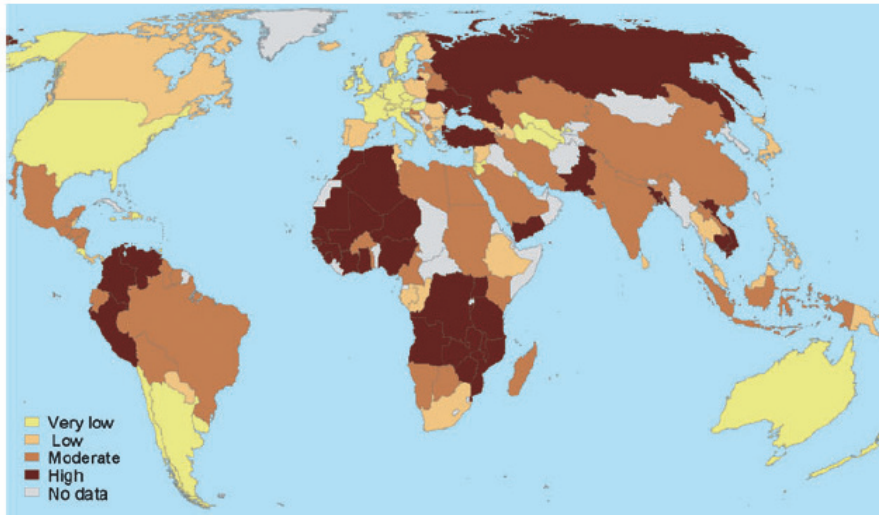
Figure 7. Vulnerability of national economies to potential climate change impacts on fisheries under SRES B2 (Allison et al., 2009). Colours represent quartiles with dark brown for the upper quartile (highest index value), yellow for the lowest quartile, and grey where no data were available.

This is supported by results presented by Cheung et al. (2010); here, even more severe impacts on marine fisheries are suggested due to climate change. Cheung et al. (2010) projected changes in global catch potential for 1066 species of exploited marine fish and invertebrates from 2005 to 2055 under climate change scenarios. Cheung et al. (2010) found that climate change may lead to large-scale redistribution of global catch potential, with an average of 30–70% increase in high-latitude regions and a decline of up to 40% in the tropics. The simulations were based climate simulations from a single GCM (GFDL CM2.1) under a SRES A1B emissions scenario (CO_2 concentration at 720ppm in 2100) and a stable-2000 level scenario (CO_2 concentration maintains at year 2000 level of 365 ppm). The limitations of applying a single GCM have been noted previously. For Indonesia, the projected change in the 10-year averaged maximum catch potential from 2005 to 2055 was around a 23% reduction under A1B. Climate change mitigation reduced this somewhat, but still, the stabilisation scenario considered by Cheung et al. (2010) suggested that a 7% reduction in maximum catch potential was possible. These changes were based upon 45 exploited species included in the analysis. Figure 8 demonstrates how this compares with projected changes for other countries across the globe, which highlights that of the 20 countries considered by Cheung et al. (2010), Indonesia experienced the most severe impact.
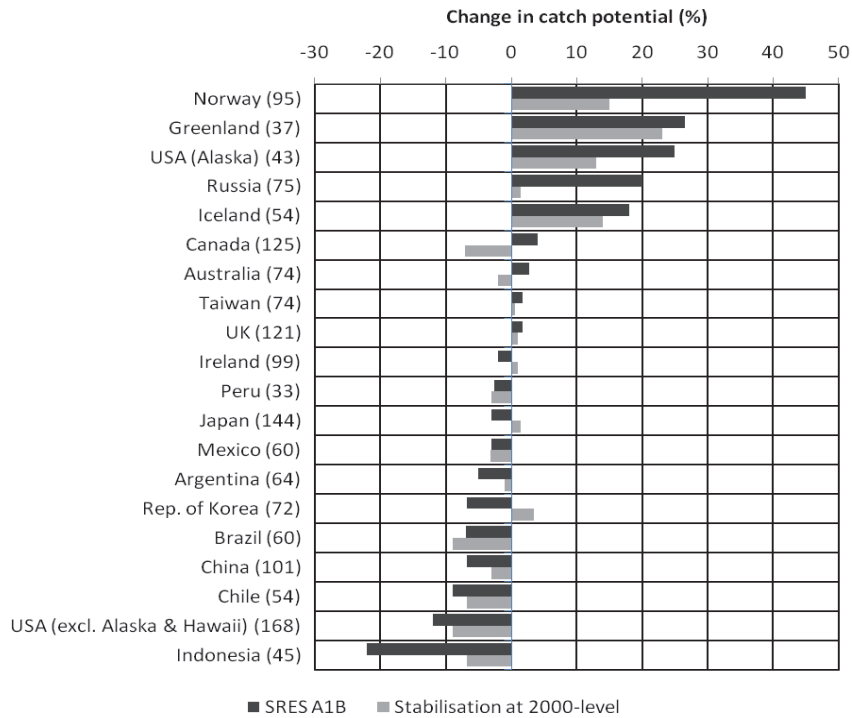
Figure 8. *Projected changes in the 10-year averaged maximum catch potential from 2005 to 2055. The numbers in parentheses represent the numbers of exploited species included in the analysis. Adapted from Cheung et al. (2010).*

National-scale or sub-national scale assessments

Literature searches yielded no results for national-scale or sub-national scale studies for this impact sector.

Water stress and drought

Headline

There are currently few studies on the impact of climate change on water stress and drought in Indonesia. One study that applied climate change simulations from only a single climate model suggests that water stress may not increase with climate change in Indonesia. Simulations that apply 21 climate models, by the AVOID programme, support this.

Supporting literature

Introduction

For the purposes of this report droughts are considered to be extreme events at the lower bound of climate variability; episodes of prolonged absence or marked deficiency of precipitation. Water stress is considered as the situation where water stores and fluxes (e.g. groundwater and river discharge) are not replenished at a sufficient rate to adequately meet water demand and consumption.

A number of impact model studies looking at water stress and drought for the present (recent past) and future (climate change scenario) have been conducted. These studies are conducted at global or national scale and include the application of global water 'availability' or 'stress' models driven by one or more climate change scenario from one or more GCM. The approaches variously include other factors and assumptions that might affect water availability, such as the impact of changing demographics and infrastructure investment, etc. These different models (hydrological and climate), assumptions and emissions scenarios mean that there are a range of water stress projections for Indonesia. This section summarises findings from these studies to inform and contextualise the analysis performed by the AVOID programme for this project. The results from the AVOID work and discussed in the next section.

Important knowledge gaps and key uncertainties which are applicable to Indonesia as well as at the global-scale, include; the appropriate coupling of surface water and groundwater in hydrological models, including the recharge process, improved soil moisture and evaporation

dynamics, inclusion of water quality, inclusion of water management (Wood et al. 2011) and further refinement of the down-scaling methodologies used for the climate driving variables (Harding et al. 2011).

## *Assessments that include a global or regional perspective*

Recent past

Recent research presented by Vörösmarty et al. (2010) describes the calculation of an '*Adjusted Human Water Security Threat'* (HWS) indicator. The indicator is a function of the cumulative impacts of 23 biophysical and chemical drivers simulated globally across 46,517 grid cells representing 99.2 million km^2. With a digital terrain model at its base, the calculations in each of the grid boxes of this model take account of the multiple pressures on the environment, and the way these combine with each other, as water flows in river basins. The level of investment in water infrastructure is also considered. This infrastructure measure (the *investment benefits factor*) is based on actual existing built infrastructure, rather than on the financial value of investments made in the water sector, which is a very unreliable and incomplete dataset. The analysis described by Vörösmarty et al. (2010) represents the current state-of-the-art in applied policy-focussed water resource assessment. In this measure of water security, the method reveals those areas where this is lacking, which is a representation of human water stress. One drawback of this method is that no analysis is provided in places where there is 'no appreciable flow', where rivers do not flow, or only do so for such short periods that they cannot be reliably measured. This method also does not address places where water supplies depend wholly on groundwater or desalination, being piped in, or based on wastewater reuse. It is based on what is known from all verified peer reviewed sources about surface water resources as generated by natural ecosystem processes and modified by river and other hydraulic infrastructure (Vörösmarty et al., 2010).

Here, the present day HWS is mapped for Indonesia. The model applied operates at 50km resolution, so, larger countries appear to have smoother coverage than smaller countries, but all are mapped and calculated on the same scale, with the same data and model, and thus comparisons between places are legitimate. It is important to note that this analysis is a comparative one, where each place is assessed *relative* to the rest of the globe. In this way, this presents a realistic comparison of conditions across the globe. As a result of this, however, some places may seem to be less stressed than may be originally considered. One example is Australia, which is noted for its droughts and long dry spells, and while there are some densely populated cities in that country where water stress is a real issue, for most

of the country, *relative to the rest of the world*, the measure suggests water stress (as measured by HWS defined by Vörösmarty et al. (2010)), is not a serious problem.

Figure 9 presents the results of this analysis for Indonesia. Indonesia is made up of thousands of islands, many of them too small to feature in this analysis which is based on grid cells of 50km resolution. Of the major islands however, all are under moderate to high levels of threat to human water security.
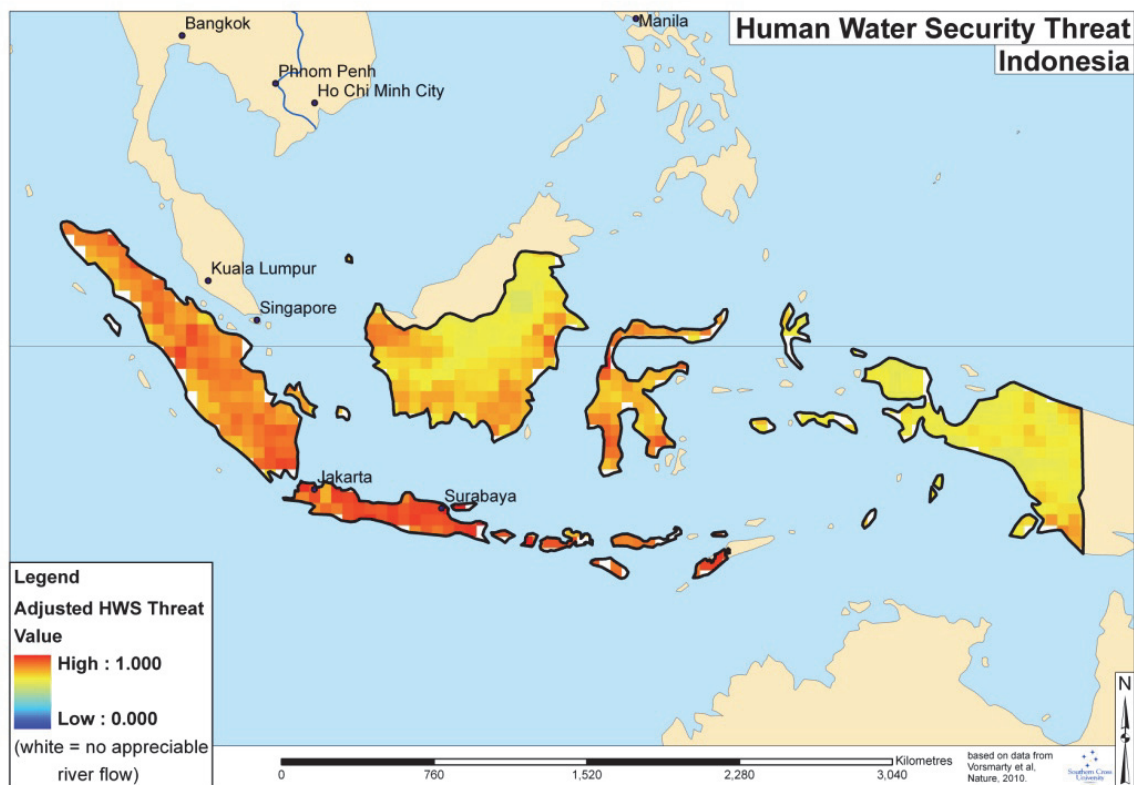
Figure 9. *Present Adjusted Human Water Security Threat (HWS) for Indonesia, calculated following the method described by Vörösmarty et al. (2010).*

Climate change studies

Rockstrom et al. (2009) applied the LPJml vegetation and water balance model (Gerten et al. 2004) to assess green-blue water (irrigation and infiltrated water) availability and requirements. The authors applied observed climate data from the CRU TS2.1 gridded dataset for a present-day simulation, and climate change projections from the HadCM2 GCM under the SRES A2 scenario to represent the climate change scenario for the year 2050. The study assumed that if water availability was less than 1,300m^3/capita/year, then the country was considered to present insufficient water for food self-sufficiency. The simulations presented by Rockstrom et al. (2009) should not be considered as definitive, however,

because the study only applied one climate model, which means climate modelling uncertainty was overlooked. The results from the two simulations are presented in Figure 10. Rockstrom et al. (2009) found that globally in 2050 and under the SRES A2 scenario, around 59% of the world's population would be exposed to "blue water shortage" (i.e. irrigation water shortage), and 36% exposed to "green water shortages" (i.e. infiltrated rain shortage For Indonesia, Rockstrom et al. (2009) found that blue-green water availability was well above the 1,300m^3/capita/year threshold in present and under climate change. Although water availability does decline with climate change, there is no indication that the country could face water scarcity in the future when considering such a measure of water stress at the national scale.
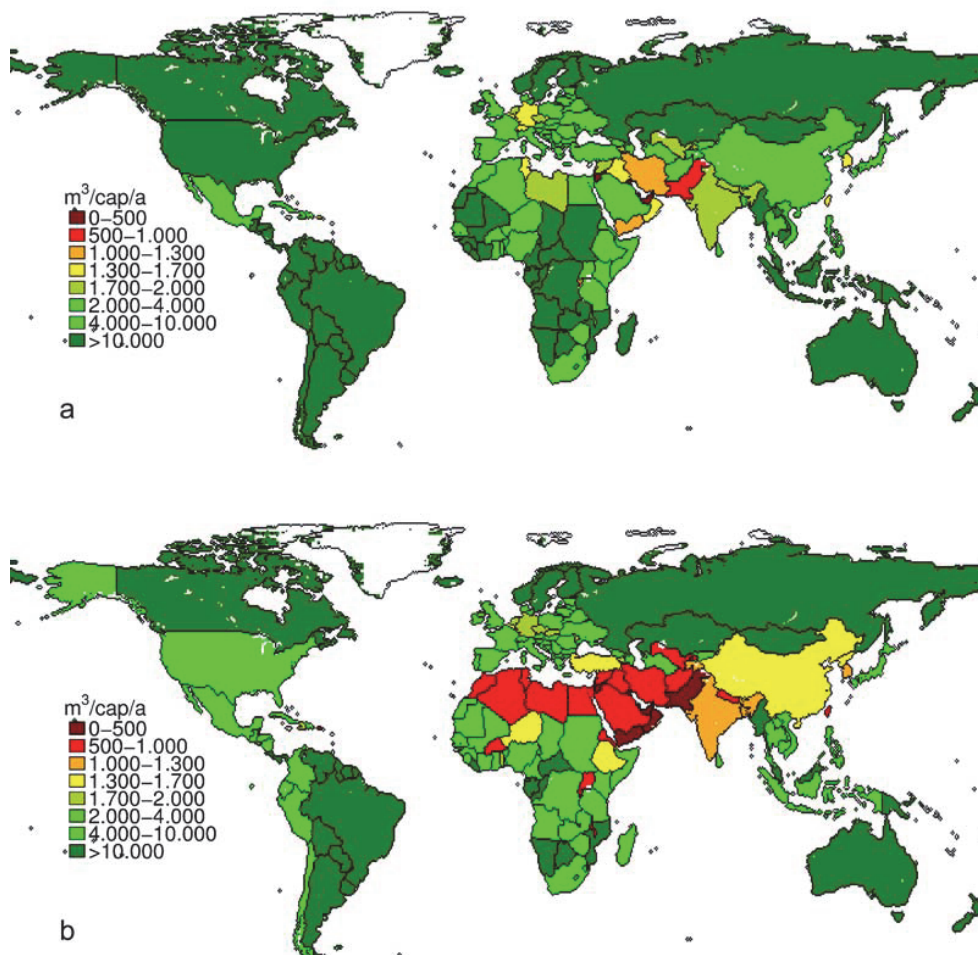
Figure 10. *Simulated blue-green water availability (m^3/capita/year) for present climate (top panel) and including both demographic and climate change under the SRES A2 scenario in 2050 (bottom panel). The study assumed that if water availability was less than 1,300m^3/capita/year, then the country was considered to present insufficient water for food self-sufficiency. The figure is from Rockstrom et al. (2009).*

National-scale or sub-national scale assessments

D'Arrigo and Wilson (2008) note that Indonesia is impacted by severe droughts that cause major food shortages over much of the country, and that these have long been linked with El Niño events in the tropical Pacific Ocean. The authors suggest that an increase in Asian monsoon intensity that is simulated by some GCMs may intensify Indonesian droughts under future warming. However, large uncertainties remain in future projections of the Asian monsoon and ENSO systems. Naylor et al. (2007) examined the potential impacts of El Niño on rice yields in Indonesia in 2050, focusing on Java and Bali. By applying climate projections from the CMIP3 multi-model dataset, they presented a projected increase in the probability of a 30-day delay in monsoon rainfall for Indonesia.

AVOID Programme Results

To further quantify the impact of climate change on water stress and the inherent uncertainties, the AVOID programme calculated water stress indices for all countries reviewed in this literature assessment based upon the patterns of climate change from 21 GCMs, following the method described by Gosling et al. (2010) and Arnell (2004). This ensures a consistent methodological approach across all countries and takes consideration of climate modelling uncertainties.

Methodology

The indicator of the effect of climate change on exposure to water resources stress has two components. The first is the number of people within a region with an *increase in exposure to stress*, calculated as the sum of 1) people living in water-stressed watersheds with a significant reduction in runoff due to climate change and 2) people living in watersheds which become water-stressed due to a reduction in runoff. The second is the number of people within a region with a *decrease in exposure to stress*, calculated as the sum of 1) people living in water-stressed watersheds with a significant increase in runoff due to climate change and 2) people living in watersheds which cease to be water-stressed due to an increase in runoff. It is not appropriate to calculate the net effect of "increase in exposure" and "decrease in exposure", because the consequences of the two are not equivalent. A water-stressed watershed has an average annual runoff less than $1000m^3$/capita/year, a widely used indicator of water scarcity. This indicator may underestimate water stress in

watersheds where per capita withdrawals are high, such as in watersheds with large withdrawals for irrigation.

Average annual runoff (30-year mean) is simulated at a spatial resolution of 0.5x0.5o using a global hydrological model, MacPDM (Gosling and Arnell, 2011), and summed to the watershed scale. Climate change has a "significant" effect on average annual runoff when the change from the baseline is greater than the estimated standard deviation of 30-year mean annual runoff: this varies between 5 and 10%, with higher values in drier areas.

The pattern of climate change from 21 GCMs was applied to MacPDM, under two emissions scenarios; 1) SRES A1B and 2) an aggressive mitigation scenario where emissions follow A1B up to 2016 but then decline at a rate of 5% per year thereafter to a low emissions floor (denoted A1B-2016-5-L). Both scenarios assume that population changes through the 21st century following the SRES A1 scenario as implemented in IMAGE 2.3 (van Vuuren et al., 2007). The application of 21 GCMs is an attempt to quantify the uncertainty due to climate modelling, although it is acknowledged that only one impacts model is applied (MacPDM). Simulations were performed for the years 2030, 2050, 2080 and 2100. Following Warren et al. (2010), changes in the population affected by increasing or decreasing water stress represent the additional percentage of population affected due to climate change, not the absolute change in the percentage of the affected population relative to present day.

Results

The results for Indonesia are presented in Figure 11 and they show no appreciable increases or decreases in population exposed to water stress with climate change.
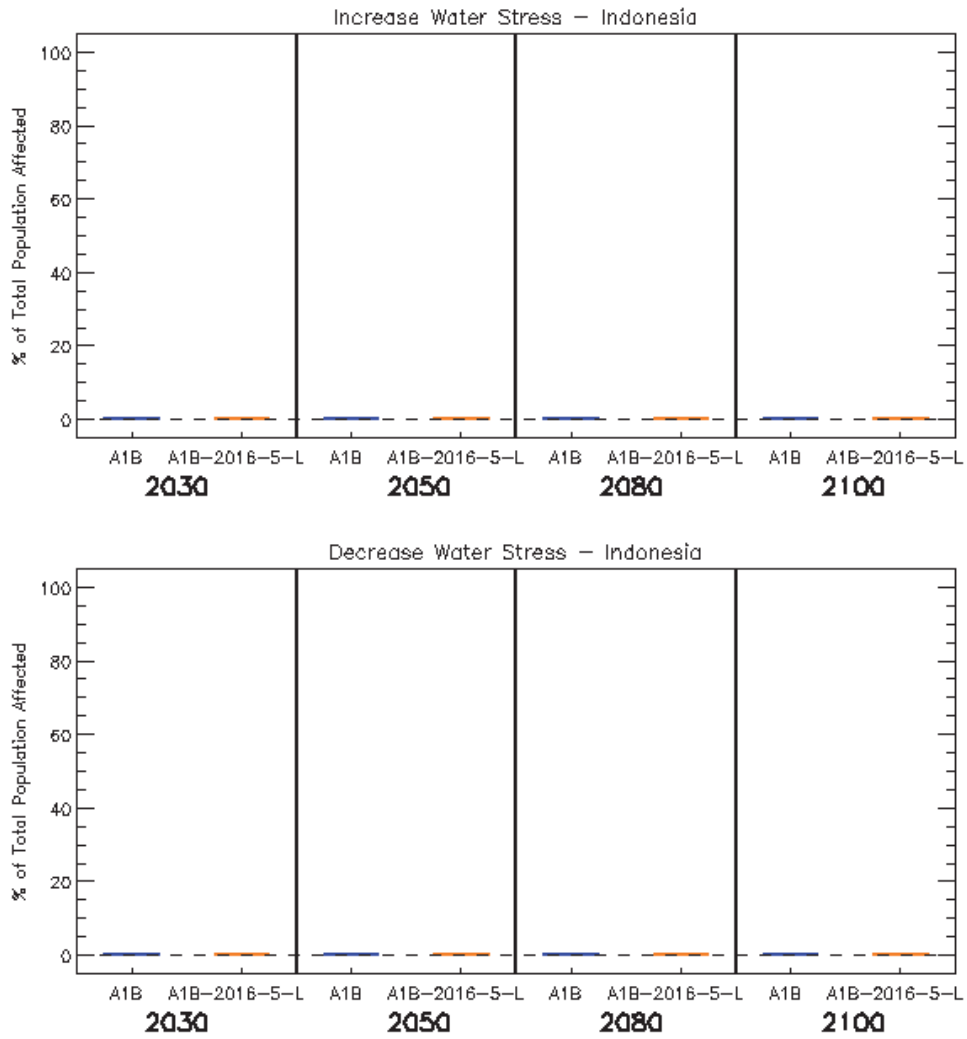
Figure 11. *Box and whisker plots for the impact of climate change on increased water stress (top panel) and decreased water stress (bottom panel) in Indonesia, from 21 GCMs under two emissions scenarios (A1B and A1B-2016-5-L), for four time horizons. The plots show the 25th, 50th, and 75th percentiles (represented by the boxes), and the maximum and minimum values (shown by the extent of the whiskers).*

Pluvial flooding and rainfall

Headline

The IPCC AR4 reported potential increases in precipitation over Indonesia under global climate change projections. However, few studies relevant to Indonesia have been published since. To this end, large uncertainties remain, particularly regarding the response of the El Niño Southern Oscillation (ENSO) to climate change.

Supporting literature

Introduction

Pluvial flooding can be defined as flooding derived directly from heavy rainfall, which results in overland flow if it is either not able to soak into the ground or exceeds the capacity of artificial drainage systems. This is in contrast to fluvial flooding, which involves flow in rivers either exceeding the capacity of the river channel or breaking through the river banks, and so inundating the floodplain. Pluvial flooding can occur far from river channels, and is usually caused by high intensity, short-duration rainfall events, although it can be caused by lower intensity, longer-duration events, or sometimes by snowmelt. Changes in mean annual or seasonal rainfall are unlikely to be good indicators of change in pluvial flooding; changes in extreme rainfall are of much greater significance. However, even increases in daily rainfall extremes will not necessarily result in increases in pluvial flooding, as this is likely to be dependent on the sub-daily distribution of the rainfall as well as local factors such as soil type, antecedent soil moisture, land cover (especially urbanisation), capacity and maintenance of artificial drainage systems etc. It should be noted that both pluvial and fluvial flooding can potentially result from the same rainfall event.

Indonesia is strongly affected by ENSO-related climate variability, with drought during El Niño events and floods during La Nina. The 1997/98 El Niño triggered forest fires over large areas. The after-effects of forest loss, including soil degradation, lead to an increased flood risk. Jakarta suffered floods in early 2007, and other parts of Java have also been afflicted

over the past decade, with some observational evidence that the flood risk is increasing (Hidayat, 2009).

Assessments that include a global or regional perspective

The IPCC AR4 (2007b) reported that mean precipitation over Southeast Asia increased in most model simulations included in the CMIP3 multi-model dataset, with a median change of 7% annually, but projected regional changes vary strongly within the region. Larger increases of 15% are projected in annual maximum precipitation over the region. The strongest and most consistent precipitation increases broadly followed the Inter-Tropical Convergence Zone (ITCZ) over northern Indonesia in June-August and southern Indonesia in December-February (IPCC, 2007b). The region could also experience a general tendency for daily precipitation extremes to become more intense under climate change, particularly where mean precipitation is expected to increase.

National-scale or sub-national scale assessments

Recent past

Aldrain and Djamil (2008) find that historic rainfall records in East Java show an increase in the ratio of rainfall during the wet season, leading to an increased threat of extreme weather in the monsoon season and more severe drought in the dry season. Hidayat (2009) note that local studies point towards increases in mean and extreme rainfall, a main cause of floods in Java.

Climate change studies

Prior to IPCC AR4, Boer and Faqih (2004) compared patterns of change across Indonesia using five GCMs, and obtained highly contrasting results. Their conclusion was that "no generalisation could be made on the impact of global warming on rainfall" in the region. Rainfall variability under climate change could be affected by changes in ENSO, and its effect on monsoon variability, which are mechanisms that are not well understood.

Fluvial flooding

Headline

Results from one recent global-scale study suggest that extreme flooding could increase in Indonesia with climate change. Simulations by the AVOID programme, based on 21 GCMs, support these results. A majority of the models show a tendency for increasing flood risk, particularly later in the century and in the A1B scenario, and in some models this increase is very large. However, few studies have made projections of changes in flood hazard under climate change in Indonesia at national or local scale. Given that severe floods have affected Indonesia several times in recent history, a recommended avenue for further research is to better quantify the risk of flooding in Indonesia under climate change scenarios.

Supporting literature

Introduction

This section summarises findings from a number of post IPCC AR4 assessments on river flooding in Indonesia to inform and contextualise the analysis performed by the AVOID programme for this project. The results from the AVOID work are discussed in the next section.

Fluvial flooding involves flow in rivers either exceeding the capacity of the river channel or breaking through the river banks, and so inundating the floodplain. A complex set of processes is involved in the translation of precipitation into runoff and subsequently river flow (routing of runoff along river channels). Some of the factors involved are; the partitioning of precipitation into rainfall and snowfall, soil type, antecedent soil moisture, infiltration, land cover, evaporation and plant transpiration, topography, groundwater storage. Determining whether a given river flow exceeds the channel capacity, and where any excess flow will go, is also not straightforward, and is complicated by the presence of artificial river embankments and other man-made structures for example. Hydrological models attempt to simplify and conceptualise these factors and processes, to allow the simulation of runoff and/or river flow under different conditions. However, the results from global-scale

hydrological modelling need to be interpreted with caution, especially for smaller regions, due to the necessarily coarse resolution of such modelling and the assumptions and simplifications this entails (e.g. a 0.5^o grid corresponds to landscape features spatially averaged to around 50-55km for mid- to low-latitudes). Such results provide a consistent, high-level picture, but will not show any finer resolution detail or variability. Smaller-scale or catchment-scale hydrological modelling can allow for more local factors affecting the hydrology, but will also involve further sources of uncertainty, such as in the downscaling of global climate model data to the necessary scale for the hydrological models. Furthermore, the application of different hydrological models and analysis techniques often makes it difficult to compare results for different catchments.

Severe flood events have affected Indonesia, and particularly Java, in recent years, such as the flooding in Jakarta in early 2007, and in the Bengawan Solo Basin (Central and East Java) in late December 2007 and early 2008, and again in 2009 (Hidayat, 2009). Although flood risk in Indonesia has been increasing, few studies have actually made projections of changes in flood hazard under climate change.

Assessments that include a global or regional perspective

Climate change studies

A global modelling study presented by Hirabayashi et al. (2008), which applied climate change simulations from a single GCM under the A1B emissions scenario, suggests for the next few decades (2001-2030) only localised decreases in the return period of what was a 100-year flood event in the 20th century. By the end of the century (2071-2100) the return period of a 100-year event was a projected to reduce to 40 years or less across the entire country, suggesting a strong and widespread increase in the probability of extreme flooding events. It should be noted, however, that results from studies that have applied only a single climate model or climate change scenario should be interpreted with caution. This is because they do not consider other possible climate change scenarios which could result in a different impact outcome, in terms of magnitude and in some cases sign of change.

National-scale or sub-national scale assessments

Recent past

There is convincing evidence that the flood risk in Indonesia is increasing. Since 1985, more than 150 flood events have been recorded in the country, 54 of which were classified as severe (Hidayat, 2009). Rainfall records in East Java show an increase in the proportion of

rainfall during the wet season, leading to an increased threat of extreme weather in the monsoon season and more severe drought in the dry season (Aldrian and Djamil, 2008). These trends may be further exacerbated by ongoing forest degradation (Wahyu et al., 2010).

Climate change studies

Literature searches yielded no results for national-scale or sub-national scale studies of future changes in flood risk in Indonesia under climate change.

AVOID programme results

To quantify the impact of climate change on fluvial flooding and the inherent uncertainties, the AVOID programme calculated an indicator of flood risk for all countries reviewed in this literature assessment based upon the patterns of climate change from 21 GCMs (Warren et al., 2010). This ensures a consistent methodological approach across all countries and takes consideration of climate modelling uncertainties.

Methodology

The effect of climate change on fluvial flooding is shown here using an indicator representing the percentage change in average annual flood risk within a country, calculated by assuming a standardised relationship between flood magnitude and loss. The indicator is based on the estimated present-day (1961-1990) and future flood frequency curve, derived from the time series of runoff simulated at a spatial resolution of $0.5°x0.5°$ using a global hydrological model, MacPDM (Gosling and Arnell, 2011). The flood frequency curve was combined with a generic flood magnitude–damage curve to estimate the average annual flood damage in each grid cell. This was then multiplied by grid cell population and summed across a region, producing in effect a population-weighted average annual damage. Flood damage is thus assumed to be proportional to population in each grid cell, not the value of exposed assets, and the proportion of people exposed to flood is assumed to be constant across each grid cell (Warren et al., 2010).

The national values are calculated across major floodplains, based on the UN PREVIEW Global Risk Data Platform (preview.grid.unep.ch). This database contains gridded estimates, at a spatial resolution of 30 arc-seconds ($0.00833°x0.00833°$), of the estimated frequency of flooding. From this database the proportion of each $0.5°x0.5°$ grid cell defined as floodplain

was determined, along with the numbers of people living in each 0.5°x0.5° grid cell in flood-prone areas. The floodplain data set does not include "small" floodplains, so underestimates actual exposure to flooding. The pattern of climate change from 21 GCMs was applied to MacPDM, under two emissions scenarios; 1) SRES A1B and 2) an aggressive mitigation scenario where emissions follow A1B up to 2016 but then decline at a rate of 5% per year thereafter to a low emissions floor (denoted A1B-2016-5-L). Both scenarios assume that population changes through the 21st century following the SRES A1 scenario as implemented in IMAGE 2.3 (van Vuuren et al., 2007). The application of 21 GCMs is an attempt to quantify the uncertainty due to climate modelling, although it is acknowledged that only one impacts model is applied (MacPDM). Simulations were performed for the years 2030, 2050, 2080 and 2100. The result represents the change in flood risk due to climate change, not the change in flood risk relative to present day (Warren et al., 2010).

Results

The results for Indonesia are presented in Figure 12. By the 2030s, the models project a range of changes in mean fluvial flooding risk over Indonesia in both scenarios, with some models projecting decreases and others increases. However, the balance is much more towards higher flood risk, with three quarters of the models projecting an increase. The largest decrease projected for the 2030s is about 30%, and the largest increase is 150%. The mean across all projections is approximately a 30% increase in average annual flood risk.

By 2100 the balance shifts even more towards higher flood risk in both scenarios, and the difference in projections from the different models also becomes greater. Both these aspects of the results are more pronounced for the A1B scenario than the mitigation scenario. Under the mitigation scenario, a minority of the models still project a decline in flood risk (down to −40%), but most models project increased flood risk. The mean over all projections is a 40% increase, and the largest increase is about +300%. Under the A1B scenario, a large majority of the models project a higher flood risk, but still a few models project decreased flood risk (down to −40%). The largest projected increase is approximately +900%, with the mean over all projections being an increase in annual average flood risk of approximately 150%.

So for Indonesia, the models show a much greater tendency for increasing flood risk, particularly later in the century and particularly in the A1B scenario. This increase in flood risk can potentially be very large. Differences between the model projections are also greater later in the century and particularly for A1B.
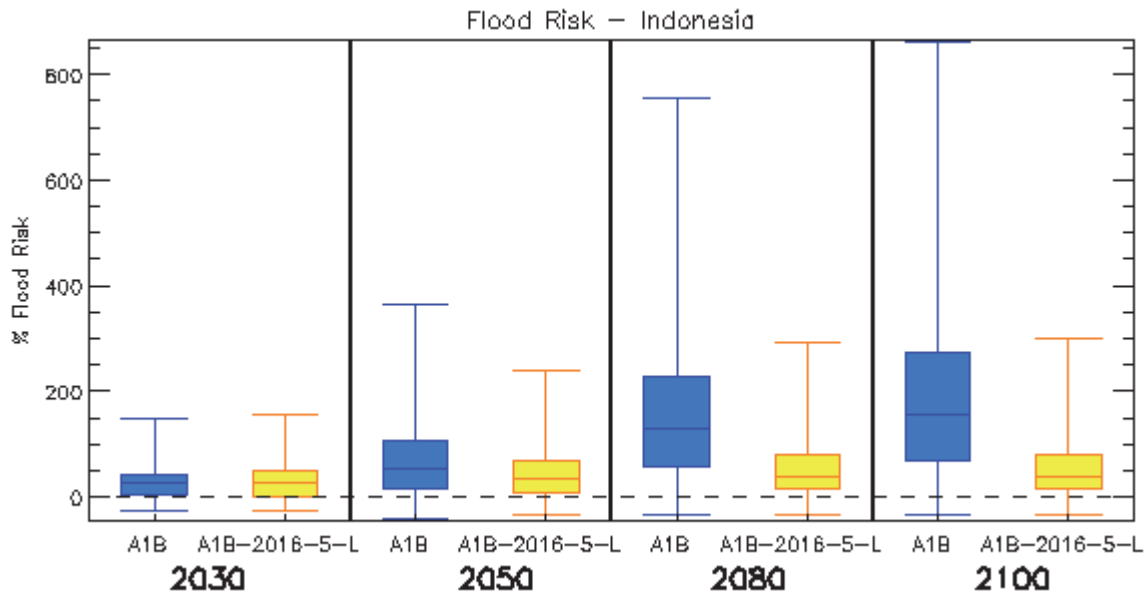
Figure 12. *Box and whisker plots for the percentage change in average annual flood risk within Indonesia, from 21 GCMs under two emissions scenarios (A1B and A1B-2016-5-L), for four time horizons. The plots show the 25th, 50th, and 75th percentiles (represented by the boxes), and the maximum and minimum values (shown by the extent of the whiskers).*

Tropical cyclones

Headline

Most studies reviewed here suggest that the frequency of landfalling tropical cyclones in Indonesia could decrease with climate change, for both West Pacific, affecting the eastern part of the country; and South Indian Ocean cyclones, affecting the western and southern regions. However, most studies reviewed suggest that the intensity of cyclones could increase with climate change, particularly for the most severe storms. The combination of these two effects, and the uncertainties in each of their magnitudes, leads to considerable uncertainty in the estimation of future cyclone damages in Indonesia under climate change.

Supporting literature

Introduction

Cyclones in the tropics are different from those that exist in mid-latitudes in the way that they form and develop. There remains an overall large uncertainty in the current understanding of how tropical cyclones might be affected by climate change because conclusions are based upon a limited number of studies. Moreover, the majority of tropical-cyclone projections are from either coarse-resolution global models or from statistical or dynamical downscaling techniques. The former are unable to represent the most-intense storms, whereas the very patterns used for the downscaling may change in itself under climate change. To this end, caution should be applied in interpreting model-based results, even where the models are in agreement.

Assessments that include a global or regional perspective

Indonesia is affected by cyclones that form in both the South Indian Ocean near the northern coast of Australia, and the West Pacific. Since all studies considered in this literature assessment separately analysed the response of cyclones in each of these basins to climate change, the basins will be considered separately here as well. The projections are similar

for the two basins; a possible decrease in cyclone *frequencies* and a possible increase in cyclone *intensities*.

South Indian Ocean

Most of the modelling studies considered simulate a decrease in the *frequency* of South Indian Ocean cyclones under climate change, but an increase in cyclone *intensity*. Note, however, that these results are aggregated over the entire basin. There is currently considerable uncertainty at the sub-basin scale, with no models able to reliably simulate whether particular portions of the basin (i.e., the Indonesian coast) will experience an increase or decrease in cyclone frequency or intensity.

Assessments of cyclone frequency

Sugi et al. (2002) conducted a ten-year timeslice experiment (experiments over a short period of time to enable ensemble simulations using reasonable amounts of computational power) using the Japan Meteorological Agency (JMA) atmosphere-only model at 120km resolution, driven by the changes in sea surface temperature (SST) and sea ice simulated by the MRI GCM under $2xCO_2$ conditions. The JMA model simulated a 57% decrease in the frequency of tropical cyclones in the South Indian Ocean. In a much finer-resolution timeslice experiment, Oouchi et al. (2006) applied the JMA model at 20km for ten years, using the SSTs and sea ice simulated by the MRI GCM under the A1B emissions scenario for the 2080-2099 time horizon. The authors found that South Indian Ocean cyclones decreased in frequency by 28%. Sugi et al. (2002) concluded that the decreases were due to increased atmospheric stability in a warmer world; the model simulated a 10% increase in the dry static stability, defined as the difference in potential temperature between the 250hPa level of the atmosphere and the land surface.

Zhao et al. (2009) applied the 50km GFDL GCM with four future SST and sea ice distributions; 1) the ensemble mean from 18 GCMs, 2) the HadCM3 GCM, 3) the GFDL GCM, and 4) the ECHAM5 GCM. The SSTs distributions were for the A1B emissions scenario for the 2081-2100 time horizon. In all four experiments, the frequency of cyclones in the South Indian Ocean basin decreased. The range of decreases was 13-41%, with three of the four models simulating decreases over 30%.

Further evidence for decreasing cyclone frequencies in this basin under climate change is presented by Sugi et al. (2009). In this study, the authors conducted timeslice experiments

with the JMA model, driven at 60km and 20km resolutions respectively, with SSTs and sea ice from three individual GCMs and the CMIP3 multi-model dataset ensemble mean, for a total of eight simulations, all under the A1B emissions scenario. For the South Indian Ocean, six simulations presented decreases in frequency (18-28%), one simulation showed little change (5%) and one simulation presented an increase (10%).

Emanuel et al. (2008) applied a hybrid statistical-dynamical downscaling method to seven GCMs under the A1B emissions scenario for the 2180-2200 time horizon. The technique "seeds" large numbers of tropical-cyclone vortices into each basin, then uses the models' large-scale climate fields (e.g., SSTs, wind shear, relative humidity) to determine whether the storms grow into cyclones or simply decay. The technique has shown considerable skill at simulating both frequency and intensity of storms over the past several decades, when driven by reanalysis data. By comparing the A1B scenario results for 2180-2200 to downscaled reanalysis data for 1980-2000, the authors concluded that South Indian Ocean cyclone numbers could decrease by 12% with climate change. The seven individual GCMs showed high consistency; all simulated a decrease, although the magnitudes varied between 2% and 22%. The spatial maps of variations in cyclogenesis under climate change presented by Emanuel et al. (2008) showed particularly large decreases near the coast of Indonesia, far higher than the basin average. There is currently very high uncertainty in these sub-basin-scale changes, however.

Only one study has simulated an increase in South Indian Ocean cyclone frequency with climate change. McDonald et al. (2005) conducted a 15-year timeslice experiment with the Hadley Centre atmospheric model (HadAM3) at 100km resolution, driven by SST and sea-ice changes from the HadCM3 GCM under the IPCC IS95a emissions scenario for the 2081-2100 time horizon. The authors compared the results of this timeslice experiment to a similar conducted for 1979-1994, but using observed SSTs and sea-ice. The 2081-2100 period showed a 10% increase in the South Indian Ocean, but this result was not statistically significant at the 5% level. The authors attributed the increase in genesis to the projected SST warming in the Indian Ocean being greater than the tropics-mean SST warming; the model also simulated reduced vertical wind shear, which is conducive to tropical cyclogenesis (formation of cyclones), for much of the eastern half of the basin.

Assessment of cyclone intensity

Despite the possible decrease in cyclone *frequency*, cyclone *intensities* in the South Indian Ocean could increase with climate change. These intensity increases follow those simulated for global cyclones, with the most intense storms expected to show the largest percentage

increases in intensity (Bender et al., 2010, Knutson et al., 2010b, Knutson et al., 2010a, Knutson et al., 2008). The 20km JMA model described by Oouchi et al. (2006) simulated a 17.3% increase in the average intensity of South Indian Ocean cyclones by 2100 under the A1B emissions scenario. The hybrid statistical-dynamical method described by Emanuel et al. (2008) showed a mean 3% increase in cyclone intensity across the seven GCMs under the A1B emissions scenario for the 2180-2200 time horizon, although it is worth noting that two GCMs simulated a decrease in mean intensities.

Further evidence for tropical cyclone intensity increases with climate change is from studies that have applied cyclone potential-intensity theory to the output of the GCMs. Yu et al. (2010) compared projections from 18 GCMs of potential-intensity changes, under the A1B emissions scenario. In an average across all GCMs, the South Indian Ocean showed increases in potential intensity of approximately 3.5% per 1°C of global-mean warming. These increases were the largest of any ocean basin, which the authors attributed to projections of reduced vertical wind shear in a warmer world; low wind shear supports cyclone genesis and maintenance. Vecchi and Soden (2007) also applied a version of potential intensity theory to the same GCM projections, finding that on average, the potential intensity of South Indian Ocean cyclones increased by 3.7% by 2100 under A1B emissions. The individual models varied in their simulations however, ranging from a 3.3% decrease to a 16.0% increase.

West Pacific

Projections of changes in tropical-cyclone frequency in the West Pacific basin remain highly uncertain, even on the sign of the change. However, several studies report a northward and eastward shift in tropical cyclogenesis in this basin under climate change, which gives greater weight to the projections of a decrease in cyclone frequency near Indonesia. (Note that the details of those already considered for the South Indian Ocean are not repeated here.)

Assessment of cyclone frequency

Bengtsson et al. (2007) conducted timeslice experiments with the atmospheric component of the ECHAM5 GCM at 60km and 40km resolutions respectively. The model was driven by the SSTs and sea ice simulated by the lower-resolution version of the GCM under the A1B emissions scenario, using the 2071-2100 time horizon for the 60km simulation and 2081-2100 for the 40km simulation. The 2081-2100 simulation was compared to a present-day simulation using the SSTs and sea ice for the 1980-2000 period. The two climate-change

experiments simulated a decrease in western Pacific tropical cyclones, with a 20% decrease in the 60km model and a 28% decrease in the 40km model. The authors attributed the decrease to a more stable atmosphere in the West Pacific, as measured by dry static stability, as well as reduced upward motion. Oouchi et al. (Oouchi et al., 2006) found that the number of West Pacific tropical cyclones declined by 38%, relative to a present-day simulation, for the 2080-2099 time horizon under the A1B emissions scenario. In agreement with Bengtsson et al. (2007), the authors concluded that the decreases were due to increased atmospheric stability in a warmer world; the model simulated a 10% increase in the dry static stability, defined as the difference in potential temperature between 250hPa level of the atmosphere and the land surface. Similarly, modest decreases in West Pacific cyclone frequency were simulated by Gualdi et al. (2008), following their application of the 120km resolution SINTEX-G model in a 30-year simulation under a $2xCO_2$ scenario.

Zhao et al. (2009) applied the 50km GFDL GCM with four future SST and sea ice distributions; 1) the ensemble mean from 18 GCMs, 2) the HadCM3 GCM, 3) the GFDL GCM, and 4) the ECHAM5 GCM. The SSTs distributions were for the A1B emissions scenario for the 2081-2100 time horizon. In all four of the experiments, the frequencies of cyclones in the West Pacific basin decreased, but the magnitude varied considerably: the GFDL GCM simulated a decrease of 5%; HadCM3 simulated a decrease of 12%; the ensemble mean from 18 GCMs simulated a 29% decrease; and ECHAM5 simulated a 52% decrease.

The eight timesclice experiments presented by Sugi et al. (2009) showed considerable variation in projected West Pacific cyclone frequencies, with three experiments simulating increases (13-64%) and five simulating decreases (14-36%). It is worth noting that three out of the four finer-resolution, 20km experiments simulated a decrease of at least 26%, including the experiment driven by the ensemble-mean SST field. The authors attributed the variations between the driving models to the variations in regional SST changes simulated by those models. Those models which simulated an SST warming in the West Pacific that was greater than the global-mean warming tended to produce increases in cyclone frequency, while those models that simulated a relatively cooler West Pacific tended to reduce the number of cyclones relative to the present-day climate.

Emanuel et al. (2008) concluded that West Pacific tropical-cyclone frequency could increase by 6%, under the A1B emissions scenario for the 2180-2200 time horizon. All seven GCMs considered in the analysis simulated an increase in frequencies of tropical cyclones. Importantly for Indonesia, however, Emanuel et al. (2008) found a northward shift in the

main Pacific tropical cyclogenesis region, which suggests that fewer storms could make landfall in Indonesia.

Further supporting evidence for fewer Pacific cyclones impacting Indonesia with climate change is provided by a study presented by Li et al. (2010), which found a substantial shift in cyclone activity away from the West Pacific and towards the central part of the basin. The authors conducted 20-year timeslice experiments with the 40km resolution ECHAM5 atmospheric model, driven by the SSTs and sea-ice from the lower-resolution version of the model from two periods; one experiment used the period 1981-2000, representing the present-day climate; the other used the period 2081-2100 from the model's A1B scenario simulation. The model simulated a 31% decrease in cyclone numbers in the West Pacific and a 65% increase in the Central Pacific, with a considerable decrease in the number of cyclones tracking near Indonesia. Unlike the findings by Zhao et al. (2009), the authors found that the regional SST warming patterns simulated by ECHAM5 in the Pacific could not explain the shift of cyclone tracks toward the Central Pacific. Rather, the reduction in cyclone numbers in the West Pacific was due to a weakening of the Pacific trade winds and a more El Niño-like basic state in ECHAM5. This resulted in changes in the mean-state vertical wind shear that suppressed nascent tropical cyclones in the West Pacific and enhanced tropical cyclogenesis in the centre of the basin.

While there is therefore considerable uncertainty in projections of tropical-cyclone frequency change in the West Pacific under climate change, the existing sub-basin-scale information—limited and uncertain as it is—suggests that fewer cyclones in this basin could affect Indonesia.

Assessment of cyclone intensity

It is, however, possible that tropical cyclones in the West Pacific could become more intense as a result of climate change. Under an extreme $6xCO_2$ scenario with the CCSM2 GCM, Stowasser et al. (2007) simulated a mean increase in the intensity of North Pacific storms, with a doubling in the frequency of storms exceeding 35 ms^{-1}. Furthermore, in their application of potential-intensity theory to 18 GCMs, Vecchi and Soden (2007) found that on average West Pacific cyclone intensities increased by 3.5% by 2100 under A1B emissions. This was confirmed by Yu et al. (2010); the mean of the 18 GCM simulations in their study showed a 2.3% increase in West Pacific potential intensity per 1°C of global-mean warming.

Knutson and Tuleya (2004) found that under a 1% per year CO_2 increase scenario, the intensity of West Pacific cyclones increased by 4-9% by the end of an 80-year simulation.

The authors also used a 9km version of the GFDL hurricane model, driven by the large-scale conditions simulated by several GCMs under the same 1% per year CO_2 increase scenario. Across all GCMs, the average wind speed of West Pacific cyclones increased by 5%, while central pressures fell by 13.6%. In their global timeslice experiment with the JMA 20km model, Oouchi et al. (2006) found that cyclone intensities increased by 4.2% in the West Pacific against the present-day climate, under the A1B emissions scenario for the 2080-2099 time horizon. These intensity changes are expected to be strongest for the most extreme storms, as suggested by Stowasser et al. (2007) for the West Pacific and by many global-scale studies (McDonald et al., 2005, Oouchi et al., 2006).

Assessment of Cyclone damages

To estimate the impact of climate change on tropical cyclone damages, Mendelsohn et al. (2011) applied the cyclone "seeding" method described by Emanuel et al. (2008) to the output of four GCMs under the A1B scenario, then constructed a damage model to estimate the damages from each landfalling storm. The model separates the additional damages from the impact of climate change on tropical cyclones from the additional damages due to future economic development. This is accomplished through applying the damages from both present-day and future tropical cyclones to the projected economic conditions in 2100 (the "future baseline"). Against a future baseline of $609.7 million in damages per year in Indonesia, two of the four GCMs considered simulated a considerable increase in cyclone damages due to climate change; the CNRM GCM ($6839.3 million) and the ECHAM5 GCM ($793.4 million). The other two GCMs showed a decrease; the GFDL GCM ($166.2 million) and the MIROC GCM ($174.3 million). The range of these changes indicates the high level of uncertainty in understanding of the response of Indian Ocean and West Pacific tropical cyclones to climate change.

National-scale or sub-national scale assessments

Literature searches yielded no results for national-scale or sub-national scale studies for this impact sector.

Coastal regions

Headline

Sea level rise (SLR) could have major impacts on Indonesia's coastal regions. A 10% intensification of the current 1-in-100-year storm surge combined with a prescribed 1m SLR could affect 39% of Indonesia's coastal GDP and 14,400km^2 of coastal land. Another study showed that the country's population exposed to SLR could increase from 600,000 in present, to 2.7 million by the 2070s, under the A1B emissions scenario. An aggressive mitigation scenario could avoid around 156,000 people out of this total being exposed to SLR.

Supporting literature

Assessments that include a global or regional perspective

The IPCC AR4 concluded that at the time, understanding was too limited to provide a best estimate or an upper bound for global SLR in the twenty-first century (IPCC, 2007b). However, a range of SLR, excluding accelerated ice loss effects was published, ranging from 0.19m to 0.59m by the 2090s (relative to 1980-2000), for a range of scenarios (SRES A1FI to B1). The IPCC AR4 also provided an illustrative estimate of an additional SLR term of up to 17cm from acceleration of ice sheet outlet glaciers and ice streams, but did not suggest this is the upper value that could occur. Although there are published projections of SLR in excess of IPCC AR4 values (Nicholls et al., 2011), many of these typically use semi-empirical methods that suffer from limited physical validity and further research is required to produce a more robust estimate. Linking sea level rise projections to temperature must also be done with caution because of the different response times of these two climate variables to a given radiative forcing change.

Nicholls and Lowe (2004) previously showed that mitigation alone would not avoid all of the impacts due to rising sea levels; adaptation would likely be needed too. Recent work by van Vuuren et al. (2011) estimated that, for a world where global mean near surface temperatures reach around 2°C by 2100, global mean SLR could be 0.49m above present

levels by the end of the century. Their sea level rise estimate for a world with global mean temperatures reaching 4°C by 2100 was 0.71m, suggesting around 40% of the future increase in sea level to the end of the 21st century could be avoided by mitigation. A qualitatively similar conclusion was reached in a study by Pardaens et al. (2011), which examined climate change projections from two GCMs. They found that around a third of global-mean SLR over the 21st century could potentially be avoided by a mitigation scenario under which global-mean surface air temperature is near-stabilised at around 2°C relative to pre-industrial times. Under their baseline business-as-usual scenario the projected increase in temperature over the 21st century is around 4°C, and the sea level rise range is 0.29-0.51m (by 2090-2099 relative to 1980-1999; 5% to 95% uncertainties arising from treatment of land-based ice melt and following the methodology used by the IPCC AR4). Under the mitigation scenario, global mean SLR in this study is projected to be 0.17-0.34m.

The IPCC 4th assessment (IPCC 2007a) followed Nicholls and Lowe (2004) for estimates of the numbers of people affected by coastal flooding due to sea level rise. Nicholls and Lowe (2004) projected for the southeast Asia region that an additional 400 thousand people per year could be flooded due to sea level rise by the 2080s relative to the 1990s for the SRES A2 Scenario (note this region also includes other countries, such as Thailand and the Philippines). However, it is important to note that this calculation assumed that protection standards increased as GDP increased, although there is no additional adaptation for sea level rise. More recently, Nicholls et al. (2011) also examined the potential impacts of sea level rise in a scenario that gave around 4°C of warming by 2100. Readings from Figure 3 from Nicholls et al. (2011) for the southeast Asian region suggest less than an approximate 20 million additional people could be flooded for a 0.5 m SLR (assuming no additional protection). Nicholls et al. (2011) also looked at the consequence of a 2m SLR by 2100, however as we consider this rate of SLR to have a low probability we don't report these figures here.

Dasgupta et al. (2009) considered 84 developing countries with a 10% intensification of the current 1-in-100-year storm surge combined with a prescribed 1m SLR. GIS inundation models were applied in the analysis and the method means that uncertainty associated with the climate system is inherently overlooked. Nevertheless, the projections give a useful indicator of the possible impact of SLR in Indonesia. Table 11 shows that in terms of the proportion of coastal GDP affected by SLR, Indonesia was found to be one of the 84 countries that experiences the most severe impacts; around 39% of coastal GDP and 14,400km^2 of coastal land affected. SLR was estimated to affect around 5.8 million people. The results presented by Dasgupta et al. (2009) contrast with a previous assessment that

estimated a 0.6m SLR for Indonesia could be associated with a land loss of around 34,000km^2 and 2.0 million people displaced (Nicholls and Mimura, 1998), although differing methodologies and magnitudes of SLR may explain the divergence.

Country	Incremental Impact: Land Area (sq. km)	Projected Impact as a % of Coastal Total	Incremental Impact: Population	Projected Impact as a % of Coastal Total	Incremental Impact: GDP (mil. USD)	Projected Impact as a % of Coastal Total	Incremental Impact: Agricultural Area (sq. km)	Projected Impact as a % of Coastal Total	Incremental Impact: Urban Extent (sq. km)	Projected Impact as a % of Coastal Total	Incremental Impact: Wetlands (sq. km)	Projected Impact as a % of Coastal Total
Africa												
South Africa	607	43.09	48,140	32.91	174	30.98	70	34.48	93	48.10	132	46.23
Egypt	2,290	13.61	2,600,000	14.68	4,600	16.67	692	5.23	627	15.30	640	28.36
Kenya	274	41.93	27,400	40.23	10	32.05	40	22.13	9	38.89	177	52.51
Americas												
Argentina	2,400	18.03	278,000	19.52	2,240	16.42	157	9.93	313	27.47	459	11.30
Brazil	6,280	15.08	1,100,000	30.37	4,880	28.48	275	16.47	960	33.67	2,590	11.48
Mexico	9,130	29.04	463,000	20.56	2,570	21.22	310	10.89	701	18.35	1,760	52.25
Peru	727	36.69	61,000	46.90	177	46.18	5	26.92	54	42.72	20	37.91
Asia												
China	11,800	17.52	10,800,000	16.67	31,200	17.15	6,640	11.66	2,900	15.70	4,360	39.77
Rep. of Korea	902	61.73	863,000	50.48	10,600	47.86	237	66.75	335	48.15	77	78.81
India	8,690	29.33	7,640,000	28.68	5,170	27.72	3,740	23.64	1,290	30.04	2,510	32.31
Indonesia	14,400	26.64	5,830,000	32.75	7,990	38.71	4,110	26.12	1,280	33.25	2,680	26.97
Saudi Arabia	1,360	41.58	243,000	42.92	2,420	40.60	0	0.00	390	45.85	715	51.04
Bangladesh	4,450	23.45	4,840,000	16.01	2,220	19.00	2,710	17.52	433	18.30	3,890	24.29

Table 11. The impact of a 1m SLR combined with a 10% intensification of the current 1-in-100-year storm surge. Impacts are presented as incremental impacts, relative to the impacts of existing storm surges. Each impact is presented in absolute terms, then as a percentage of the coastal total; e.g. 9.93% of Argentina's coastal agricultural land is impacted. The table is adapted from a study presented by Dasgupta et al. (2009), which considered impacts in 84 developing countries. Only those countries relevant to this review are presented here and all incremental impacts have been rounded down to three significant figures.

Hanson et al. (2010) investigated population exposure to global SLR, natural and human subsidence/uplift, and more intense storms and higher storm surges, for 136 port cities across the globe. Their analysis suggests that Indonesia is in the top 5 of the globe's most highly impacted countries to SLR, which is largely supportive of the results presented by Dasgupta et al. (2009). Future city populations were calculated using global population and economic projections, based on the SRES A1 scenario up to 2030. The study accounted for uncertainty on future urbanization rates, but estimates of population exposure were only presented for a rapid urbanisation scenario, which involved the direct extrapolation of population from 2030 to 2080. All scenarios assumed that new inhabitants of cities in the future will have the same relative exposure to flood risk as current inhabitants. The study is similar to a later study presented by Hanson et al. (2011) except here, different climate change scenarios were considered, and published estimates of exposure are available for more countries. Future water levels were generated from temperature and thermal expansion data related to greenhouse gas emissions with SRES A1B (un-mitigated climate change) and under a mitigation scenario where emissions peak in 2016 and decrease subsequently at 5% per year to a low emissions floor (2016-5-L). Table 12 shows the aspects of SLR that were considered for various scenarios and Table 13 displays regional population exposure for each scenario in the 2030s, 2050s and 2070s. By comparing the projections in Table 13 with the estimates for exposure in the absence of climate change that are presented in Table 14, the vulnerability of Indonesia to SLR is clear. For example, in present day there are around 600,000 people in Indonesia exposed to SLR and in the absence of climate change in the 2070s this increases to around 1.5 million. With climate change in the 2070s, and under the FAC (Future City All Changes) scenario the exposed population is 2.7 million under un-mitigated A1B emissions. Hanson et al. (2010) also demonstrated that aggressive mitigation scenario could avoid an exposure of around 156,000 people in Indonesia, relative to un-mitigated climate change (see Table 14) in 2070.

Scenario		Water levels				
		Climate			Subsidence	
Code	Description	More intense storms	Sea-level change	Higher storm surges	Natural	Anthropogenic
FNC	Future city	V	x	x	X	x
FRSLC	Future City Sea-Level Change	V	V	x	V	x
FCC	Future City Climate Change	V	V	V	V	x
FAC	Future City All Changes	V	V	V	V	V

Table 12. Summary of the aspects of SLR considered by Hanson et al. (2010). 'V' denotes that the aspect was considered in the scenario and 'x' that it was not.

Rapid urbanisation projection

2030						2050						2070					
Country	Ports	Water level projection				Country	Ports	Water level projection				Country	Ports	Water level projection			
		FAC	FCC	FRSLC	FNC			FAC	FCC	FRSLC	FNC			FAC	FCC	FRSLC	FNC
CHINA	15	17,100	15,500	15,400	14,600	CHINA	15	23,000	19,700	18,700	17,400	CHINA	15	27,700	22,600	20,800	18,600
INDIA	6	11,600	10,800	10,300	9,970	INDIA	6	16,400	14,600	13,600	12,500	INDIA	6	20,600	17,900	15,600	13,900
US	17	8,990	8,960	8,830	8,460	US	17	11,300	11,200	10,800	9,970	US	17	12,800	12,700	12,100	10,700
JAPAN	6	5,260	4,610	4,430	4,390	JAPAN	6	6,440	5,280	5,000	4,760	JAPAN	6	7,800	5,970	5,580	5,070
INDONESIA	4	1,420	1,200	1,200	1,170	INDONESIA	4	2,110	1,610	1,610	1,500	INDONESIA	4	2,680	1,830	1,830	1,530
BRAZIL	10	833	833	833	802	BRAZIL	10	929	929	929	879	BRAZIL	10	940	940	940	864
UK	2	497	497	478	459	UK	2	609	609	564	521	UK	2	716	716	640	569
CANADA	2	459	433	422	405	CANADA	2	549	512	486	457	CANADA	2	614	585	545	489
REP. Of KOREA	3	344	344	331	441	REP. Of KOREA	3	361	361	341	318	REP. Of KOREA	3	377	377	325	303
GERMANY	1	257	257	253	248	GERMANY	1	287	287	273	269	GERMANY	1	309	309	290	280
RUSSIA	1	177	177	177	177	RUSSIA	1	202	202	173	173	RUSSIA	1	226	226	197	169
AUSTRALIA	5	162	162	157	157	AUSTRALIA	5	197	197	191	181	AUSTRALIA	5	196	196	186	175
SOUTH AFRICA	2	30	30	30	29	SAUDI ARABIA	1	33	33	33	27	SAUDI ARABIA	1	38	38	38	29
SAUDI ARABIA	1	24	24	24	22	SOUTH AFRICA	2	28	28	28	27	SOUTH AFRICA	2	30	30	30	27
FRANCE	1	15	15	15	15	FRANCE	1	19	19	19	17	FRANCE	1	23	23	23	18
ITALY	1	2	2	2	2	ITALY	1	4	4	4	3	ITALY	1	6	6	6	4
MEXICO	0	0	0	0	0	MEXICO	0	0	0	0	0	MEXICO	0	0	0	0	0

Table 13. *National estimates of population exposure (1,000s) for each water level projection (ranked according to exposure with the FAC (Future City All Changes) scenario) under a rapid urbanisation projection for the 2030s, 2050s and 2070s. Estimates for present day exposure and in the absence of climate change (for 2070 only) for comparison are presented in Table 14. Data is from Hanson et al. (2010) and has been rounded down to three significant figures.*

| Country | Ports | Population exposure | | | | |
| | | Current | 2070. Rapid urbanisation, FAC water level scenario | | | Exposure avoided |
			No climate change	A1B un-mitigated	Mitigated (2016-5-L)	
CHINA	15	8,740	18,600	27,700	26,500	1,140
UNITED STATES	17	6,680	10,700	12,800	12,300	505
RUSSIA	1	189	169	226	197	28
JAPAN	6	3,680	5,070	7,800	7,290	515
SOUTH AFRICA	2	24	27	30	29	0
INDIA	6	5,540	13,900	20,600	18,900	1,670
BRAZIL	10	555	864	940	926	14
MEXICO	0	0	0	0	0	0
CANADA	2	308	489	614	599	15
AUSTRALIA	5	99	175	196	190	6
INDONESIA	4	602	1,530	2,680	2,520	156
REP. Of KOREA	3	294	303	377	343	34
UK	2	414	569	716	665	51
FRANCE	1	13	18	23	20	2
ITALY	1	2	4	6	6	0
GERMANY	1	261	280	309	295	15
SAUDI ARABIA	1	15	29	38	35	3

Table 14. Exposed population (1,000s) in present (current), and in the 2070s in the absence of climate change (no climate change), with unmitigated climate change (A1B un-mitigated), and mitigated climate change (mitigated 2016-5-L), under the rapid urbanisation and FAC (Future City All Changes) water level scenarios. The final column shows the potential avoided exposure, as a result of mitigation. Data is from Hanson et al. (2010) and has been rounded down to three significant figures.

Hanson et al. (2011) also present estimates of the exposure of the world's large port cities (population exceeding one million inhabitants in 2005) to coastal flooding due to SLR and storm surge, now and in the 2070s. Population exposure was calculated as a function of elevation against water levels related to the 1 in 100 year storm surge. The analysis assumed a homogenous SLR of 0.5m by 2070. For tropical storms a 10% increase in extreme water levels was assumed, with no expansion in affected area; while for extratropical storms, a 10% increase in extreme water levels was assumed. A uniform 0.5 m decline in land levels was assumed from 2005 to the 2070s in those cities which are historically susceptible (usually port cities located in deltas). This approach provided a variable change in extreme water level from around 0.5m in cities only affected by global SLR, to as much as 1.5m for cities affected by global SLR, increased storminess and human-induced subsidence. Population projections were based upon the UN medium variant, where global population stabilises at around 9 billion by 2050. Figure 13 shows that Indonesia presented the 11th highest increased exposure from SLR relative to present in the 2070s, out of the countries Hanson et al. (2011) considered. Generally, exposure change in developing country cities is more strongly driven by socioeconomic changes, while developed country cities see a more significant effect from climate change. The results confirm previous findings from global-scale studies that Indonesia displays medium-to-high vulnerability to SLR (Dasgupta et al., 2009, Nicholls and Mimura, 1998, Hanson et al., 2010).
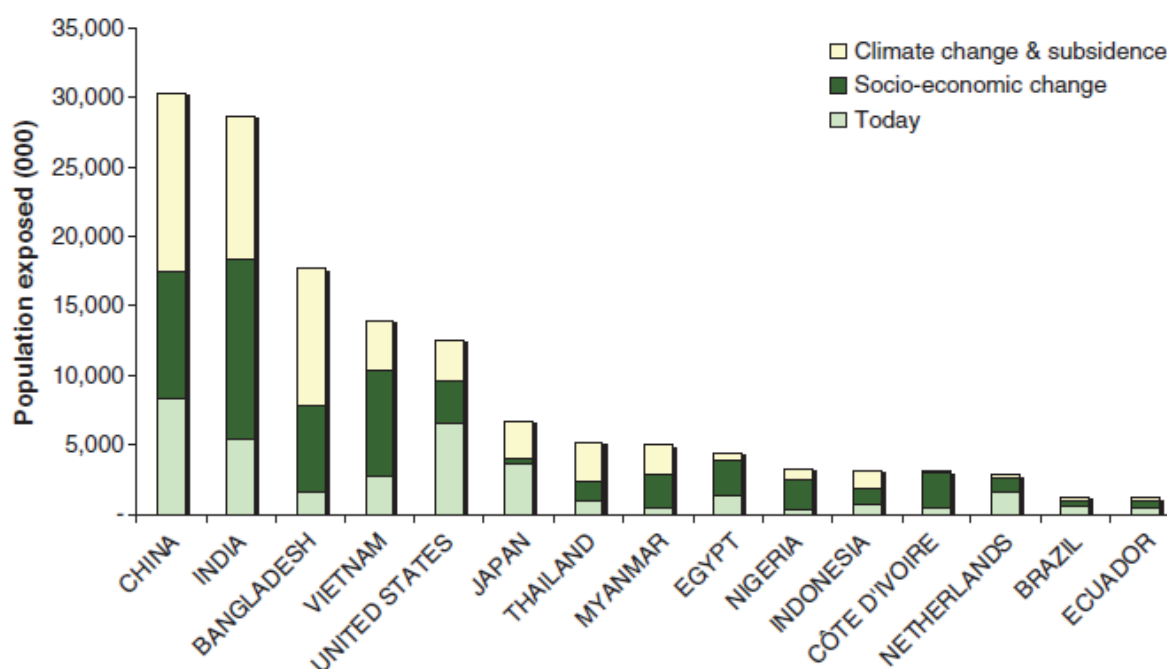
Figure 13. *The top 15 countries in the 2070s for exposure to SLR, based upon a global analysis of 136 port cities (Hanson et al., 2011). The proportions associated with current exposure, climate change and subsidence, and socio-economic changes are displayed.*

To further quantify the impact of SLR and some of the inherent uncertainties, the DIVA model was used to calculate the number of people flooded per year for global mean sea level increases (Brown et al., 2011). The DIVA model (DINAS-COAST, 2006) is an integrated model of coastal systems that combines scenarios of water level changes with socio-economic information, such as increases in population. The study uses two climate scenarios; 1) the SRES A1B scenario and 2) a mitigation scenario, RCP2.6. In both cases an SRES A1B population scenario was used. The results are shown in Table 15.

	A1B		RCP	
	Low	**High**	**Low**	**High**
Additional people flooded (1000s)	320.65	2212.81	219.11	1414.30
Loss of wetlands area (% of country's total wetland)	19.28%	27.75%	16.66%	24.92%

Table 15. *Number of additional people flooded (1000s), and percentage of total wetlands lost by the 2080s under the high and low SRES A1B and mitigation (RCP 2.6) scenarios (Brown et al., 2011).*

119

National-scale or sub-national scale assessments

Marfai and King (2008) used GIS inundation techniques to assess the impact of 1.2m and 1.8m SLR changes for the Semarang coastal area, which is located on the northern part of Central Java Province. Semarang has a total area of about 373km^2 and a population of approximately 1.5 million, which makes it the fifth largest city in Indonesia. It is one of the most important harbours of the Central Java region and the city of Semarang plans to develop and become the centre of national development. Therefore the projections presented by Marfai and King (2008) (see Table 16) have important implications for planning and adaptation in the region.

Land use	Affected area (ha)		Total value (€million)	
	1.2m SLR	1.8m SLR	1.2m SLR	1.8m SLR
Agriculture and plantation area	527	712	42	57
Bare land, beach and yards	775	930	1	1
Built up areas	1320	1716	1584	2059
Fishpond areas	1943	2335	184	212
Total	4567	5594	1812	2330

Table 16. Estimation of the vulnerability of the Semarang coastal area to SLR. Data is from Marfai and King (2008) and has been rounded down to four significant figures.

References

AGRIMONEY. 2010. *La Nina rains wash out Indonesia coffee hopes* [Online]. Available: http://bit.ly/eBolai [Accessed 12 June 2011].

AINSWORTH, E. A. & MCGRATH, J. M. 2010. Direct Effects of Rising Atmospheric Carbon Dioxide and Ozone on Crop Yields. *In:* LOBELL, D. & BURKE, M. (eds.) *Climate Change and Food Security.* Springer Netherlands.

ALDRIAN, E. & DJAMIL, Y. S. 2008. Spatio-temporal climatic change of rainfall in East Java Indonesia. *International Journal of Climatology,* 28**,** 435-448.

ALLISON, E. H., PERRY, A. L., BADJECK, M.-C., NEIL ADGER, W., BROWN, K., CONWAY, D., HALLS, A. S., PILLING, G. M., REYNOLDS, J. D., ANDREW, N. L. & DULVY, N. K. 2009. Vulnerability of national economies to the impacts of climate change on fisheries. *Fish and Fisheries,* 10**,** 173-196.

ARNELL, N., OSBORNE, T., HOOKER, J., DAWSON, T., PERRYMAN, A. & WHEELER, T. 2010. Simulation of AVOIDed impacts on crop productivity and food security. *Work stream 2, Report 17 of the AVOID programme (AV/WS2/D1/R17).*

ARNELL, N. W. 2004. Climate change and global water resources: SRES emissions and socio-economic scenarios. *Global Environmental Change,* 14**,** 31-52.

AVNERY, S., MAUZERALL, D. L., LIU, J. F. & HOROWITZ, L. W. 2011. Global crop yield reductions due to surface ozone exposure: 2. Year 2030 potential crop production losses and economic damage under two scenarios of O_3 pollution. *Atmospheric Environment,* 45**,** 2297-2309.

BENDER, M. A., KNUTSON, T. R., TULEYA, R. E., SIRUTIS, J. J., VECCHI, G. A., GARNER, S. T. & HELD, I. M. 2010. Modeled impact of anthropogenic warming on the frequency of intense Atlantic hurricanes. *Science,* 327**,** 454-8.

BENGTSSON, L., HODGES, K. I., ESCH, M., KEENLYSIDE, N., KORNBLUEH, L., LUO, J.-J. & YAMAGATA, T. 2007. How may tropical cyclones change in a warmer climate? *Tellus A,* 59**,** 539-561.

BETTS, R. A., BOUCHER, O., COLLINS, M., COX, P. M., FALLOON, P. D., GEDNEY, N., HEMMING, D. L., HUNTINGFORD, C., JONES, C. D., SEXTON, D. M. H. & WEBB, M. J.

2007. Projected increase in continental runoff due to plant responses to increasing carbon dioxide. *Nature,* 448**,** 1037-1041.

BOER, R. & FAQIH, A. 2004. Current and Future Rainfall Variability in Indonesia. AIACC Technical Report 021.

BROWN, S., NICHOLLS, R., LOWE, J.A. and PARDAENS, A. (2011), Sea level rise impacts in 24 countries. Faculty of Engineering and the Environment and Tyndall Centre for Climate Change Research, University of Southampton.

CHAKRABORTY, S. & NEWTON, A. C. 2011. Climate change, plant diseases and food security: an overview. *Plant Pathology,* 60**,** 2-14.

CHEUNG, W. W. L., LAM, V. W. Y., SARMIENTO, J. L., KEARNEY, K., WATSON, R. E. G., ZELLER, D. & PAULY, D. 2010. Large-scale redistribution of maximum fisheries catch potential in the global ocean under climate change. *Global Change Biology,* 16**,** 24-35.

CIA 2011. World Factbook. US Central Intelligence Agency.

D'ARRIGO, R. & WILSON, R. 2008. El Niño and Indian Ocean influences on Indonesian drought: implications for forecasting rainfall and crop productivity. *International Journal of Climatology,* 28**,** 611-616.

DASGUPTA, S., LAPLANTE, B., MURRAY, S. & WHEELER, D. 2009. Sea-level rise and storm surges: a comparative analysis of impacts in developing countries. Washington DC, USA: World Bank.

DINAS-COAST Consortium. 2006 DIVA 1.5.5. Potsdam, Germany: Potsdam Institute for Climate Impact Research (on CD-ROM)

DOLL, P. & SIEBERT, S. 2002. Global modeling of irrigation water requirements. *Water Resources Research*. Vol: 38   Issue: 4. Doi: 10.1029/2001WR000355.

EMANUEL, K., SUNDARARAJAN, R. & WILLIAMS, J. 2008. Hurricanes and Global Warming: Results from Downscaling IPCC AR4 Simulations. *Bulletin of the American Meteorological Society,* 89**,** 347-367.

FALKENMARK, M., ROCKSTRÖM, J. & KARLBERG, L. 2009. Present and future water requirements for feeding humanity. *Food Security,* 1**,** 59-69.

FAO. 2008. *Food and Agricultural commodities production* [Online]. Available: http://faostat.fao.org/site/339/default.aspx [Accessed 1 June 2011].

FAO. 2010. *Food Security county profiles* [Online]. Available: http://www.fao.org/economic/ess/ess-fs/ess-fs-country/en/ [Accessed 1 Sept 2011].

GERTEN D., SCHAPHOFF S., HABERLANDT U., LUCHT W., SITCH S. 2004 . Terrestrial vegetation and water balance: hydrological evaluation of a dynamic global vegetation model *International Journal Water Resource Development* 286:249–270.

GORNALL, J., BETTS, R., BURKE, E., CLARK, R., CAMP, J., WILLETT, K., WILTSHIRE, A. 2010. Implications of climate change for agricultural productivity in the early twenty-first century. *Phil. Trans. R. Soc. B*, DOI: 10.1098/rstb.2010.0158.

GOSLING, S., TAYLOR, R., ARNELL, N. & TODD, M. 2011. A comparative analysis of projected impacts of climate change on river runoff from global and catchment-scale hydrological models. *Hydrology and Earth System Sciences,* 15**,** 279–294.

GOSLING, S. N. & ARNELL, N. W. 2011. Simulating current global river runoff with a global hydrological model: model revisions, validation, and sensitivity analysis. *Hydrological Processes,* 25**,** 1129-1145.

GOSLING, S. N., BRETHERTON, D., HAINES, K. & ARNELL, N. W. 2010. Global hydrology modelling and uncertainty: running multiple ensembles with a campus grid. *Philosophical Transactions of the Royal Society A: Mathematical, Physical and Engineering Sciences,* 368**,** 4005-4021.

GUALDI, S., SCOCCIMARRO, E. & NAVARRA, A. 2008. Changes in Tropical Cyclone Activity due to Global Warming: Results from a High-Resolution Coupled General Circulation Model. *Journal of Climate,* 21**,** 5204-5228.

HANSON, S., NICHOLLS, R., RANGER, N., HALLEGATTE, S., CORFEE-MORLOT, J., HERWEIJER, C. & CHATEAU, J. 2011. A global ranking of port cities with high exposure to climate extremes. *Climatic Change,* 104**,** 89-111.

HANSON, S., NICHOLLS, R., S, H. & CORFEE-MORLOT, J. 2010. The effects of climate mitigation on the exposure of worlds large port cities to extreme coastal water levels. London, UK.

HARDING, R., BEST, M., BLYTH, E., HAGEMANN, D., KABAT, P., TALLAKSEN, L.M., WARNAARS, T., WIBERG, D., WEEDON, G.P., van LANEN, H., LUDWIG, F., HADDELAND, I. 2011. Preface to the "Water and Global Change (WATCH)" special collection: Current knowledge of the terrestrial global water cycle. *Journal of Hydrometeorology*, DOI: 10.1175/JHM-D-11-024.1.

HIDAYAT, F. 2009. Floods and climate change - observations from Java. *Center for River Basin Organizations and Management, Solo, Central Java, Indonesia*.

HIRABAYASHI, Y., KANAE, S., EMORI, S., OKI, T. & KIMOTO, M. 2008. Global projections of changing risks of floods and droughts in a changing climate. *Hydrological Sciences Journal-Journal Des Sciences Hydrologiques,* 53**,** 754-772.

HONORINE, S. 2010. *La Nina Creates Concerns About Indonesia's Harvest* [Online]. Voice of America. Available: http://bit.ly/bHwXtY [Accessed 12 June 2011].

IFPRI. 2010. *International Food Policy Research Institute (IFPRI) Food Security CASE maps. Generated by IFPRI in collaboration with StatPlanet.* [Online]. Available: www.ifpri.org/climate-change/casemaps.html [Accessed 21 June 2010].

IGLESIAS, A., GARROTE, L., QUIROGA, S. & MONEO, M. 2009. Impacts of climate change in agriculture in Europe. PESETA-Agriculture study. *JRC Scientific and Technical Reports.*

IGLESIAS, A. & ROSENZWEIG, C. 2009. Effects of Climate Change on Global Food Production under Special Report on Emissions Scenarios (SRES) Emissions and Socioeconomic Scenarios: Data from a Crop Modeling Study. . Palisades, NY: Socioeconomic Data and Applications Center (SEDAC), Columbia University.

IPCC 2007a. Climate Change 2007: Impacts, Adaptation and Vulnerability. Contribution of Working Group II to the Fourth Assessment Report of the Intergovernmental Panel on Climate Change. *In:* PARRY, M. L., CANZIANI, O. F., PALUTIKOF, J. P., VAN DER LINDEN, P. J. & HANSON, C. E. (eds.). Cambridge, UK.

IPCC 2007b. Climate Change 2007: The Physical Science Basis. Contribution of Working Group I to the Fourth Assessment Report of the Intergovernmental Panel on Climate Change *In:* SOLOMON, S., QIN, D., MANNING, M., CHEN, Z., MARQUIS, M., AVERYT, K. B., TIGNOR, M. & MILLER, H. L. (eds.). Cambridge, United Kingdom and New York, NY, USA.

IPCC 2007c. Summary for Policymakers. *In:* PARRY, M. L., CANZIANI, O. F., PALUTIKOF, J. P., VAN DER LINDEN, P. J. & HANSON, C. E. (eds.) *Climate Change 2007: Impacts, Adaptation and Vulnerability. Contribution of Working Group II to the Fourth Assessment Report of the Intergovernmental Panel on Climate Change.* Cambridge: Cambridge University Press.

IRAWAN, B. 2003. Multilevel Impact Assessment and Coping Strategies against El Niño: Case of Food Crops in Indonesia. *CGPRT Center Working Paper 75.* CGPRT.

IRIN. 2010. *TIMOR-LESTE: La Niña blow to crops* [Online]. Available: http://www.irinnews.org/Report.aspx?ReportID=90624 [Accessed 12 June 2011].

KISHORE, K., SETIANA, A., SUBBIAH, A. R., SRIBIMAWATI, T., DIHARTO, S., ALIMOESO, S. & ROGERS, P. 2000. Indonesia Country Case Study: Impacts and Responses to the 1997-98 El Niño Event. *In:* GLANTZ, M. H. (ed.) *Reducing the Impact of Environmental Emergencies Through Early Warning and Preparedness: The Case of El Niño-Southern Oscillation (ENSO).* Joint project of the United Nations Environment Programme and the National Center for Atmospheric Research.

KNMI. 2009. *Effects of El Niño on world weather* [Online]. KNMI. Available: http://www.knmi.nl/research/global_climate/enso/effects/ [Accessed 12 June 2011].

KNUTSON, T. R., MCBRIDE, J. L., CHAN, J., EMANUEL, K., HOLLAND, G., LANDSEA, C., HELD, I., KOSSIN, J. P., SRIVASTAVA, A. K. & SUGI, M. 2010a. Tropical cyclones and climate change. *Nature Geoscience,* 3**,** 157-163.

KNUTSON, T. R., MCBRIDE, J. L., CHAN, J., EMANUEL, K., HOLLAND, G., LANDSEA, C., HELD, I., KOSSIN, J. P., SRIVASTAVA, A. K. & SUGI, M. 2010b. Tropical cyclones and climate change: supplementary material. *Nature Geoscience,* 3**,** Online supplementary material.

KNUTSON, T. R., SIRUTIS, J. J., GARNER, S. T., VECCHI, G. A. & HELD, I. M. 2008. Simulated reduction in Atlantic hurricane frequency under twenty-first-century warming conditions. *Nature Geosci,* 1**,** 359-364.

KNUTSON, T. R. & TULEYA, R. E. 2004. Impact of CO_2-Induced Warming on Simulated Hurricane Intensity and Precipitation : Sensitivity to the Choice of Climate Model and Convective Parameterization. *Journal of Climate***,** 3477-3495.

LATIF, M. & KEENLYSIDE, N. S. 2009. El Niño/Southern Oscillation response to global warming. *Proceedings of the National Academy of Sciences of the United States of America,* 106**,** 20578-20583.

LI, T., KWON, M., ZHAO, M., KUG, J.-S., LUO, J.-J. & YU, W. 2010. Global warming shifts Pacific tropical cyclone location. *Geophysical Research Letters,* 37**,** 1-5.

LOBELL, D. B., BANZIGER, M., MAGOROKOSHO, C. & VIVEK, B. 2011. Nonlinear heat effects on African maize as evidenced by historical yield trials. *Nature Clim. Change,* 1**,** 42-45.

LOBELL, D. B., BURKE, M. B., TEBALDI, C., MASTRANDREA, M. D., FALCON, W. P. & NAYLOR, R. L. 2008. Prioritizing climate change adaptation needs for food security in 2030. *Science,* 319**,** 607-610.

LUCK, J., SPACKMAN, M., FREEMAN, A., TRE˛BICKI, P., GRIFFITHS, W., FINLAY, K. & CHAKRABORTY, S. 2011. Climate change and diseases of food crops. *Plant Pathology,* 60**,** 113-121.

MARFAI, M. & KING, L. 2008. Potential vulnerability implications of coastal inundation due to sea level rise for the coastal zone of Semarang city, Indonesia. *Environmental Geology,* 54**,** 1235-1245.

MASUTOMI, Y., TAKAHASHI, K., HARASAWA, H. & MATSUOKA, Y. 2009. Impact assessment of climate change on rice production in Asia in comprehensive consideration of process/parameter uncertainty in general circulation models. *Agriculture, Ecosystems & Environment,* 131**,** 281-291.

MCDONALD, R. E., BLEAKEN, D. G., CRESSWELL, D. R., POPE, V. D. & SENIOR, C. A. 2005. Tropical storms: representation and diagnosis in climate models and the impacts of climate change. *Climate Dynamics,* 25**,** 19-36.

MENDELSOHN, R., EMANUEL, K. & CHONABAYASHI, S. 2011. The Impact of Climate Change on Global Tropical Cyclone Damages.

NASA. 1999. *La Niña Factsheet: The Effects of La Niña* [Online]. Available: http://earthobservatory.nasa.gov/Features/LaNina/la_nina_1.php [Accessed 12 June 2011].

NAYLOR, R. L., BATTISTI, D. S., VIMONT, D. J., FALCON, W. P. & BURKE, M. B. 2007. Assessing risks of climate variability and climate change for Indonesian rice agriculture.

Proceedings of the National Academy of Sciences of the United States of America, 104**,** 7752-7757.

NAYLOR, R. L. & MASTRANDREA, M. D. 2010. Coping with Climate Risks in Indonesian Rice Agriculture: A Policy Perspective. *In:* FILAR, J. A. & HAURIE, A. (eds.) *Uncertainty and Environmental Decision Making.* Springer US.

NELSON, G. C., ROSEGRANT, M. W., KOO, J., ROBERTSON, R., SULSER, T., ZHU, T., RINGLER, C., MSANGI, S., PALAZZO, A., BATKA, M., MAGALHAES, M., VALMONTE-SANTOS, R., EWING, M. & LEE, D. 2009. Climate change. Impact on Agriculture and Costs of Adaptation. Washington, D.C.: International Food Policy Research Institute.

NELSON, G. C., ROSEGRANT, M. W., PALAZZO, A., GRAY, I., INGERSOLL, C., ROBERTSON, R., TOKGOZ, S., ZHU, T., SULSER, T. & RINGLER, C. 2010. Food Security, Farming and Climate Change to 2050. *Research Monograph, International Food Policy Research Institute.* Washington, DC.

NICHOLLS, R. J. & MIMURA, N. 1998. Regional issues raised by sea-level rise and their policy implications. *Climate Research,* 11**,** 5-18.

NICHOLLS, R. J. and LOWE, J. A. (2004). "Benefits of mitigation of climate change for coastal areas." *Global Environmental Change* **14**(3): 229-244.

NICHOLLS, R. J., MARINOVA, N., LOWE, J. A., BROWN, S., VELLINGA, P., DE GUSMÃO, G., HINKEL, J. and TOL, R. S. J. (2011). "Sea-level rise and its possible impacts given a 'beyond 4∘C world' in the twenty-first century." *Philosophical Transactions of the Royal Society A* **369**: 1-21.

OOUCHI, K., YOSHIMURA, J., YOSHIMURA, H., MIZUTA, R., KUSUNOKI, S. & NODA, A. 2006. Tropical Cyclone Climatology in a Global-Warming Climate as Simulated in a 20 km-Mesh Global Atmospheric Model: Frequency and Wind Intensity Analyses. *Journal of the Meteorological Society of Japan,* 84**,** 259-276.

PARDAENS, A. K., LOWE, J., S, B., NICHOLLS, R. & DE GUSMÃO, D. 2011. Sea-level rise and impacts projections under a future scenario with large greenhouse gas emission reductions. *Geophysical Research Letters,* 38**,** L12604.

PARRY, M. L., ROSENZWEIG, C., IGLESIAS, A., LIVERMORE, M. & FISCHER, G. 2004. Effects of climate change on global food production under SRES emissions and socio-

economic scenarios. *Global Environmental Change-Human and Policy Dimensions,* 14**,** 53-67.

PHILIP, S. Y. 2009. *Exploring El Niño mechanisms in climate models.* Phd, Universiteit Utrecht (Research at KNMI, De Bilt).

QUINN, W. H., ZOPF, K. S., SHORT, K. S. & KUO YANG, R. T. W. 1978. Historical trends and statistics of the Southern Oscillation El Niño and Indonesian droughts. *Fishery Bulletin,* 7**,** 663-678.

RAMANKUTTY, N., EVAN, A. T., MONFREDA, C. & FOLEY, J. A. 2008. Farming the planet: 1. Geographic distribution of global agricultural lands in the year 2000. *Global Biogeochemical Cycles,* 22**,** GB1003.

RAMANKUTTY, N., FOLEY, J. A., NORMAN, J. & MCSWEENEY, K. 2002. The global distribution of cultivable lands: current patterns and sensitivity to possible climate change. *Global Ecology and Biogeography,* 11**,** 377-392.

REICHLER, T. & KIM, J. 2008. How well do coupled models simulate today's climate? *Bulletin of the American Meteorological Society,* 89**,** 303-+.

ROCKSTROM, J., FALKENMARK, M., KARLBERG, L., HOFF, H., ROST, S. & GERTEN, D. 2009. Future water availability for global food production: The potential of green water for increasing resilience to global change. *Water Resources Research,* 45.

RODGERS, C. 2009. ADB Approach to Climate Change Adaptation and Water Security. *COP15.* Copenhagen.

STOWASSER, M., WANG, Y. & HAMILTON, K. 2007. Tropical Cyclone Changes in the Western North Pacific in a Global Warming Scenario. *Journal of Climate,* 20**,** 2378-2396.

SUGI, M., MURAKAMI, H. & YOSHIMURA, J. 2009. A reduction in global tropical cyclone frequency due to global warming. *SOLA,* 5**,** 164-167.

SUGI, M., NODA, A. & SATO, N. 2002. Influence of the Global Warming on Tropical Cyclone Climatology: An Experiment with the JMA Global Model. *Journal of the Meteorological Society of Japan,* 80**,** 249-272.

TATSUMI, K., YAMASHIKI, Y., VALMIR DA SILVA, R., TAKARA, K., MATSUOKA, Y., TAKAHASHI, K., MARUYAMA, K. & KAWAHARA, N. 2011. Estimation of potential changes

in cereals production under climate change scenarios. *Hydrological Processes,*Special Issue: Japan Society of Hydrology and water resources, 25 (17), 2715-2725.

VAN VUUREN, D., DEN ELZEN, M., LUCAS, P., EICKHOUT, B., STRENGERS, B., VAN RUIJVEN, B., WONINK, S. & VAN HOUDT, R. 2007. Stabilizing greenhouse gas concentrations at low levels: an assessment of reduction strategies and costs. *Climatic Change,* 81**,** 119-159.

VAN VUUREN, D. P., ISAAC, M., KUNDZEWICZ, Z. W., ARNELL, N., BARKER, T., CRIQUI, P., BERKHOUT, F., HILDERINK, H., HINKEL, J., HOF, A., KITOUS, A., KRAM, T., MECHLER, R. & SCRIECIU, S. 2011. The use of scenarios as the basis for combined assessment of climate change mitigation and adaptation. *Global Environmental Change,* 21**,** 575-591.

VECCHI, G. A. & SODEN, B. J. 2007. Effect of remote sea surface temperature change on tropical cyclone potential intensity. *Nature,* 450**,** 1066-70.

VECCHI, G. A. & WITTENBERG, A. T. 2010. El Niño and our future climate: where do we stand? *Wiley Interdisciplinary Reviews: Climate Change,* 1**,** 260-270.

VOROSMARTY, C. J., MCINTYRE, P. B., GESSNER, M. O., DUDGEON, D., PRUSEVICH, A., GREEN, P., GLIDDEN, S., BUNN, S. E., SULLIVAN, C. A., LIERMANN, C. R. & DAVIES, P. M. 2010. Global threats to human water security and river biodiversity. *Nature,* 467**,** 555-561.

WAHYU, A., KUNTORO, A. A. & YAMASHITA, T. 2010. Annual and Seasonal Discharge Responses to Forest/Land Cover Changes and Climate Variations in Kapuas River Basin, Indonesia. *Journal of international development and cooperation,* 16**,** 81-100.

WARREN, R., ARNELL, N., BERRY, P., BROWN, S., DICKS, L., GOSLING, S., HANKIN, R., HOPE, C., LOWE, J., MATSUMOTO, K., MASUI, T., NICHOLLS, R., O'HANLEY, J., OSBORN, T., SCRIECRU, S. (2010) The Economics and Climate Change Impacts of Various Greenhouse Gas Emissions Pathways: A comparison between baseline and policy emissions scenarios, AVOID Report, AV/WS1/D3/R01. http://www.metoffice.gov.uk/avoid/files/resources-researchers/AVOID_ WS1_D3_01_20100122.pdf.

WELCH, J. R., VINCENT, J. R., AUFFHAMMER, M., MOYA, P. F., DOBERMANN, A. & DAWE, D. 2010. Rice yields in tropical/subtropical Asia exhibit large but opposing

sensitivities to minimum and maximum temperatures. *Proceedings of the National Academy of Sciences of the United States of America,* 107**,** 14562-14567.

WOOD, E.F., ROUNDY, J.K., TROY, T.J., van BEEK, L.P.H., BIERKENS, M.F.P., BLYTH, E., de ROO, A., DOLL, P., EK, M., FAMIGLIETTI, J., GOCHIS, D., van de GIESEN, N., HOUSER, P., JAFFE, P.R., KOLLET, S., LEHNER, B., LETTENMAIER, D.P., PETERS-LIDARD, C., SIVAPALAN, M., SHEFFIELD, J., WADE, A. & WHITEHEAD, P. 2011. Hyperresolution global land surface modelling: Meeting a grand challenge for monitoring Earth's terrestrial water. *Water Resources Research,* 47, W05301.

WOS. 2011. *Web of Science* [Online]. Available: http://thomsonreuters.com/products_services/science/science_products/a-z/web_of_science [Accessed August 2011].

WU, W., TANG, H., YANG, P., YOU, L., ZHOU, Q., CHEN, Z. & SHIBASAKI, R. 2011. Scenario-based assessment of future food security. *Journal of Geographical Sciences,* 21**,** 3-17.

YU, J., WANG, Y. & HAMILTON, K. 2010. Response of Tropical Cyclone Potential Intensity to a Global Warming Scenario in the IPCC AR4 CGCMs. *Journal of Climate,* 23**,** 1354-1373.

ZHAO, M., HELD, I. M., LIN, S.-J. & VECCHI, G. A. 2009. Simulations of Global Hurricane Climatology, Interannual Variability, and Response to Global Warming Using a 50-km Resolution GCM. *Journal of Climate,* 22**,** 6653.